INFORMATION TO USERS

This reproduction was made from a copy of a document sent to us for microfilming. While the most advanced technology has been used to photograph and reproduce this document, the quality of the reproduction is heavily dependent upon the quality of the material submitted.

The following explanation of techniques is provided to help clarify markings or notations which may appear on this reproduction.

1. The sign or "target" for pages apparently lacking from the document photographed is "Missing Page(s)". If it was possible to obtain the missing page(s) or section, they are spliced into the film along with adjacent pages. This may have necessitated cutting through an image and duplicating adjacent pages to assure complete continuity.

2. When an image on the film is obliterated with a round black mark, it is an indication of either blurred copy because of movement during exposure, duplicate copy, or copyrighted materials that should not have been filmed. For blurred pages, a good image of the page can be found in the adjacent frame. If copyrighted materials were deleted, a target note will appear listing the pages in the adjacent frame.

3. When a map, drawing or chart, etc., is part of the material being photographed, a definite method of "sectioning" the material has been followed. It is customary to begin filming at the upper left hand corner of a large sheet and to continue from left to right in equal sections with small overlaps. If necessary, sectioning is continued again—beginning below the first row and continuing on until complete.

4. For illustrations that cannot be satisfactorily reproduced by xerographic means, photographic prints can be purchased at additional cost and inserted into your xerographic copy. These prints are available upon request from the Dissertations Customer Services Department.

5. Some pages in any document may have indistinct print. In all cases the best available copy has been filmed.

University
Microfilms
International

300 N. Zeeb Road
Ann Arbor, MI 48106

Schmermund, John Thomas

A PHOTOIONIZATION DETECTOR FOR HPLC USING A MICROPROCESSOR - CONTROLLED INTERFACE

City University of New York PH.D. 1984

PLEASE NOTE:

In all cases this material has been filmed in the best possible way from the available copy. Problems encountered with this document have been identified here with a check mark _√_.

1. Glossy photographs or pages _____
2. Colored illustrations, paper or print _____
3. Photographs with dark background _____
4. Illustrations are poor copy _____
5. Pages with black marks, not original copy _✓_
6. Print shows through as there is text on both sides of page _____
7. Indistinct, broken or small print on several pages _✓_
8. Print exceeds margin requirements _____
9. Tightly bound copy with print lost in spine _____
10. Computer printout pages with indistinct print _____
11. Page(s) _____ lacking when material received, and not available from school or author.
12. Page(s) _____ seem to be missing in numbering only as text follows.
13. Two pages numbered _____. Text follows.
14. Curling and wrinkled pages _✓_
15. Other _____

A PHOTOIONIZATION DETECTOR FOR HPLC USING

A MICROPROCESSOR-CONTROLLED INTERFACE.

by

JOHN THOMAS SCHMERMUND

A dissertation submitted to the Graduate Faculty in Chemistry in partial fulfillment of the requirements for the degree of Doctor of Philosophy, the city university of New York.

1984

This manuscript has been read and accepted for the Graduate Faculty in Chemistry in satisfaction of the dissertation requirement for the degree of Doctor of Philosophy.

25 July 1984
date

David C. Locke
Chairman of Examining Committee

25 July 1984
date

A. M.
Executive Officer

Joseph Reichstein

Arthur D Bakey

Supervisory Committee

The City University of New York

1984

Abstract

A Microprocessor-Controlled Photoionization Detector

for High Performance Liquid Chromatography

by

John Thomas Schmermund

Adviser: David C. Locke

The purpose of this investigation was to develop a highly sensitive and selective detector for high performance liquid chromatography (HPLC) and detect trace levels of pharmaceuticals in animal feed.

The initial study included the design of a high output vacuum ultraviolet lamp(VUV) and the construction of an ion chamber to collect the photoionized species formed after total vaporization of the column effluent.

Although the initial data was promising, limitations in the selection of aqueous mobile phases was noted due to the quenching of photoionized species by the vaporized mobile phase.

A microprocessor-controlled system was developed which could be used for complex, even thermally unstable mixtures separated by any mode of HPLC. The system described in this thesis has the flexibility to be used with both normal and reverse-phase LC with only minor modifications.

The new system was applied to the trace level analysis of pharmaceuticals spiked in animal feed. Excellent results were achieved for the separation of phenobarbital with a detection level of 30 ng. In addition, amantadine used as an antiviral, could be separated and detected on a reverse-phase system down to 250 ng.

Acknowledgements

I would like to express my sincere appreciation to Professor David C. Locke, my research advisor, for his many years of encouragement and support.

I am grateful to Professor A.D. Baker and J. Glickstein for spending their valuable time to read and comment on this thesis. I also thank Dr. E. Lau and Dr. F. Chow at Du Pont Pharmaceuticals for many hours of useful discussion. I am also grateful for the outstanding typing of Donna Lucas.

My sincere and deep gratitude goes to my parents, Ida and John for their many sacrifices through the years. I also thank my mother and father-in-law, Frances and Louis Sadaka for their support and concern. Special thanks are due Gail Sadaka for her encouragement, optimism and enthusiasm.

The greatest thanks are to my wife, Carrie. Her understanding, encouragement and many sacrifices were invaluable without which this thesis would not be possible.

TABLE OF CONTENTS

Chapter 1

Chapter 2

Chapter 3

Chapter 4

Chapter 5

Chapter 6

Applications of the LC-GC PID Interface

in Pharmaceutical Assays

LIST OF FIGURES

Figure

LIST OF TABLES

Chapter 1

Introduction

Major advances in columns, pumps and control systems have been achieved over the last ten years in high performance liquid chromatography (HPLC). The slowest area of growth has been in the introduction of new types of detectors which can monitor the eluent from a column with both sensitivity and selectivity. A detector which is sensitive to all compounds has not been developed, even though several concepts have been proposed. The LC detectors presently available are not as versatile as the thermal conductivity (TCD) or flame ionization (FID) detector used in gas chromatography.

The most versatile and adaptable detectors are based on the principles of ultraviolet absorbance, refractive index changes, redox reactions or fluorescence after excitation by a UV-visible light source[1]. A review of basic parameters is important to compare the performance, capabilities and disadvantages of these detectors.

The ultraviolet detector, the most frequently used, functions as a compound type or class detector. Aromatic hydrocarbons show high selectivity while alkanes yield a low response except below 210 nM.

There is extreme variability in sensitivity and wavelength of response within a class of aromatic hydrocarbons[2]. Therefore, the UV detector is specific and cannot function as a univerasl detector. In the reverse situation, a refractive index detector will respond to every solute, but with a minimal sensitivity. An RI detector, used in the differential mode with the reference side containing only the solvent, detects the solute in the sample side by a response to the difference in the refractive index between the solvent and solute. As the molecular weight increases, the refractive index increases but the sensitivity is, at best, usually in the low milligram range.

The amperometric detector based on electrochemical reactions at an electrode, often glassy carbon, shows high sensitivity and good selectivity for aromatic phenolic groups such as catecholamines and other biological molecules, but is limited by the composition of the mobile phase, which generally must be a highly conducting solvent with ions present[3-6].

Therefore, the percentage of organic modifiers should be lower than 30% with a buffer present which will not interfere with the redox reaction taking place within the cell. These requirements, in addition to a high noise level, eliminate the LC-EC from most quantitative work except for very specific analytical methodologies used in clinical chemistry.

The remaining HPLC detectors, some of which have recently become available commercially, are all basically experimental and thus have limited applications since they require special techniques to operate them. They can be divided into several categories such as: (a) production of ions which are detected by conduction[7,8]; (b) production of electromagnetic radiation including ß-induced fluorescence[9,10]; chemiluminescence[11] and atomic emission[12]; (c) separation of sample and solvent with detection of the sample such as an LC-MS interface[13] or (d) the use of chemical reactions in either a post or pre-column reactor[14].

The most obvious need in HPLC is a mass sensitive detector which has a good response to different classes of compounds. The purpose of this investigation is to develop such an LC detector based on ionization produced by a high flux of photons from a vacuum UV lamp. The high energy photons cause formation of ions within the detector cell. Once ions are formed, a polarizing voltage applied between two electrodes causes a current to flow within that circuit which can be measured by an electrometer. The current produced should be a linear function of solute concentration in the gas or vapor stream. This ionization method offers the possibility of high sensitivity with controlled selectivity by interchanging sources. Each source will produce a different threshold of ionization which increases the selectivity.

The fundamental physical process underlying the operation of all ionization detectors is the conduction of an electrical current by either a liquid or gas. In the liquid phase, however, ion-solvent interaction and the recombination reaction of the ion-electron pair formed by the photons from the vacuum UV lamp occurs more rapidly and thus greatly decreases the signal compared with a gas phase detector. The liquid phase version of the PID has been described in a recent publication[15].

Vapor Phase Detectors

The first application of photoionization to the detection of solutes in the evaporated effluent from an HPLC column was explored by Schmermund and Locke[16]. Photoionization in GC was described earlier in the literature. The use of a detector originally designed for GC in HPLC applications had not been explored prior to our work. Electrically charged atoms, molecules or free electrons can be detected in an inert gas such as helium or argon. Lovelock[17] studied photoionization as one of many methods which yield a sensitive technique for the detection of molecules in the gas phase. A source of ionization, such as a vacuum UV lamp, causes the specific ionization of gases and vapors with an ionization potential equal to or less than the energy of the lamp. Thus, photoionization occurs when an irradiated species absorbs a quantum of energy at the appropriate level and then undergoes an electronic transition to an ionized form. Ions produced at or above the threshold level are detectable with a current amplifier or electrometer in an appropriate polarized circuit. The first unit designed for a commercial application PID in GC was a device designed by Robinson and Brubaker[18].

These detectors were designed so that optimization involved not only the electrodes and ion chamber, but also the vacuum UV lamp. The original detectors used a lamp which was not sealed, but required a high vacuum system to provide a continuous flow of gas. The first PID designs were based on a direct connection between the compartment where photons were formed and the ionization chamber[19-27]. The required radiation in all of these detectors was produced using a glow discharge. Forming the electrical discharge required the careful regulation of several parameters including the separation of the electrodes, optimization of the acceleration voltage and discharge current. Thus, difficulties in the operation of the detector limited applications of the original designs.

Freeman[29] et al used a microwave discharge in high purity helium as a PID source. The purified helium at a reduced pressure of approximately 1 Torr resulted in a 21 eV ionization source. The advantage of using the helium discharge was that organic compounds and even some inorganic species could be detected. This line at 21 eV is capable of ionizing virtually any atomic or molecular species. The increased background current generated by the high energy output of the lamp lowers its sensitivity in relation to other PID detectors such as the argon lamp detector.

Sevcik[30] attempted the first separation of the VUV lamp from the sample compartment. The lamp, filled with a gas such as hydrogen at reduced pressure, was operated with a window of lithium fluoride which was transparent to 11.8 eV radiation. This system provided a source of photons with known energy and readily interchangeable sources. The original detectors suffered from lamp contamination and sputtering of the electrode material on the window surface, reducing the photon flux. Sensitivity decreased with a simultaneous decrease in the signal to noise ratio as the intensity of the radiation was attenuated. A similar design developed by Ostojic and Sternberg[31] using a sealed lamp as the source of ionizing photons showed an equivalent response to selected compounds. The VUV radiation was obtained from a mixture of hydrogen and argon covering the ionization range of 9.5 - 11.5 eV which could ionize practically all molecular species. The broad spectrum of molecular hydrogen is emitted, with the 121.5 nM Lyman-α line predominating. A 10 cm column of plasma within the sealed lamp was produced by circular electrodes approximately 1 cm in diameter and coaxial with the glass envelope of the lamp. A photon flux of 1×10^{10} photons/second was produced at a pressure of 1 Torr or less, when a current of 15-50 mA was applied. The use of deuterium instead of hydrogen increased the useful life of the lamp.

The next major advance in the development of the GC-PID was reported by Driscoll et al[32] in 1976. Subsequent publications reviewed the applications of this first truly practical, commercialized PID applied to specific GC separations[33-38]. The detector described in these articles was a very stable unit with a sealed lamp. A smaller cell volume with electrodes protected from direct illumination by the VUV lamp reduced the background noise. In addition, the high photon output increased ionization efficiency over previous designs and yielded a response better than the flame ionization detector for most organic compounds. The stable 10.2 eV lamp sealed to the ionization chamber and modified for high temperature operations resulted in a 100-fold increase in linear dynamic range: linearity was better than 10^7 and approached 10^8 with dilution of the solute. This range is larger than any other GC detector.

Design of the gas phase HPLC-PID evolved from the detectors of Sevcik and Ostojic[31] with special consideration given the requirement of HPLC detectors such as low cell volume and minimal mixing within the cell. Both the liquid and gas phase detectors were investigated, but quenching in the liquid phase, which is approximately 10^3 greater than in the gas phase, precluded a highly sensitive device for a great variety of compounds. The design, construction and operation of the gas phase HPLC-PID is described in detail in chapter 3 and 4.

The recent investigation by Krull et al[39] based on our original concept, has shown several additional applications. Their system vaporizes the total HPLC column effluent with subsequent detection using a PID manufactured by HNU Systems, (Newton, Massachussetts) founded by Driscoll[32-38]. Either the entire vaporized eluent or a fraction obtained by using a splitter was transferred to the high temperature PID (Model P-52). This HPLC-PID system was applied to a large number of organic compounds. A series of N-substituted aniline derivatives showed similar sensitivities when compared to data which we obtained on the original HPLC-PID[16]. Linearity extended over three orders of magnitude with the following detection limits: N, N' - dimethyl- aniline (20 pg), N-methylaniline (25 pg) and N,N'-diethylaniline (80 pg). In addition, this paper emphasized one of the major limitations of the HPLC-PID interface, which was the lower response caused by specific solvents and, in particular, most polar mobile phases such as methanol, acetonitrile and water. A summary of the characteristics is contained in Table I.

Table I

Gas Phase Photoionization Detectors

	Lovelock	Price	Freeman	Sevcik	Locke	Sternberg	Yamane	NHU	Schmermund& Locke
Ionization Efficiency	10^{-4}	10^{-3}	10^{-3}	1.6×10^{-4}	10^{-4}	5×10^{-5}	---	8×10^{-4}	10^{-6}
Background Current (A)	5×10^{-10}	2×10^{-10}	6×10^{-9}	9×10^{-11}	5×10^{-11}	3×10^{-11}	---	10×10^{-12}	1×10^{-11}
Linear Dynamic Range	10^{4}	10^{5}	10^{4}	10^{5}	10^{5}	10^{5}	10^{3}	10^{7}	10^{4}
Minimum Detectable Quantity (gm/sec)	---	1×10^{-12}	4×10^{-11}	2×10^{-12}	2×10^{-10}	3×10^{-10}	---	2×10^{-12}	1×10^{-11}
Noise (A)	---	10^{-3}	4×10^{-11}	3×10^{-13}	10^{-12}	5×10^{-13}	1.6×10^{-1}	2×10^{-14}	4×10^{-14}
Type Of Lamp	Ar	Ar	He	H_2	Ar	Ar, H_2	Ar	H_2	He, H_2
Sealed Lamp	No	No	No	Yes	No	Yes	No	Yes	Yes
Temperature Range	---	---	250	100	---	350	---	250	80

Liquid Phase Detectors

A brief description of the liquid phase system should help in the understanding of the evaluation of the HPLC-PID from the original concept. The liquid phase has specific limitations present in all condensed phases. The limitations are lower sensitivity because of rapid capturing of previously ionized species and a high background due to the conductivity of the mobile phase. The use of a one-photon ionization technique with incoherent light sources similar to the type used for the vapor phase detector was applied to a flowing liquid stream. The results of this study are contained in reference 15.

A laser two-photon technique has been explored by Yamada and Voigtman et al[41-44]. High-power tunable laser excitation sources exist and a pulsed laser source has been particularly advantageous because of its high luminosity resulting in a highly sensitive detector and good coherence for a small sample volume. Most of the systems discussed have been targeted for condensed ring systems which yield the highest sensitivity.

The laser-excited windowless flow cell was operated simultaneously in the fluorescence, photoacoustic, and two-photon modes. Voigtman[45] found that aqueous solutions did not cause significant interference for reverse-phase. It was also reported that the ionization efficiency was 10^{-2} compared with the liquid phase detector described in reference 15.

The New Detector: Initial Design Concepts

The initial design was evaluated for reverse-phase applications and two approaches were considered to make it more amenable to highly polar mobile phases usually containing a large percentage of water. The first was a lower flowrate which could be achieved by using microbore technology and the second was a column switching method. Microbore columns require a flowrate of 10-40 µl/min. and could reduce the total volume of evaporated solvent which flows through the detector. A preliminary study showed that attenuation of the response still existed with acetonitrile and methanol. In addition, the configuration of the flash-evaporator became crucial and a well-resolved mixture tended to blend together in the evaporation chamber, thus losing the benefits of microbore technology. Yet another problem was the inability to control flowrates accurately. Background noise in the detector varied with the flowrate, and caused tremendous changes in detection levels, if not totally obliterating the signal.

The adaptation of valve switching to HPLC has been quite successful. Therefore, the focus of this study was on the development of a valve switching system which could trap and concentrate the solute, followed by thermal desorption so that the solute could be converted into a vapor flowing into a GC-PID. A general system was considered for both normal and reverse-phase applications. This simple concept still requires complex instrumentation including a microprocessor to control the timing and sequencing of events. Applications in both normal and reverse-phase will be discussed and separations will be demonstrated.

Summary

A microprocessor-controlled system was developed which could be used for complex, even thermally unstable mixtures separated by any mode of HPLC. The system described in this thesis has the flexibility to be used with both normal and reverse-phase LC with only minor modifications. Examples of the application of each of these LC modes will be described in the following chapters.

References - Chapter 1

(1) Snyder, L.; Kirkland, J.; "Introduction to Modern Liquid Chromatography", 2nd John Wiley and Sons: New York, NY, 1979; Chapter 4.

(2) Drushel, Harry V.; J. Chrom. Sci., 21, 375 (1983).

(3) Kissinger, P.T.; Anal. Chem.; 49, 447A (1977).

(4) Kissinger, P.T.; Felice, L.J.; Miner, D.J.; Preddy, C.R.; Shoup, R.E.; "Contemporary Topics in Analytical and Clinical Chemistry", Vol. 2; Plenum: New York, NY, 1978

(5) Kissinger, P.T.; Felice, L.J.; Riggin, R.M.; Pachla, L.A.; Wenke, D.C.; Clin. Chem., 20, 992 (1974).

(6) Riggin, R.M.; Kissinger, P.T.; Anal. Chem., 49, 530 (1977).

(7) Popovich, D.J.; Dixon, J.B.; Ehrlich, B.J. J. Chrom. Sci., 17, 643 (1979).

(8) Mowery, R.A.; Juvet, R.S.; J. Chrom. Sci, 12, 687 (1974).

(9) Malcolme-Lawes, D.J.; Warwick, P.; Gifford, L.A.; J. Chromatogr., 176, 157 (1979).

(10) Malcolme-Lawes, D.J.; Anal. Proc., 19, 365 (1982).

(11) Birks, J.W.; Kuge, M.C.; Anal. Chem. 1980, 52, 897.

(12) Cope, M.J.; Anal. Proc., 17, 273 (1980).

(13) Henion, J.; Anal. Chem., 55, 2275 (1983)

(14) Lawrence, A.H.; Anal. Chem., 54, 2385 (1982)

(15) Locke, D.C.; Dhingra, B.S.; Baker, A.D.; Anal. Chem., 54, 447 (1982).

(16) Schmermund, J.T.; Locke, D.C., Anal. Lett., 619, (1975).

(17) Lovelock, J.E.; Nature, 188, 401. (1980)

(18) Robinson, C.F.; Brubaker, W.M.; U.S Patent 2,959,677, 1960.

(19) Roesler, J.F.; Anal. Chem., 36, 1900, (1964).

(20) Locke, D.C.; Meloan, C.E.; Anal. Chem., 37, 389 (1965).

(21) Yamane, M.; J. Chromatogr., 9, 162 (1962).

(22) Yamane, M.; J. Chromatogr., 11, 158 (1963).

(23) Yamane, M.; J. Chromatogr., 14, 355 (1964).

(24) Price, J.G.W.; Fenimore, D.C.; Simmonds, P.G.; Zalatkis, A.; Anal. Chem., 40, 541 (1968).

(25) Watanabe, K.; J. Chem. Phys., 26, 542 (1957).

(26) Lovelock, J.E.; Lipsky, S.R.; J. Am. Chem. Soc., 82, 431 (1960).

(27) Rosiek, J.; Gudowski, W.; LaSa, J.; Chem. Anal., 21, 1251 (1976).

(28) Freeman, R.R.; Wentworth, W.E.; Anal. Chem., 43, 1987 (1971).

(29) Sevcik, J.; Krysl, S.; Chromatographia, 6, 375 (1973).

(30) Ostojic, N.; Sternberg, Z.; Chromatographia, 7, 3 (1974).

(31) Driscoll, J.N.; Clarici, J.B.; Chromatographia, 9, 567 (1976).

(32) Jaramillo, L.F.; Driscoll, J.N.; J. High Res. Chromatogr. CC, 2, 536 (1979).

(33) Driscoll, J.N.; Spaziani, F.F.; Res./Dev., 27, 50 (1976).

(34) Driscoll, J.N.; Am. Lab, 8, 71 (1976).

(35) Driscoll, J.N.; Ford, J.; Jaramillo, L.F.; J. Chromatogr., 158, 171 (1978).

(36) Jaramillo, L.F.; Driscoll, J.N.; J. Chromatogr., 186, 637 (1979).

(37) Driscoll, J.N.; Marshall, J.K.; Jaramillo, L.F.; Hewitt, G.; Alongi, V.; Am. Lab, 12, 84 (1980).

(38) Kuang-Hua, Xie; Krull, I.S.; Pittsburgh Conference, Abst. No. 076, 1983.

(39) Yamada,; Koji, K.; Ogawa, T.; Bunseki Kagaku, 31, 247 (1982).

(40) Voightman, E.; Jurgensen, A.; Winefordner, J.D. Anal. Chem., 53, 1921 (1981).

(41) Voightman, E.; Winefordner, J.D.; Anal. Chem., 54, 1834 (1982).

(42) Lai, E.P.C.; Su, S.Y.; Voightman, E.; Winefordner, J.D.; Chromatographia, 15, 645 (1982).

(43) Voightman, E.; Winefordner, J.D.; J. Liq. Chrom., 5, 2113 (1982).

(44) Voightman, E.; Winefordner, J.D.; J. Liq. Chrom., 6, 1275 (1983).

Chapter 2

Theory of Photoionization and Detector Response

The absorption of high energy ultraviolet radiation by molecules sets off a complex series of processes. The photon-molecule interaction can lead to competing processes such as dissociation and ionization. Associated with these effects are predissociation and preionization caused by the presence of overlapping unstable potential curves in the same energy region[1]. Ionization of the molecule may also take place leaving the ion in an excited state, leading to the process of fluorescence as the ion decays to its own ionic ground state.

Preionization and Predissociation

Radiationless transitions may be expected when the overlapping of discrete energy levels by a continuous range of levels occurs as in the case of autoionization for atomic systems. However, for molecules, two processes can take place instead of the single autoionization process. Both processes give rise to the reduction of the lifetime of the discrete state and make themselves known by the broadening of the rotational lines in absorption and the breaking off of the bonds or their branches at definite rotational levels in emission. The processes are distinguished by the products of the radiationless transition.

The radiationless transition takes place either into an unstable state or into a stable state above the dissociation limit in the more familiar case. The net effect of the process is the disintegration of the molecule into atomic or molecular fragments; i.e., the molecule dissociates and the process is called predissociation. Thus, the absorption of a photon can lead to the population of an excited, stable molecular state from which there is the probability of a radiationless transition into an unstable state. The instability in turn gives rise to dissociation into fragments in either their ground or excited states. The end product consists of the molecular ion and an ejected electron and is analogous to the atomic case of autoionization in the other process. For this to occur in molecules, the stable discrete state has to lie adjacent to an ionic state (usually the lowest vibrational state of the ion) and the radiationless transition resulting in an ion plus an electron is called preionization. Observation of the process in absorption is possible only in the far ultraviolet, since the radiationless transition has to take place into an ionic state[2]. Predissociation, on the other hand, requires only that there be an adjacent unstable state for which the selection rules allow a reasonable probability of a radiationless transition. Effects of predissociation can, therefore, be observed in the near ultraviolet and in the vacuum ultraviolet (VUV).

Molecular Photoionization

Photoionization can be represented by:

$$R + h\nu \longrightarrow R^+ + e^-$$

This is a general equation showing the process for molecule R. The process is initiated by the absorption of a photon by the molecule. In general, if the molecule has an ionization potential equal to or less than the energy of the photon, photoionization can occur. The following reactions contribute to the ion current within the PID.

Reaction	Rate	
$AB + h\nu \longrightarrow AB^*$	$R_1 = I_a - I$	(1)
$AB^* \longrightarrow AB^+ + e^-$	$R_2 = K_2 [AB^*]$	(2)
$AB^* \longrightarrow A + B$	$R_3 = K_3 [AB^*]$	(3)
$e^- + \text{anode} \longrightarrow \text{current, } i$	$R_{4a} = K_{4a} [e^-]$	(4)
$AB^+ + \text{cathode} \longrightarrow AB$	$R_{4b} = K_{4b} [AB^+]$	(5)
$AB^+ + e^- + M \longrightarrow AB + M$	$R_5 = r [AB^+] [e^-]$	(6)
$AB^* + M \longrightarrow AB + M$	$R_6 = K_6 [AB^*] [M]$	(7)

Here, AB is an ionizable solute which is in the vaporized solvent and has a concentration [AB] and M is the vaporized solvent with concentration [M]. The initial photon flux is I_o and the number of photons absorbed per second is (I_o-I). This is equivalent to the number of moles of AB* produced per second since, in general, one photon excites one molecule. Equation 2 expresses the preionization and equation 3 the predissociation process. The rate constant for recombination of the positive ion and electron is r (equation 6).

When the absorption cross section (the probability that the excited state will ionize) of the photoionized molecule is considered, the rate for equation (1) can be rewritten as:

$$AB + h\nu \longrightarrow AB^*$$

$$R_1 = I_o\,(1-\exp\,[-\,\alpha\,[AB]\,L]) \quad . \qquad (8)$$

Where α is the absorption cross section, and L is the path length within the detector cell. A reduction or quenching of the photoion concentration occurs according to equations (6) and (7). An increase in these rates or the appearance of other removal mechanisms will consequently lead to increased quenching of the measured photocurrent for compounds which are photoionizable. Similarly, any decrease in these removal rates will enhance the PID response. The main concern in the detector design should, therefore, be a reduction in the competing removal rates.

Quenching Effects

Several other mechanisms also can occur to remove photoions before they can be measured. Driscoll[3] proposed a quenching reaction via electron capture. This can be explained as follows:

$$EC + e^- \longrightarrow EC^- \qquad R_7 = K_7 [e^-] [EC] \qquad (9)$$

$$EC^- + AB^+ \longrightarrow AB + EC \qquad R_8 = K_8 [EC^-] [AB^+] \qquad (10)$$

In these reactions, EC is a compound which can attach or capture an electron. The higher the concentration of EC, the greater the rate of equation 10, and in some cases can become much greater than R_6 and consequently increases the quenching of the PID signal. An example is the reduction of background current due to oxygen quenching. The positive ions produced by photoionization can be neutralized much more efficiently by O_2 than by e^- and a series of reactions which indicates this is:

$$e^- + O_2 \xrightarrow{k} O_{2-} \qquad (11)$$

$$e^- + AB^+ \xrightarrow{k2} AB \qquad (12)$$

$$O_{2-} + AB^+ \xrightarrow{k3} AB \qquad (13)$$

where k_3 and k_2 both will reduce the measured photoion current.

The vapors of several of the common polar mobile phases, such as acetonitrile, methanol, and isopropanol will cause this quenching effect. In some instances, solvents have a large electron-capture cross-section such as CCl_4, CH_2Cl_2 and other chlorinated hydrocarbons in general. For example, when a small plug of acetonitrile is evaporated into a flowing stream of n-hexane vapor, a large negative peak is noted when the acetonitrile elutes through the PID cell,. Also, dissolved air in the mobile phase will have a similar quenching effect on the detector response. The effect of CO_2 within the vapor phase causes a slight quenching of the PID response when compared with a carrier gas such as He which is transparent to virtually all wavelengths. Freedman[4] studied this quenching and concluded that about 30% was due to a reduction in the initial photon flux I_o, caused by the CO_2 absorption at 10.2 ev and the remainder caused by the CO_2 removing the photoions according to equation (7).

Absorption Cross-Section

It should be noted that some solvents that have a higher ionization potential than source energy can lower the detector response in a mode other than quenching. They absorb light and thus decrease I_o. In table II, it can be seen that methane, ethane, and other hydrocarbons have a significant absorption coefficient at 10.2 eV compared with negligible values for both argon and helium. Even so, argon is preferable as PID carrier gas since it minimizes the PID ion removal processes; consequently an argon carrier gas provides at least a 40% greater response than nitrogen. This difference is apparently due to the increased drift velocity of the electrons in argon compared to nitrogen[5]. The increased electron drift velocity enhances the collection of the electrons by the PID and also minimizes the recombination of the photoions and electrons caused by the decreased electron concentration.

Table II

Ionization Potentials and Absorption Coefficients for Various Gases and Vapors

Ionization Potentials

Gas or Vapor	Ionization Potential (ev)	Absorption Coefficient 10.2 ev (cm^{-})
Methane	12.6	400
Ethane	11.65	550
Propane	11.07	1592
n-Butane	10.63	2531
n-Pentane	10.35	2909
n-Hexane	10.18	3531
n-Heptane	10.08	3851
Argon	15.67	negligible
Helium	24.58	negligible

Absorption of Photons in the PID cell

The probability that a photon will be absorbed by a solute within the PID cell depends upon the absorption cross-section of the substance, r. In terms of the Beer-Lambert law,

$$I = I_o \exp(-\sigma N [AB] L) \qquad (14)$$

where N is Avogadro's number and L is the pathlength of the cell. The probability that the excited state will ionize as defined in equation 2 will depend upon the photoionization efficiency, n, where

$$n = \frac{K_2}{K_2 + K_3 + K_6} \qquad (15)$$

If steady state conditions are assumed, the formation rate of AB* (the excited state) will equal its rate of removal. Therefore, combining equations 1, 2 and 6,

$$I_o - I = K_2 [AB^*] + K_3 [AB^*] + K_6 [AB^*] [M] \qquad (16)$$

Since the concentration of M should be in such large excess, the [M] $\simeq$ 1 and equation (16) becomes:

$$I_o - I = [AB^*] [K_2 + K_3 + K_6] \qquad (17)$$

Recombination reaction (6) can be suppressed with high voltage applied to the electrodes of the cell to "pull" the ions apart, in which case the rate of ion formation equals the rate of ion collection, and

$$K_4 [AB^+] = K_2 [AB^*] \qquad (18)$$

$$I_a - I = \frac{K_4(AB+)K_2+K_3+K_6)}{K_2} = \frac{(K_4(AB+)(K_2+K_3+K_6)}{n} \qquad (19)$$

Substitution into equation (17) gives:

$$I_o - I = K_4 [AB^+] \frac{K_2 + K_3 + K_6}{K_2} = K_4 [AB^+] \frac{1}{\eta}$$

and thus,

$$I_o - I = \frac{i}{F} \frac{1}{\eta} \qquad (21)$$

where i is the ion current which is amplified to give the PID signal and F is the Faraday.

Combining the expression for the Beer-Lambert law (eqn.14) and equation (20),

$$I_o - I = I_o [\, 1-\exp (-r\, NL\, [AB])] = \frac{i}{Fn} \qquad (22)$$

Freedman[6] expanded this function in a Taylor series and neglected all terms with exponents greater than unity, to yield

$$i = I_o\, F\, n\, r\, NL\, [AB] \qquad (23)$$

Thus, in a specific experimental system, the response of the detector is proportional to ionization efficiency, absorption cross-section and molar concentration. The product $r\eta$ is the photoionization cross section, r_i which expresses the probability that a molecule will both absorb a photon and ionize from the resulting excited state. It has been attempted to calculate molecular photoionization cross-sections[7]. These calculations are complex, but show that the photoionization cross section depends directly on the photon energy and ionization potential. When the PID is considered using a photoionizable species AB, equation (22) can be rewritten as:

$$\frac{i}{[AB]} = I_o F n r NL = K r n \qquad (24)$$

where $K = I_o FNL$ is a proportionality constant which is fixed by the PID, therefore,

$$\frac{i}{[AB]} Kri + R \qquad (25)$$

where R is the molar response.

These factors, which influence the signal produced by the detector, have been considered by Sevick, et al[8], Freedman[4,6], Senum[9], Casida[10] and Driscoll[6,7].

Relative detector sensitivities were investigated using a wide variety of organic compounds and calculating the results on the basis of molar sensitivity relative to benzene (in a paper published by Langhorst[13]). The equation which was used is as follows:

$$SM = \frac{A}{A\,(B_z)} \quad \frac{B\,(Bz)}{B} \qquad (26)$$

where A is the peak area of the compound of interest, A (Bz) is the peak area of a benzene sample, B is the molar concentration of the compound of interest (millimoles/ml) in a non-photoionizable solvent and B (Bz) is the molar concentration of the benzene standard solution (millimoles/ml).

The relative sensitivity normalized to benzene on a weight basis is calculated using the following equation.

$$S = \frac{A}{A\,(Bz)} \quad \frac{C\,(Bz)}{C} \qquad (27)$$

where C is the concentration of the compound under analysis (μg ml) and $C_{(Bz)}$ is the concentration of benzene in standard solution (μg ml)

Table III

Molar Sensitivity of Typical HPLC Solvents Relative to Benzene

COMPOUND	IONIZATION POTENTIAL (eV)	MOLAR SENSITIVITY RELATIVE TO BENZENE SM (B_z)
n-pentane	10.35	0.021
n-hexane	10.18	0.032
n-heptane	10.08	0.075
2,2,4-Trimethylpentane	9.84	0.080
Cyclohexane	9.88	0.18
Diethylether	9.53	0.36
Tetrahydrofuran	9.45	0.39
Methylene Chloride	11.35	0.015
Ethyl Acetate	10.15	0.020

It can be seen from the data for alkanes that the sensitivity of the detector response increases as carbon number increases. Langhorst[13] concluded that for n-alkanes a linear relationship exists which is related to carbon number and can be expressed as

$$SM = 0.715\ n - 0.475 \qquad (28)$$

where SM is the molar sensitivity relative to benzene and n is the carbon number.

Perhaps the most important conclusion to be drawn from Table III is that even compounds which have ionization potentials above the source energy will produce a photocurrent. Two factors are important and will cause species to photoionize between 10.2 and 10.9 eV, the upper limit of transmission for the standard magnesium fluoride windows used on the HNU detector VUV lamps. The energy gap between molecules in excited vibrational states and the ground state of the ion can be up to 0.4 eV less than the ionization potential of the molecule.

In addition, impurities in the lamp can give rise to other emission bands between 10.2 and 10.9 eV. These two factors will cause species with ionization potentials between 10.2 and 10.9 eV to give a small PID response. The actual response will depend on such factors as voltage applied to the electrodes, the lamp window and gas used to fill the particular lamp.

The removal of the mobile phase vapor prior to detection of the solute is essential to achieve low detection limits particularly in trace analysis since even low levels of solvent vapor will decrease the response. The detector discussed in Chapters 5 and 6 was designed to overcome lower response caused by attenuation of photons and background photocurrent from the solvent.

References Chapter 2

(1) Mann, Geoffrey V.; "Photoionization Processes in Gases", Wiley: New York, NY, 1961.

(2) Sampson, J.A.R.; "Vacuum Ultraviolet Spectrophotometry", Wiley: New York, NY, 1959.

(3) Driscoll, J.N.;J. Chromatogr. Sci., 134, 49 (1977).

(4) Freedman, A.; J. Chromatogr., 190, 263 (1980).

(5) Kaye, G.W.C.; Laby, T.H.; "Tables of Physical and Chemical Constants", Wiley, New York, NY, 1959

(6) Freedman, A.; J. Chromatogr., 236, 11 (1982).

(7) Schweig, A.; Thiel, W.; J. Chem. Phys., 60, 951 (1974).

(8) Sevcik, J.; Krysl, S.; Chromatographia, 6, 375 (1973).

(9) Senum, G.I.; J. Chromatogr., 205, 413 (1981).

(10) Casida, M.E.; Casida, K.C.; J. Chromatogr., 200, 35 (1980).

(11) Driscoll, J.N.; J. Chromatogr. Sci., 20, 91 (1982).

(12) Jaramillo, L.; Driscoll, J.N.; J. Chromatogr., 186, 637 (1979).

(13) Langhorst, M.; J. Chromatogr. Sci., 19, 98 (1981).

Chapter 3

Design of the Original HPLC - PID

The original design of an HPLC-PID required vaporization of the total effluent from the column, which was then exposed to high energy vacuum UV photons from a discharge lamp. The solute, which was photoionized by a source less energetic than required to photoionize the mobile phase, produced ions in proportion to the absolute concentration. The current flowing within the cell through polarized electrodes was amplified and the resulting current produced was linearly related to the solute concentration. This chapter considers the design and construction of that PID and its experimental parameters.

Ionization Chamber

The detector was constructed of an ionization chamber with collector electrodes, and a replaceable vacuum UV lamp. Interchangeable lamps are desirable because of the energy-selectivity which can be achieved and because of the ease of cleaning the window separating the ion chamber and reduced pressure area containing the gas mixtures. Several materials were investigated for the ion chamber. Primary conditions included stability at elevated temperature, a high dielectric constant, superior thermal and electrical insulating properties and chemical resistance.

The material which exhibited the best properties (Table IV) was polytetrafluoroethylene (TFE), the most common form of Teflon®. This material can be machined, but requires special precautions to obtain a smooth finish to prevent leakage from the cell.

A TFE rod, one inch (1") in diameter, was selected to provide the correct dimensions for the ion chamber. A cylindrical hole was machined to accept a gold coated electrode which was press-fitted into the Teflon® cylinder. The gold plating increased conductivity while also increasing chemical resistance. Vapors from the LC mobile phase created corrosion problems with all but the most chemically resistant materials. Since the coefficient of expansion (Table IV) of the Teflon® is high, the Teflon® cylinder was heated to approximately 200°C and the electrode was readily inserted into the bored-out cavity. Electrical connection was made to the power supply (Harrison Model 6515) using Belden 8240 RG 58/U shielded cable. This cable was used for all of the electrical connections. Electrical leads were kept as short as possible to reduce noise and electrical pickup from Radio Frequency Interference (RFI) and Electromagnetic Interference (EMI) sources. The collector voltage was generally set at 1000 volts, although variations between 500 and 1500 volts gave little variation in observed current. However, the higher the voltage, the greater the risk of arcing between the electrodes in the cell.

Properties of Fluorocarbons

Type	Polytrifluoro-chlorocthylene (PTFCE)"Kel-F"	Polytetrafluoro-ethylene (PTFE)	Fluorinated ethylene propylene (FEP)
PHYSICAL PROPERTIES			
Specific Gravity	2.10 - 2.15	2.1 - 2.3	2.14 - 2.17
Ther Cond, BTu/hr/sq.ft./of/ft.	0.145	0.14	0.12
Coef of Ther. Exp., per° F x 10^{-5}	3.99	7.5 - 8.4	5.3 - 10.7
Water Absorption (24 hr.), %	0.00	0.01	0.01
MECHANICAL PROPERTIES			
Hardness (Rockwell)	R110 - 115	R35 - 55	30 - 45
Elongation (in Zin), %	125 - 175	250 - 350	250 - 330
ELECTRICAL PROPERTIES			
Volume Resisitivity, ohm-cm	10^{18}	10^{18}	2×10^{18}
Detectric Constant			
60 cycles	2.6 - 2.7	2.1	2.1
10^{6} cycles	2.30 - 2.37	2.1	2.1
HEAT RESISTANCE			
Max. Rec. Svc. Temp., F	380	550	400

The gold-plated brass electrode had a 3 mm diameter hole drilled through the body. A tungsten inner electrode 1 mm in diameter was positioned concentrically within the outer electrode and held in place with Teflon® spacers. The positioning of the electrodes within the detector assembly reduced the intensity of ionizing UV radiation passing down the axes of the concentric electrodes, thus reducing the background signal. In addition, the close proximity of the electrodes to the window maximized the photocurrent which was generated. Radiation in this range is rapidly attenuated as discussed in Chapter 2.

Tungsten has a high work function and is mechanically strong, with high chemical resistance. However, obtaining a good electrical connection to the tungsten rod was difficult since conventional soldering methods are ineffective. A spot-weld provided both mechanical strength and a good electrical contact.

VUV Lamp Designs

Perhaps the most crucial component of the detector assembly is the vacuum UV lamp. Most of the commercial sealed lamps constructed for PID units contain a mixture of hydrogen and argon which produces an output in the 9.5 - 11.5 eV range, covering the ionization energy of practically all organic molecular species which would be separated by a GC column.

Similarly, rare gas discharge lamps with lower output energies provide selectivity, when a mobile phase contains a component with a low photoionization potential. The desirable characteristics of a lamp include a photon discharge of 10^{10} photons/second for greater ionization efficiency, high output stability and a long lamp life.

Several designs were considered based on the papers by Sevcik[1] et at and Ostojic et al[7]. The study included the following parameters, all of which had to be optimized:

1) The size, shape, geometry and materials used to construct the lamp electrodes.

2) The configuration of the area in which the plasma is formed, and a suitable material of construction or cooling technique to withstand high internal temperatures.

3) A window which transmits selected wavelengths, and a method for attaching the window to the lamp while retaining the vacuum seal.

Numerous articles describe the construction of rare gas light sources for the vacuum ultraviolet. Most of this development work which was performed because of a recent renewed interest in vacuum ultraviolet adsorption spectroscopy and molecular photoionization, has greatly stimulated development of rare gas lamps with emission continua. All of the rare gases, when properly excited, emit continuous spectra with little structure except for a few emission lines which prove useful as wavelength standards. Either a condensed discharge or a microwave discharge may be used to excite such continua with useful intensities, although the mechanisms and the spectral characteristics may be different.

Table V

Pressure and Operating Conditions of Vacuum UV Lamps

Gas	Pressure (Torr)	Wavelength (A°)	Energy (eV)
Kr	0.1	1235.8	10.03
Xe	0.1	1295.6	9.57
H_2:He (10:90%)	0.1-1.0	1216.0	10.30

The lower wavelength values for a rare gas continuum depend on the operating pressure of the lamp. The experimental design of the lamp used for the PID requires the investigation of materials suitable for high temperature operation and which would contribute essentially no contamination of gas within the lamp. The initial design consisted of an aluminum housing as one electrode with a pyrex glass tube and Kovar® metal cylinder at the opposite end (Figure 1). This configuration allowed the easy installation of a window without using an all glass lamp. After several attempts, however, the idea was abandoned because of lamp contamination and sputtering of metal on the window surface.

An all glass lamp was constructed using a 2 mm quartz inner tube with the electrodes sealed into pyrex glass. The first lamp utilized a water-cooled jacket which cracked after several hours of use so that the final design (Figure 2) was an air-cooled lamp. A high vacuum filling system was constructed to control the pressure and filling of the lamp prior to sealing. A block diagram is shown in Figure 3.

Spectral Characteristics of Lamps

The main vacuum ultraviolet emission continua excited by a condensed discharge (at pressure of 0.1 - 10 torr) are: He, 600-100 A°; Ne, 744-1000 A°; Ar, 1070-1650 A°; Kr, 1250-1850 A°; Xe, 1470-2250 A°[3].

However, when the excitation is carried out at higher pressures (200 mm - 600 mm), additional strong emission continua appear at longer wavelengths. For example, the helium continuum extends to 4000 A°, and the krypton, argon and xenon continua extend to above 3000 A°. It is also possible to blend mixtures of rare gases to produce more intense line sources, but extension of the continua is not feasible since mixtures of rare gases produce an output corresponding to the gas with the lowest ionization potential. Thus, a mixture of xenon and krypton will not produce a continuum extending from 1260 A° to 2250 A° because the ionization potential of xenon (12.13 eV) is less than that of krypton (13.97 eV); consequently, the emission produced by a mixture of e.g. 99.98% krypton and only 0.02% xenon, is largely xenon emission and no krypton emission whatsoever[4]. Similarly, in a mixture of argon (15.76 eV) and xenon, only the xenon continuum appears. Likewise, in a mixture of argon and krypton, only the krypton continuum will appear[5]. In the case of hydrogen, the so-called Lyman-α line at 1216 A° is the ionizing wavelength of interest and is intensified when a 10:90% mixture of hydrogen and helium is used. Pressure and operating conditions are given in Table IV.

Figure 1

Metal-Glass Vacuum UV Lamp

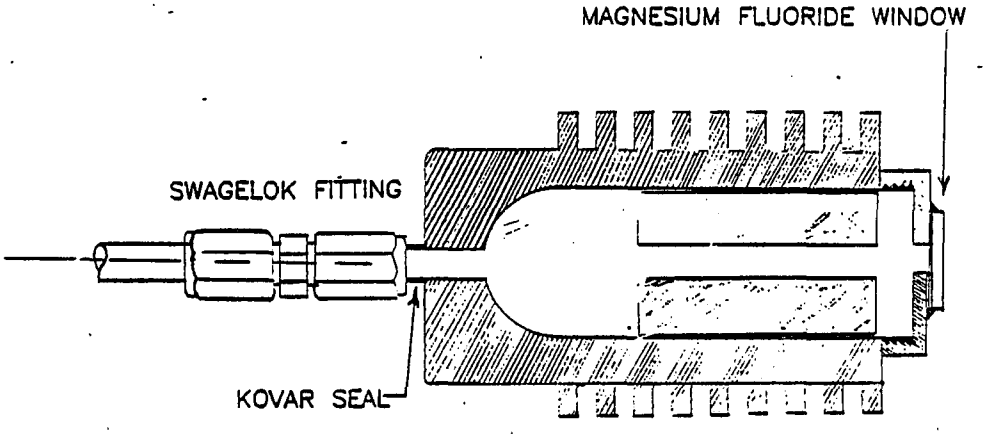
MAGNESIUM FLUORIDE WINDOW
SWAGELOK FITTING
KOVAR SEAL

Figure 2

Glass UV Lamp and Detector Assembly

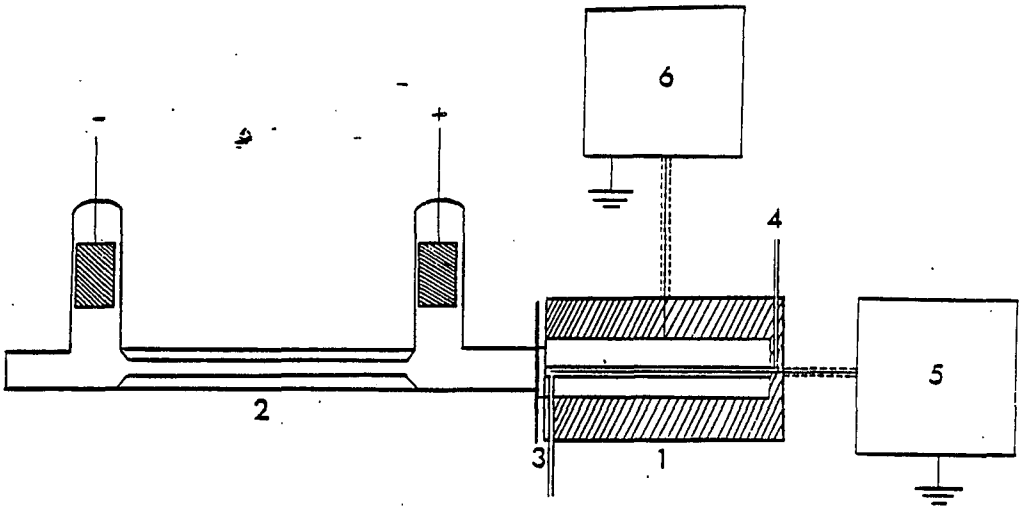

1. Teflon detector block
2. VUV lamp
3. Vapor inlet
4. Vapor outlet
5. Electrometer
6. Detector power supply

VACUUM UV LAMP AND DETECTOR ASSEMBLY

Figure 3

High-Vacuum Lamp Filling System

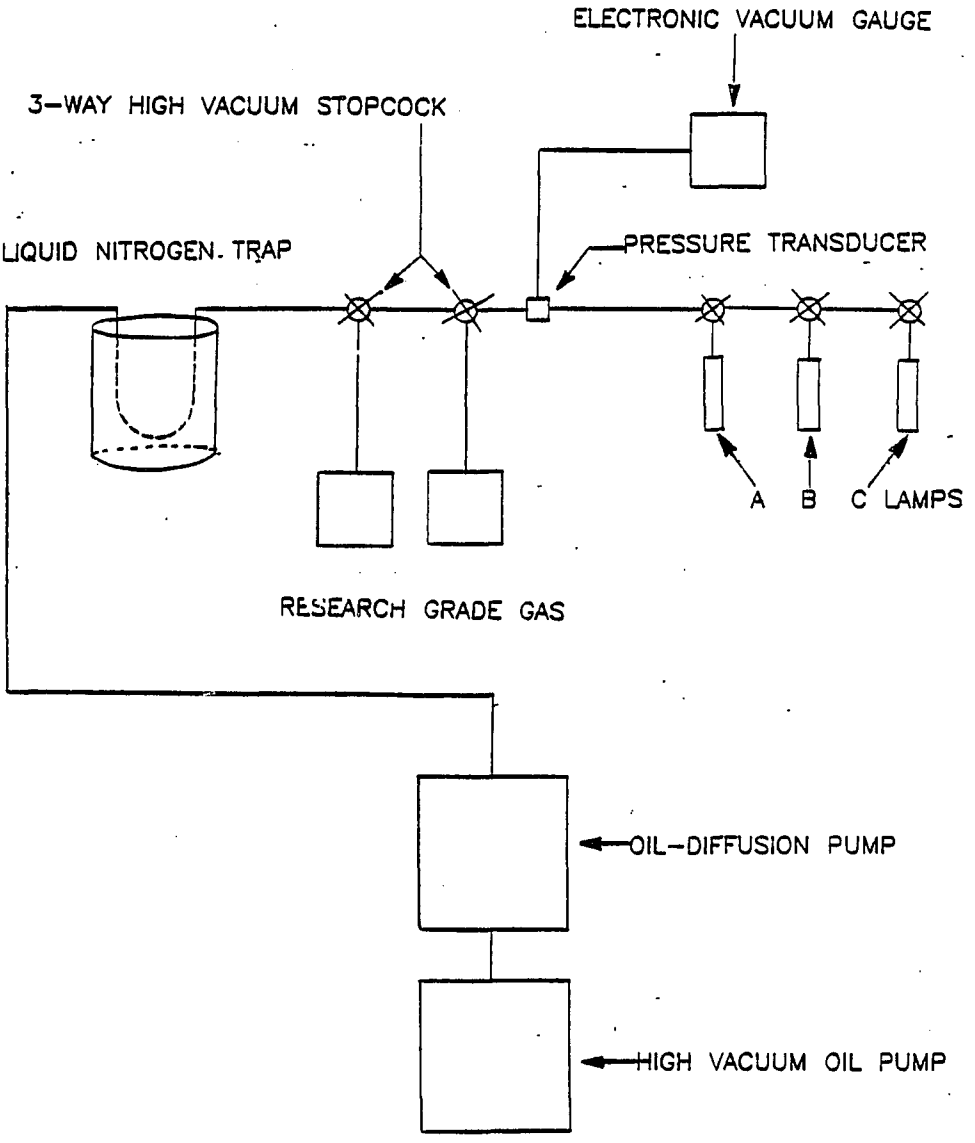

HIGH-VACUUM LAMP FILLING STATION

The filling procedure consisted of initially baking the lamp at 200°C for 24 hours, then removing the assembly and attaching it to point A in Figure 3. The 3-way stopcock was opened and the pressure inside the glass envelope was decreased to 10^{-6} Torr and held at that pressure for at least 6 hours while the glass envelope of the lamp was heated occasionally with a flame to remove traces of moisture or entrapped gases. The stopcock at point B was rotated to slowly allow either of the filling gases to enter the lamp. The needle valve control was operated to allow the high vacuum pump to gradually reduce the pressure within the lamp while monitoring the decrease on the electronic vacuum gauge. The quality of the lamp was checked by initiating a DC discharge and operating the lamp for one hour to determine if the discharge color varied. For example, a krypton lamp, used most frequently because of its spectral output, normally had a white to slighly-blue color. When an air leak was present, the color changed to a deep blue and gradually the discharge was extinguished. Research grade gases (Union Carbide, Linden, N.J.) were required because of trace nitrogen present in other commercial grades.

The lamp power supply was a Power Designs Pacific Model HV 1545 with variable voltage from 0-5000 volts at 20 mA with the negative terminal at ground potential. Filling pressures are specified in Table IV. A voltage greater than 2000 volts was usually required to initiate and sustain a discharge. The lamp discharge also could be initiated by using a Tesla coil.

Window Materials

Selection of a suitable window material must be based on several parameters including:

1) The spectral cut-off.
2) Stability to VUV and mechanical strength.
3) Inertness when exposed to solute and mobile phase vapors at elevated temperatures.
4) Transmittance of the crystal.

The most commonly used window materials include LiF, MgF_2, CaF_2, BaF_2 and synthetic sapphire ($\alpha A l_2 O_3$). Thus, the useful number of solid materials in the vacuum UV region is extremely limited and consists mainly of the alkaline earth fluorides.

The selection of the crystal should be made in conjunction with the rare gas used in the discharge lamp so that the crystal is transparent to the radiation of interest, but filters out extraneous wavelengths. The krypton and xenon lamp were utilized most frequently because of the types of compounds which were photoionized in conjunction with the mobile phase.

In general, the krypton lamp serves as the best compromise. Therefore, either a lithium fluoride or magnesium fluoride window is the most appropriate considering the respective cut-off wavelengths of all the available crystals (Table VI). These data, which represent 25°C conditions are not strictly true under the operating conditions of the PID cell, because temperature has a significant effect on the transmission properties of the crystals.

A decrease in transmission is observed when the temperature increases. In addition, a rather sudden decrease in transmittance, commencing at 1100 A° (11.2 eV) in LiF, is attributed to excitation to the first excitation level whose maximum appears at 12.0 eV at the maximum, the transmittance below 1050 A° will be virtually zero for anything other than a thin film.

Table VI

Transmission of Window Materials in the Vacuum UV Region

Window Material	Wavelength of 50% Transmission of Window Materials (A°)
Lithium Fluoride (LiF)	1125
Magnesium Fluoride (MgF_2)	1110
Calcium Fluoride (CaF_2)	1235
Barium Fluoride (BaF_2)	1550
Sapphire (α-Al_2O_3)	1600

The observed decrease in transmittance of the other crystals is presumably due to similar optical transitions. Since a variation in binding energy occurs with ionic size, as the ions in the crystal become larger, the absorption peaks are shifted to lower energy for similar crystal structures. This is observed in the short-wavelength transmittance for the four alkaline earth fluorides.

Window-to-Lamp Seal

In our lamp design, the window is sealed directly to the glass housing of the lamp. Several types of cement were investigated to obtain a fast drying seal which would not be influenced by the high energy photons emitted from the lamp. After investigating epoxy, silver chloride and high temperature waxes, Apiezon W vacuum wax was selected because it was easy to apply and a vacuum-tight seal was obtained in all cases. The one disadvantage was that the maximum temperature of the detector electrodes was 80°C due to the melting point of the wax.

Vaporization Chamber

The effluent from the column was completely vaporized at a high temperature prior to flowing into the PID detector. A GC injection port was connected to the end of the LC column with 1/16 in. x 0.010 in 316 stainless steel tubing, using the shortest possible length. The design of the heater assembly is detailed in Figure 4. The optimal length was 10 cm with minimal dead volume. A variable voltage transformer connected to a 50 watt cartridge heater maintained the temperature at 300°C . A thermocouple continously monitored the temperature. The chief limitation of this detector design was to maintain a temperature high enough to produce constant vaporization but to avoid excessive temperatures which cause extensive pyrolysis of both samples and mobile phase, causing deposition of breakdown products on the window. Thus, solutes boiling higher than 300°C, high molecular weight materials, polymers, ionics and other nonvaporizable materials are not amemmable to this design.

Figure 4

Vaporization Oven

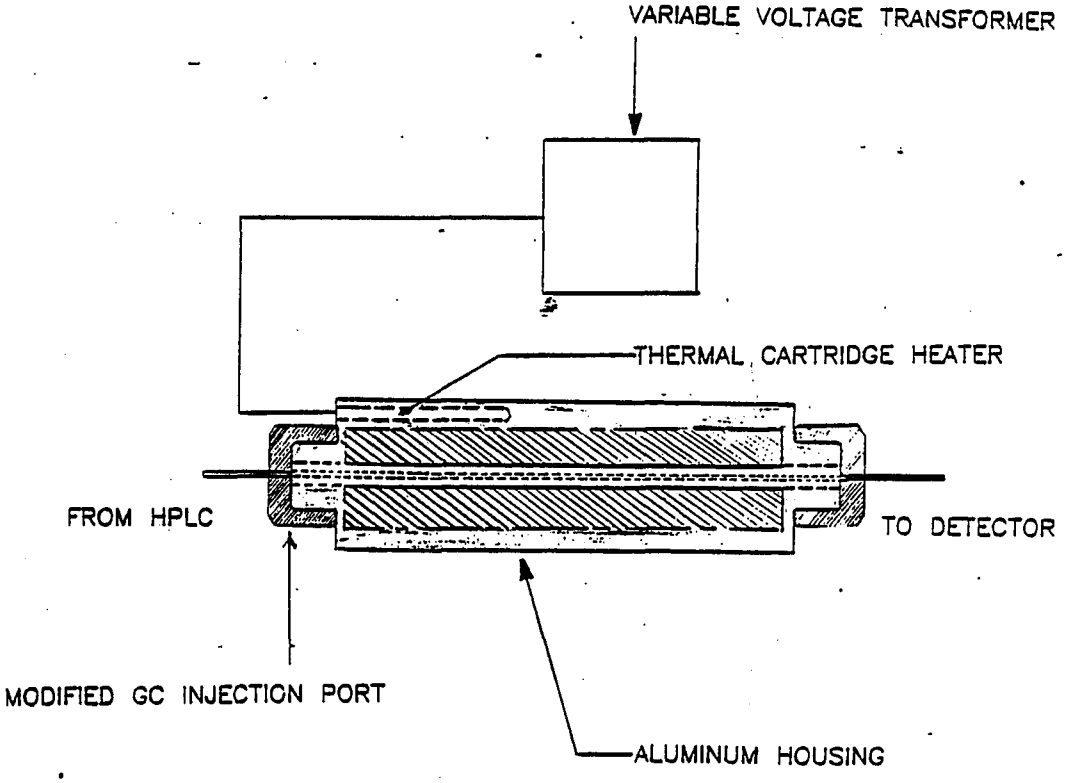

VAPORIZATION INTERFACE OVEN

Detector Parameters

The detector was evaluated using p-methylaniline which had an optimum retention time and also responded well at 254 nm in the U V. The krypton lamp was selected since it was stable and did not cause photoionization of most common mobile phases. Separation of substituted anilines was achieved using a pentane mobile phase modified with 0.5% methanol. The low boiling point of these solvents allowed easy vaporization.

1. Minimum Detectable Quantity (MDQ)

This value may be determined by several methods, including injection of known volumes at known solute concentrations or by using an exponential dilution flask. The value in table I was determined by the former method. Measured volumes of solutions of known concentration were injected into a short column packed with glass beads. Thus, retention was due only to the void volume of the column, but allowed the detector to see sharp, gaussian chromatographic peaks. Peak areas were converted to units of coulombs from the known sensitivities of the electrometer and recorder.

The peak noise level of the detector system was determined similarly from the recorder output (using a Honeywell 193) to be about 4×10^{-14} A. The mass flowrate of p-methylaniline producing a peak twice the noise level was taken to be the MDQ and was approximately 1×10^{-11} gm/sec. This value agrees with data published by HNU systems for the Model P52 detector.

Linear Dynamic Range (LDR)

The linear dynamic range indicates the range of sample concentrations that can be injected into the detector and produce a linear response. The value for our detector was determined by plotting the current versus sample weight values on log-log paper. A line of unit slope was obtained from MDQ to at least 10^{-6} grams/second, i.e. yielding an LDR of 10^{5}.

Ionization Efficiency (IE)

The detector sensitivity was found as above to be 1 x 10^{-3} coulombs/gram for p-methylaniline, or almost 0.1 coulombs/mole. If complete ionization of a mole of solute could occur, 10^{5} coulombs would result and thus the ionization efficiency is about 10^{-6}. This value is lower than those shown in Table I, Chapter 1 and is probably due to a less intense VUV lamp. A microwave discharge has been reported to produce 10^{17} photons/second as compared with a maximum of 10^{9} photons/second from a continuous DC discharge[4]. Obviously, this is a major improvement which could be made.

Background Current

This value, about 10^{-11}, is backed out with the electrometer (Keithley 610B) which measures the current flowing within the detector cell.

Relative Response

Any absorbing molecules with an ionization potential less than the energy of the absorbed photon can in principle be ionized. Molecules with higher ionization potentials have zero ionization cross-sections, and should generally be transparent in the vacuum UV. Fortuitously, most common solvents used as HPLC eluents have ionization potentials exceeding the energy of photons from rare gas discharges, while most solutes which would be separated by LC are more easily ionized. Table VII lists several of these solvents and their ionization potentials.

Table VII

Ionization Potentials of LC Solvents

Solvent	IP (eV)	Solvent	IP (eV)	Solvent	IP (eV)
n-pentane	10.35	Benzene	9.23	MeOAc	10.24
Hexane	10.18	Ethyl Ether	9.55	MeCN	12.20
Isooctane	9.84	$CHCl_3$	11.42	i-PrOH	10.09
n-Decane	10.19	CH_2Cl_2	11.35	n-PrOH	10.15
Cyclohexane	9.88	THF	9.45	ETOH	10.50
CS_2	10.08	Acetone	9.69	HOAc	10.36
$n\text{-}C_4H_9Cl$	10.67	Dioxane	9.56	H_2O	12.59

Solvents evaluated include n-pentane, diethyl ether, methanol, and their mixtures. No signal was obtained for these solvents. In this detector design, Apiezon W is used to seal the MgF_2 window to the discharge tube. The detector temperature consequently cannot exceed about 80°C. Solvents boiling at temperatures higher than this, such as acetonitrile, condense in the detector and short out the electrodes. However, the introduction of solutions of acetonitrile in pentane to the detector gave no signal, indicating the compatability of this useful solvent with the photoionization detector but as noted before, quenching of other signals will occur. Similarly, water is not detected although MgF_2 windows are required to prevent steam-etching.

Numerous substituted anilines, aromatic hydrocarbons, chlorinated compounds and oxygenated compounds as solutions in pentane/methanol mixtures have been tested in the detector. All solutes with ionization potentials less than the source excitation energy gave signals of roughly the same order of magnitude.

References Chapter 3

(1) Pruett, Kenneth; "Compass Corrosion Guide", Technical Publications: La Mesa, CA, 1978, Section 3.

(2) Tanaka, Y,; J. Opt. Soc. Am., 45, 710 (1955).

(3) Tanaka, Y,; Jursa, A.S.; Le Blanc, F.T.; J. Opt. Soc. Am., 48, 304 (1958).

(4) Wilkinson, P.G.; J. Opt. Soc. Am., 45, 1044 (1955).

(5) Tanaka, Y,; Jursa, A.S.; J. Opt. Soc. Am., 50, 1118 (1960).

(6) Duncanson, A.; Stevenson, R.W.H.; Proc. Phys. Soc., 72, 1001 (1958).

Chapter 4

Applications of the Original HPLC-PID[1]

The packing originally selected for our HPLC study was Corasil I and II manufactured by Waters Associates, Inc. This silica was selected since, at the time of the study, it was one of the best silica gel porous layer beads available. The Corasils are spherical particles consisting of a solid glass core 37-50 μ min diameter coated with either a single or double layer of fine silica particles[2]. The nitrogen surface areas are about 7 m^2/g for Corasil I and 14 m^2/mg for Corasil II[3]. The higher surface area of Corasil II allows its use as a relatively weak adsorbent, as well as a support, like Corasil I for bonding. Initial work also involved Porasil, a series of spherical silica beads of different but controlled average pore sizes (100-1500A) and surface areas (1.5 - 480 m^2/g). They can be used as solid adsorbent supports for bonded phases and also for gel permeation chromatography involving the separation of polymers[4]. Their extremely high porosity restricted their use in HPLC so that the bonded phases were evaluated by GC. Another porous layer bead utilized in the HPLC bonded phases was Vydac, manufactured by the Separations Group[5].

This is a high efficiency, spherical core-porous siliceous surface material of carefully controlled particle size in the 30-44 μm range, with a free fall density of 1.4 g/cc, and of low, homogeneous surface activity. The nitrogen surface area is 12 m^2/g and the average pore size is 57 A° in diameter[5]. The deactivation of residual hydroxyl groups on silica surfaces has been well established[6,7].Silanes such as DMCS and trimethylchlorosilane will react with the residual hydroxyl groups to "end-cap" a column or deactivate the surface. It is also possible to take advantage of the reactivity of the surface hydroxyl groups of silicas to synthesize chemically bonded phases for chromatography. There are three types of reactions which can be performed on the silica surface: esterification, reaction with an organo-chlorosilane, and chlorination followed by treatment with an organometallic.

Slurry Packing Apparatus

The apparatus used to pack columns in a down flow orientation is shown in Figure 6. The column blank (2.1 mm x 1 m, 316SS) was throughly cleaned by scrubbing the interior walls with a hot detergent solution (Micro Laboratory Solvent) using a long pipe cleaner, and then rinsed first with distilled water for several minutes followed by a series of organic solvents including methanol, acetone and chloroform before drying with nitrogen. A porous frit was attached with swagelok fittings to the outlet of the column and the column was filled with the same liquid mixture used to suspend the packing material. Slurries containing approximately 20% (by weight) of the packing material were prepared and degassed using an ultrasonic bath. The slurry was added to the reservoir (3/8" OD tubing), and pressurized with a Whitey high pressure pump (Whitey Engineering, Inc). The slurry was pumped rapidly into the column blank at the highest possible pressure (3000 psi) to produce the best column performance.

Figure 5

Slurry Packing Apparatus

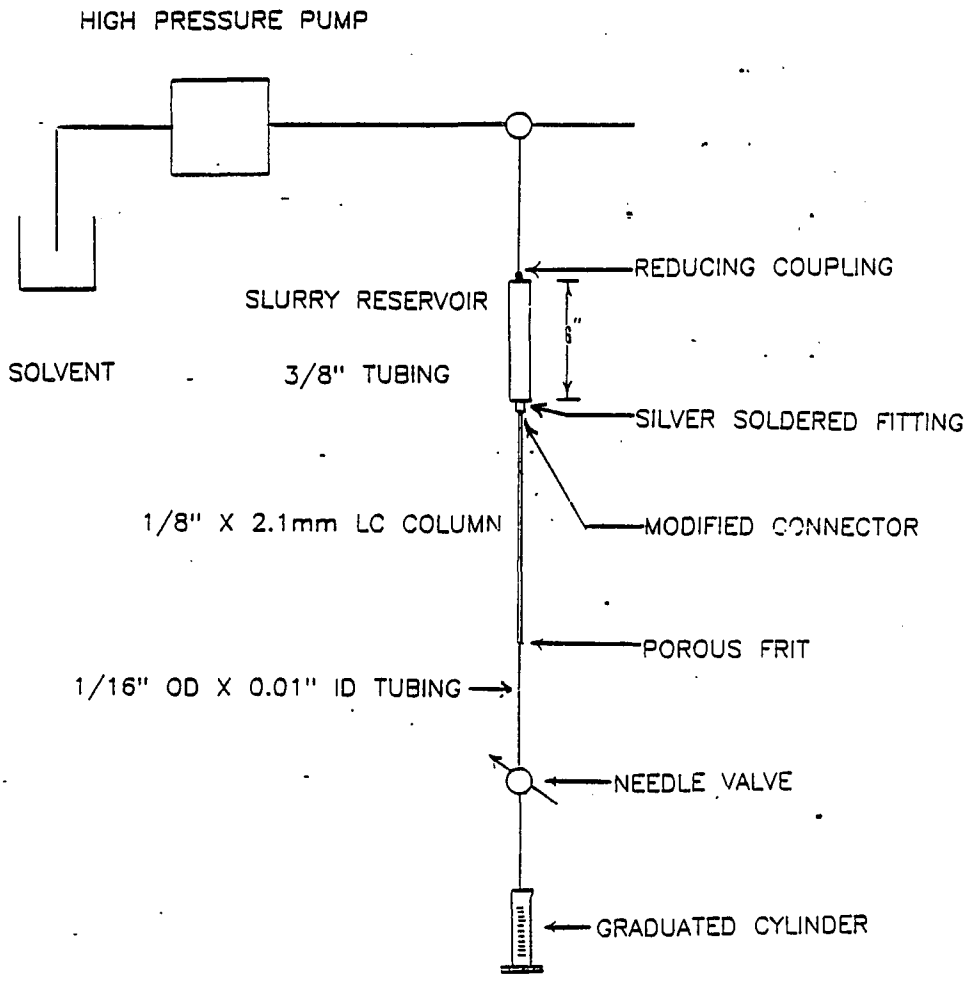

SLURRY PACKING APPARATUS

Mobile Phase

All solvents, including reagent grade, had to be purified to remove trace components detectable by the photoionization detector. Alkanes were washed with concentrated sulfuric acid and dried over sodium metal. Molecular sieves, particularly 4A and 3A were the most universally useful and efficient of the drying agents. The water content in most solvents was reduced to less than 0.008%[17]. The final purification step for each solvent was distillation through a 1 meter Vigreaux column. If the solvent could be distilled from impurities, the resulting liquid could be used directly in the mobile phase, otherwise, further purification was required. Prior to pumping the mobile phase through the HPLC column, it was degassed for 5-10 minutes with helium.

Chromatographic Separations

A normal phase system was used because of the type of functional groups bonded onto the surface. The bonded phases were initially evaluated using either the UV or RI detector and then adapted to the PID detector. A separation of p- and m-chloroaniline was achieved using a 80 cm x 2.1 mm column packed with Corasil-I chemically-bonded with 1.1% chlorobenzyl groups. The separation in Figure 7 was obtained with a mobile phase of heptane modified with 0.50% isopropanol.

The mobile phase was changed to pentane modified with 1.0% MeOH when the photoionization detector was used (Figure 8), because of the lower boiling point and higher photoionization potential of these solvents. A difference in peak height is evident which indicates almost a 10-fold increase in sensitivity using the photoionization detector compared with the UV detector. A similar separation of nitroanilines was also achieved. Detection was accomplished using the PID (Figure 9). It would be expected that a nitroaniline should yield a high relative response using a PID.

The separation of a series of ketones is illustrated in Figure 10 which provides an example of the clear advantage of the photoionization detector over the UV detector. The sensitivity of the PID to these compounds is at least 2 orders of magnitude greater than that of the RI detector. This chromatogram also shows that the effluent evaporator system does not cause appreciable solute mixing and band broadening. It should also be noted that the response of the photoionization detector towards p-methylaniline was at least a factor of 2 times greater than that of a 254 nm UV monitor which responds maximally to such compounds.

Figure 6

Separation of m-chloroaniline and o-chloroaniline
Using a 254 nm UV Detector

Column	80 cm x 2.1 mm
Eluant	0.50% Isopropanol in n-Heptane
Flowrate	2.0 ml/minute
Detector	0.05 AUFS @ 254 nm
Temperature	Ambient
Packing	1.1% Chlorobenzyl-Corasil-I
Sample	10 µg each of o-chloroaniline and m-chloroaniline

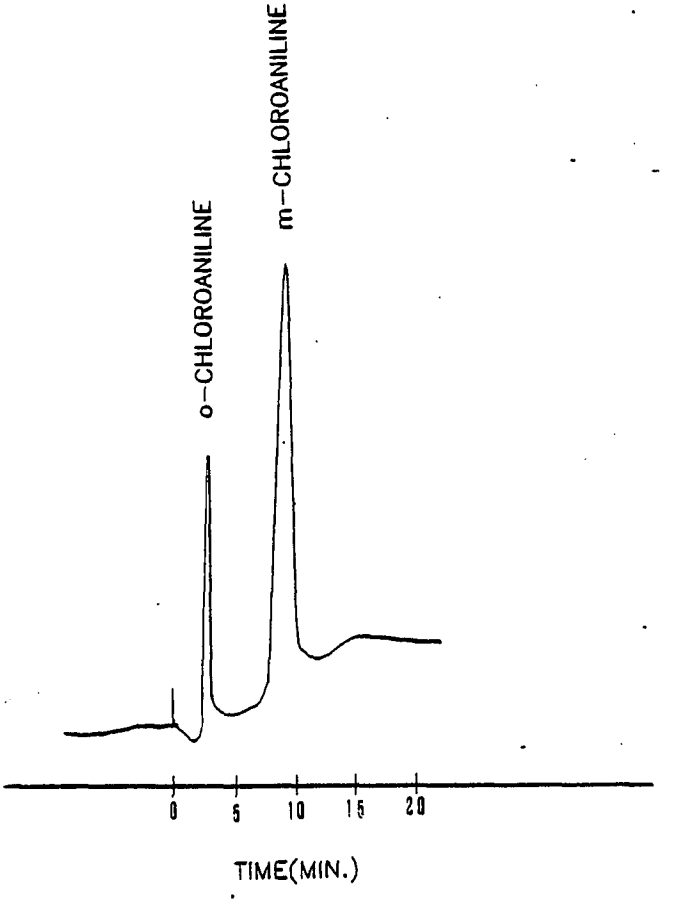

SEPARATION OF m-CHLOROANILINE AND
o-CHLOROANILINE USING A UV DETECTOR

Figure 7

Separation of m-chloroaniline and o-chloroaniline Using a PID

Column	80 cm x 2.1 mm
Eluant	1.0% MeOH in n-Pentane
Flowrate	2.0 ml/minute
Temperature	Ambient
Packing	1.1% Chlorobenzyl-Corasil-I
Sample	1 µg each of o-chloroaniline and m-chloroaniline

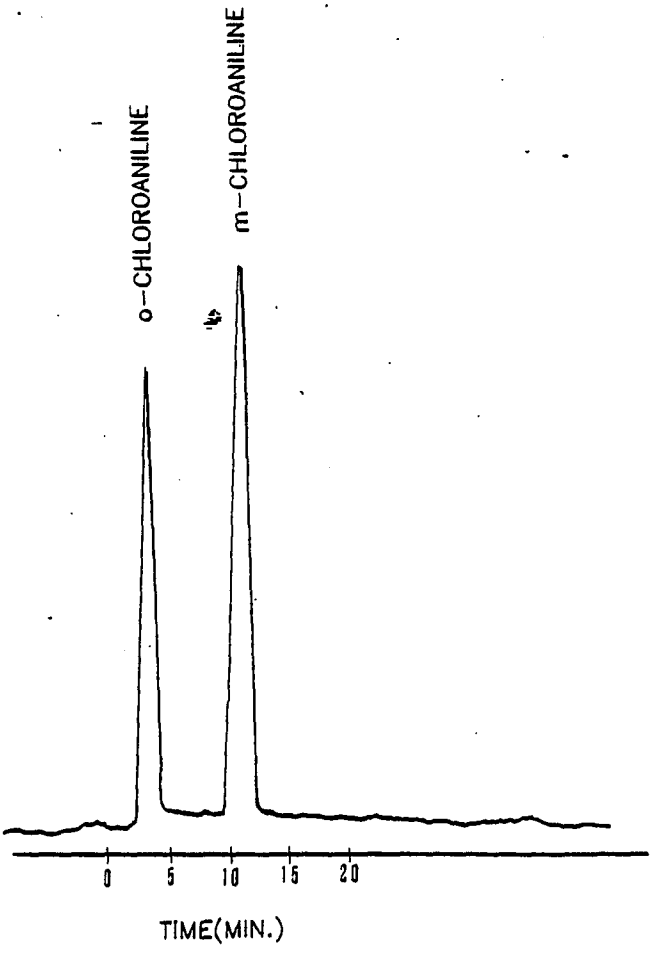

SEPARATION OF m-CHLOROANILINE AND
o-CHLOROANILINE USING A PID

Figure 8

Separation of p-Nitro and o-Nitroaniline

Using a Photoionization Detector

Column	80 cm x 2.1 mm
Eluant	1.0% MeOH in n-pentane
Flowrate	2.0 ml/minute
Temperature	Ambient
Packing	1.1% Chlorobenzyl-Corasil-I
Sample	1 µg each of o-nitroaniline and p-nitroaniline

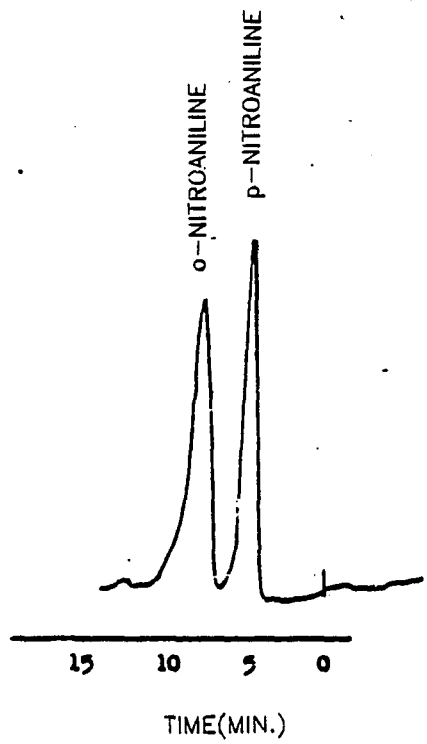

SEPARATION OF o-NITROANILINE AND
p-NITROANILINE USING A PID

Figure 9

Separation Of Ketones Using A PID

Column	80 cm x 2.1 mm
Eluant	0.5% MeOH in n-pentane
Flowrate	2.0 ml/minute
Temperature	Ambient
Packing	1.1% Chlorobenzyl-Corasil-I
Sample	5 µg each of 3-hexanone, 2-octanone and cyclopentanone

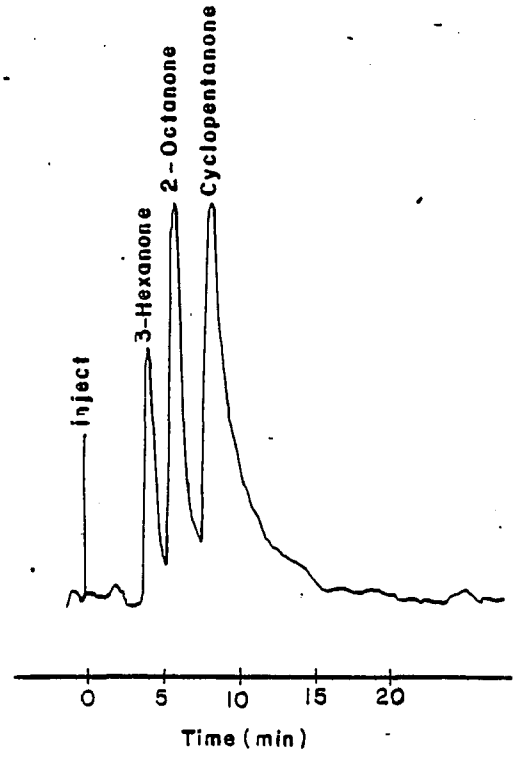

SEPARATION OF KETONES USING A PID DETECTOR

References Chapter 4

(1) Schmermund, J.T.; Locke, D.C.; Anal. Lett., 619, (1975).

(2) Little, J.N.; Horgan, D.F.; Bombaugh, K.J.; J. Chrom. Sci., 8, 625 (1970).

(3) Majors, R.E.; J. Chrom. Sci., 8, 338 (1970).

(4) Guillemin, L.; Deleuil, M.; Cirendini, S.; Vermont, J.; Anal. Chem., 43, 2015 (1971).

(5) Promotional literature from the Separations Group, Hesperia, California

(6) Snyder, L.R.; Ward, J.W.; J. Phys. Chem., 70, 3941 (1966).

(7) Rowan, R.; Sorrell, J.B.; Anal. Chem., 42, 1716 (1970).

(8) Riddick, J.A.; Anal. Chem., 30, 793 (1958).

Chapter 5

An Automated System to Interface an HPLC to a PID Using Column Switching

The total vaporization of the mobile phase causes the problems outlined in Chapter 3: a decrease in sensitivity due to solvent vapor-quenching of the ionized species, condensation within the detector cell, and etching of the window with reverse-phase solvent systems. Acetonitrile acts as an excellent electron-capturing species with a pronounced decrease in the baseline even when a sample of acetonitrile is injected into a stream of argon flowing into a PID. The removal of the photoionized species occurs via electron capture. This is detailed as follows[1]:

$$AB + h\nu \longrightarrow AB^*$$

$$AB^* \longrightarrow AB^+ + e^-$$

$$EC + e^- \longrightarrow EC^-$$

$$EC^- + AB^+ \longrightarrow AB + EC$$

in which AB is a photoionizable compound and EC is a compound such as acetonitrile which is able to attach an electron. Figure 10 shows a typical quenching effect caused by acetonitrile. Therefore, a method to separate the mobile phase from the solutes prior to introduction into the PID is desirable. After considering the previous approaches, a technique called multidimensional column chromatography (sometimes referred to as column switching) was investigated.

Column Switching Techniques

Column switching in GC has been performed with both packed and capillary columns[2,3,4]. In the GC case, the use of a different stationary phase in each column gives different selectivity and retention so that solutes unseparated on the primary column can be further resolved on the secondary column. In certain cases, either differential pressure or high temperature switching valves are used.

The use of column switching in HPLC was first reported by Huber et al[5], but pioneering work by Snyder[6] and Scott[7] in low pressure LC provided the initial concepts. Recently, a number of papers have been published on the subject of HPLC column switching[8-24].

Figure 10

PID Quenching Effect

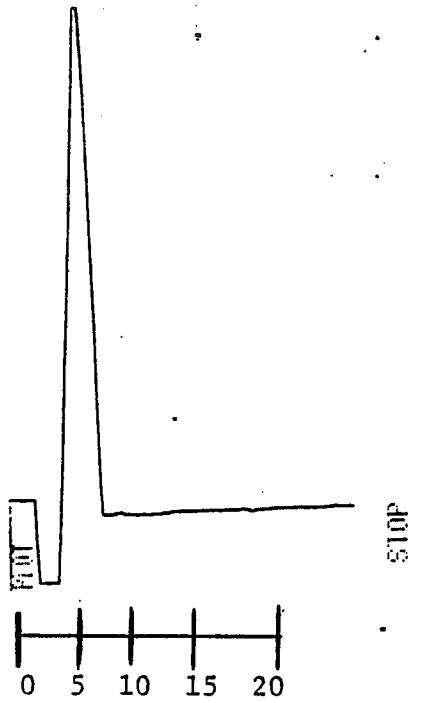
FEED
STOP
0
5
10
15
20
Time (min)

One of the major technical problems in the past was the automatic timing of the valve switching. With a low cost microprocessor, it is now possible to switch columns accurately at pre-determined times. The new generation of computing integrators usually incorporates an external event relay interface to allow several different devices to be controlled in a fixed timing sequence during an analysis. In addition, automatic column switching demands a very stable chromatographic system if accurate switching by time alone is used[25-28].

The application of multidimensional chromatography in HPLC, can, in principle, be off-line or on-line. Off-line multidimensional LC, used frequently in past years, is carried out by collection of solutes at the detector exit from the first column and reinjection of the collected fraction onto a second column. On-line multidimensional HPLC is achieved through coupling to a second column by means of a high pressure switching valve which either traps a defined volume of collected sample, usually in a loop, and directs it to the second column called (heart cutting) or diverts the mobile phase containing the desired solute(s) from the first to the second column for a timed interval to provide on-column concentration.

Multiple dimensions are introduced into the chromatography separation system by using a new solvent system or new stationary phases in the secondary columns. The differences in column selectivity achievable by multidimensional chromatography results in a significant improvement in resolution and in a reduction of the number of components which interfere with the analyte. This gradual enrichment of the analyte relative to the interfering matrix constituents in a multistage process generally precludes extensive clean-up of samples. A specfic application of column switching is the on-line coupling of a normal phase and reverse-phase HPLC system. The flexibility which can result from using either mode of LC increases the usefulness of an LC-GC interface to a PID. Sonnefeld et al[29] described a method for the on-line coupling for a normal-phase HPLC system to a reversed-phase HPLC system. The method utilized a diamine column for a on-column concentration of a selected fraction from a normal-phase aminosilane column followed by a solvent exchange procedure and gradient elution focusing of the analyte species onto a reversed-phase octadecylsilane column.

The two chromatographic systems were interfaced with a dual six-port HPLC valve assembly containing the "concentrator" column. The valves were arranged such that the "concentrator" column can be alternately coupled to: (1) the outlet of the normal-phase column for on-line concentration of the desired fraction; (2) an inert gas purging cycle; (3) the "head" of the reversed-phase guard column. A six-port valve is coupled between the guard column and the head of the analytical column to allow for the venting of the inert gas during the transfer of the solutes from the concentrator column to the guard column.

Compound Chromatography

Another technique, called compound chromatography, was considered in our design of a LC-GC PID interface. The combined technique of LC-GC can be implemented through a continuous or a two step procedure. The latter implies that the two chromatographic methods are used independently of each other, LC being employed as a micro-preparative technique prior to subsequent GC.

Thus, compound chromatography is essentially a combination of LC and GC techniques, integrated into a single procedure for qualitative and quantitative analysis of complex mixtures. A partial separation is carried out on an LC column, and then a GC column is used to separate the eluent from the components and/or to resolve further the compounds being analyzed. In general, the LC can be applied to the separation of compounds that are difficult to resolve by GC alone; This also allows use of a GC detector, which is desirable since a versatile and highly sensitive detector for LC has not yet been developed.

A particularly promising combination of LC and GC is that in which a modified gas chromatograph is used essentially as a detector for LC. The GC column is intended only for the separation of the highly volatile solvent from the compounds of interest, the boiling point of which usually exceed that of the solvent by more than 100°C, thus allowing the use of a very short GC column. This method can also be used for the analysis of thermally labile compounds in some applications, since the solvent can be separated rapidly from these compounds on a GC column at a lower temperature.

The most important advantages of compound chromatography as applied to the analysis of volatile and thermally labile components include the following: (1) high sensitivity; (2) versatility; (3) selective detection by using specific GC detectors and (4) applicable to micro and preparative LC.

Combining LC and GC Systems

The idea of using a gas chromatograph as a detector for LC was first proposed about 15 years ago.[28] In the short (30 cm) GC column the highly volatile solvent was separated from one or more high-boiling components of the analyzed mixture by injecting drops of the eluent from the LC column into the GC. The composition of each drop is recorded on the GC chromatogram as individual peaks after separation on the column. The total quantity of the solute components is determined by adding the peak areas or heights of the same solutes together. A similar system was described by Majors[30].

An example of the combination of LC with GC is the separation of petroleum fractions by LC with isolation of the fractions followed by a second separation using GC. About 70 components can be detected and identified in the petroleum fractions boiling up to 100°C[30].

Automating the LC-GC Interface

A more complex valving system was required in our approach to coupling an LC system to a GC since sequencing requires the use of a sophisticated microprocessor controller. We combine the ability for column switch, changing LC mode, and thermally desorbing the LC solvent, into a unique interface. This is the first attempt to apply these techniques to a single, universal, LC-GC interface using a photoionization detector.

Microprocessor - Controller

A simple controller can be used for basic column switching techniques, but the requirements of our interface, which has 7 individual valves, temperature control and integrated flow controllers, demands a sophisticated microprocessor with several hundred step memory.

A unit manufactured by Systec, Inc. for specific control functions was modified for our system. Figure 11 is a block diagram of the microprocessor with all of the interconnections. The block diagram of the flow system in Figure 12 illustrates the overall fluid and electrical control systems. A contact closure from the modified Micromeritics Model 725 Autosampler is converted to a digital pulse on the input board (Figure 12) which starts the program to run on the microprocessor to control all of the subsequent timing and sequencing functions.

The CPU is based on a 6502 microprocessor chip which combined with RAM and ROM memory constituted the microcomputer. The 6502 regulates all operations of the microcomputer based on the sequence of instructions that has been programmed into memory from the keyboard. A quartz crystal provides timing to the 6502 to synchronize the transfer of data.

Figure 11

SLIC - 1400 Microprocessor - Controller

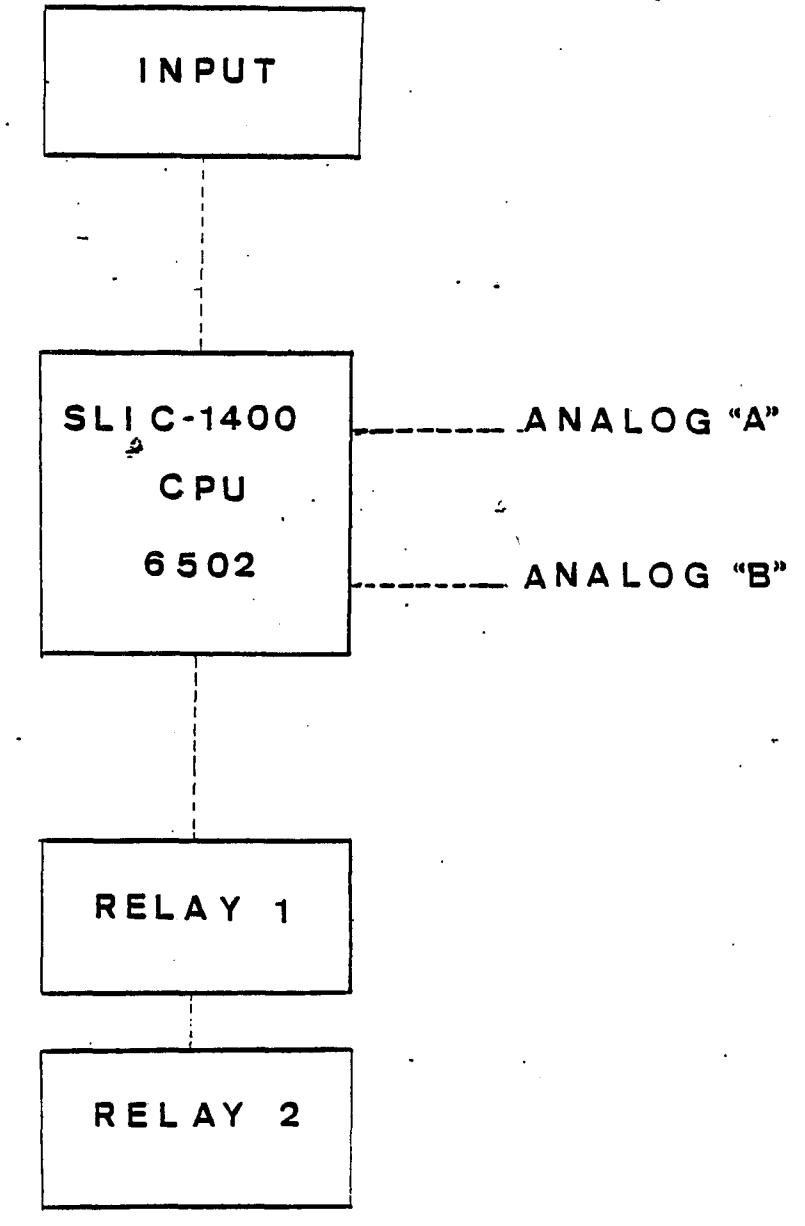

MICROPROCESSOR CONTROLLER

Figure 12

Block Diagram of Fluid Controls on the LC-GC-PID Interface

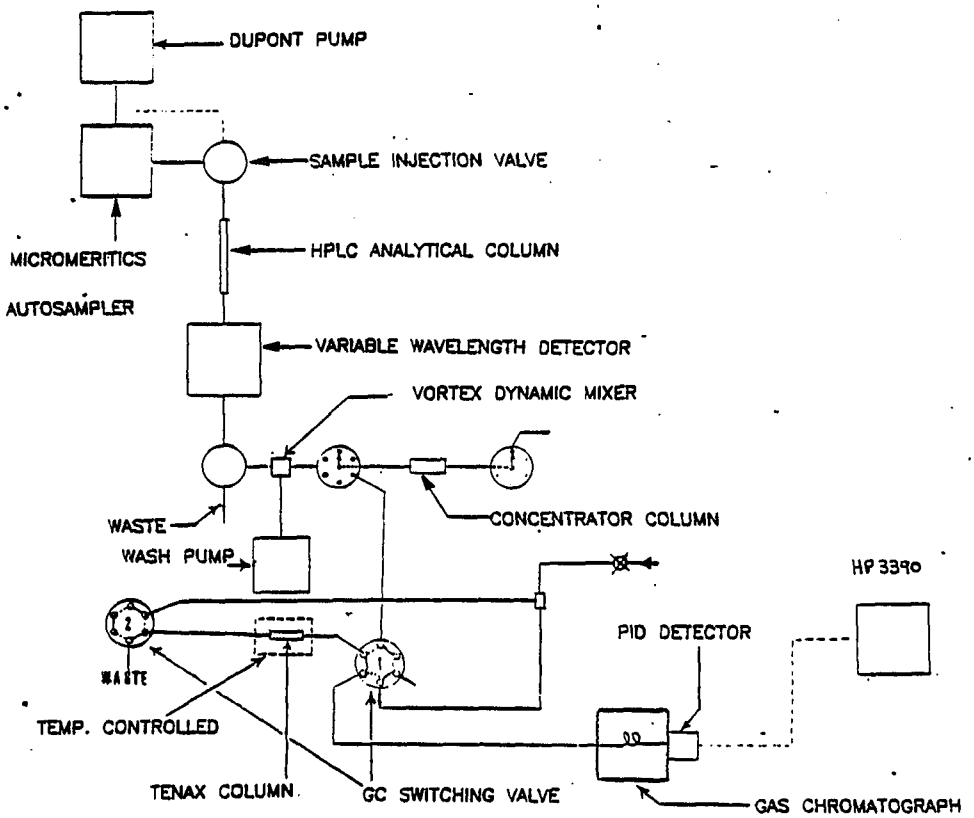

LC-GC/PID FLUID CONTROLS

This CPU is an 8-bit microprocessor which means that the basic unit of information, the byte, is 8 bits wide. Further, all information is transferred to and from memory, and to and from the input output (I/O) devices, 8 bits at a time. All information transfers between the 6502 and external devices is on the 8-line data bus. The data bus is bidirectional so the same lines are used to transfer information both into and out of the 6502 microprocessor.

The 6502 microprocessor executes programs by recalling an instruction from memory, executing it and then recalling the next instruction. A special register, called the program counter, determines which memory location will be accessed next. The program counter is automatically incremented after each memory access so that it addresses the next consecutive memory location. It can address any location in the 64 K-byte address space of the 6502 because the program counter is 16 bits wide.

The SLIC-1400 has both an analog and digital output, both of which were utilized in the LC-GC PID interface. The analog output provides a continuously variable voltage which was used to control the flowrate of both pumps in Figure 12. A controlled voltage ramp allowed the pump to reach a specified flowrate over a designated time interval so that a rapid pressure change could be avoided. Sudden pressure changes can damage a column by collapsing the column packing.

The digital output was cascaded to provide 16 individual channels. Each channel contained a 10 amp relay which provides a contact closure either to switch a valve or to start a thermal cycle. Figure 13 shows the schematic of the output box. The contact closure which could be for any time interval was programmed from the keyboard. A contact closure of 10 seconds would advance the valve to the next position to control valve switching. The electronic interconnections to the solenoid are also detailed in Figure 13 which shows the activation of the pneumatic control valve by applying 12 volts.

Figure 13

Solenoid Valve Control Electrical Schematic

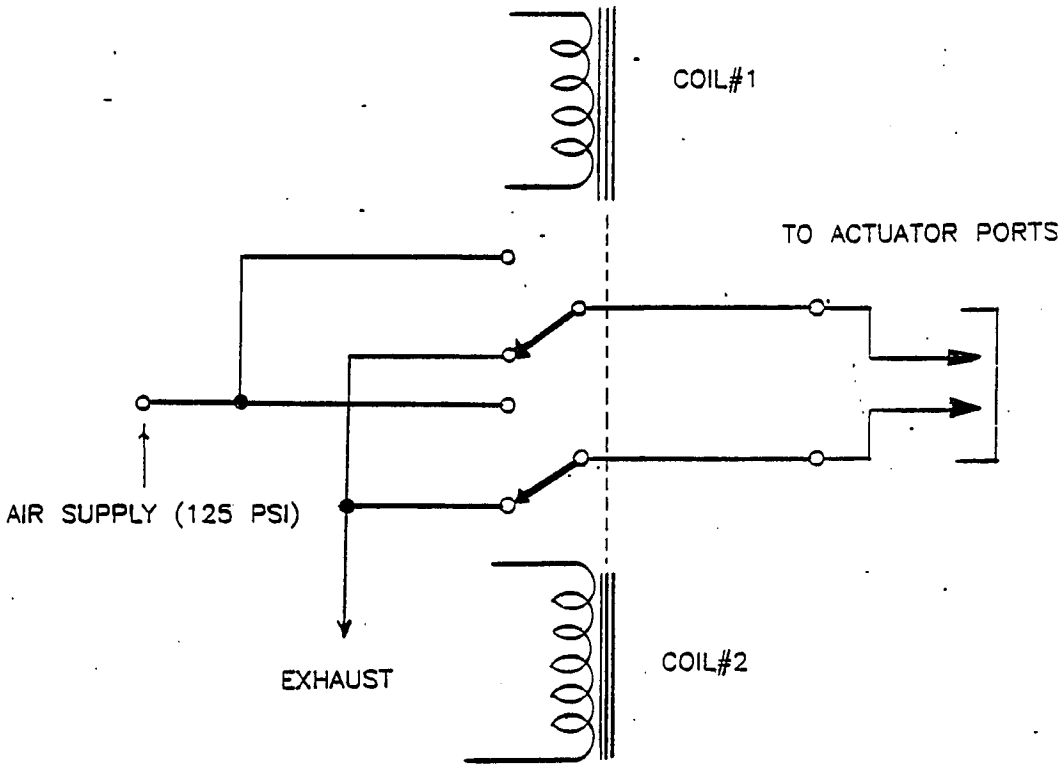

SOLENOID VALVE CONTROL

Thermal Desorption Unit

The thermal desorption unit (Figure 14) was also controlled by a contact closure from the SLIC-1400 output board. The heater contained a precise temperature control with a closed-loop proportional feedback system. Figure 15 shows the electrical schematic of the heater circuit. The temperature accuracy of this circuit, which depends on the input sensitivity of the CA 3059, the thermistor used, and the level of temperature being controlled is the order of $\pm 0.2°C$[36]. The ramp portion of the circuit in Figure 15 controls the voltage applied to the triac. The triac is not gated when the magnitude of the ramp voltage is less than a predetermined voltage with this approach. This mode of operation produces an "on" period that decreases as the sensor temperature increases. Thus, the triac is never off all of the time. The increments of power are based on the number of line voltage half-cycles that occur during the time-base period. A half-second time base allows 60 half-cycle periods of operation. The heat can then be changed in increments of 1.6 percent.

Figure 14

Thermal Desorption Unit

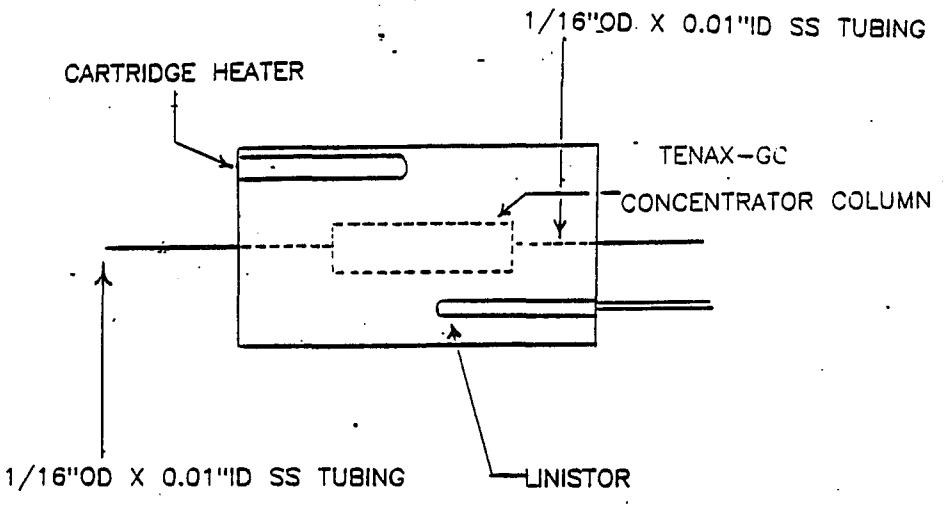

THERMAL DESORPTION UNIT

Figure 15

Proportional Temperature Controller

Thermal Desorption Unit

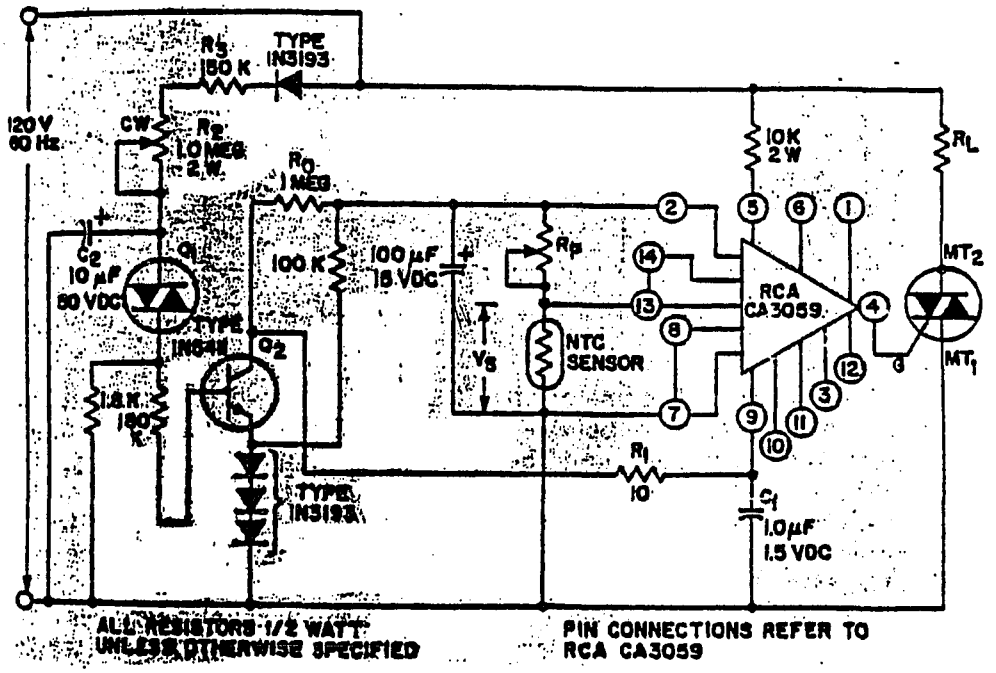
120 V
60 Hz
R_3
150 K
TYPE
IN3193
CW
R_2
1.0 MEG
2 W.
R_D
1 MEG
C_2
10 μF
50 VDC
Q_1
TYPE
IN5441
Q_2
100 K
100 μF
15 VDC
R_P
V_S
NTC
SENSOR
1.8 K
180
K
TYPE
IN3193
R_1
10
C_1
1.0 μF
1.5 VDC
10K
2 W
R_L
RCA
CA3059
MT_2
G
MT_1
ALL RESISTORS 1/2 WATT
UNLESS OTHERWISE SPECIFIED
PIN CONNECTIONS REFER TO
RCA CA3059

The zero-voltage switch (CA 3059) allows the power to be switched on at the high point of the AC cycle. Also, less Radio Frequency Interference (RFI) is produced and thus interference with the microprocessor is decreased. A linistor (linear thermistor) was selected to provide better temperature control over the range of 35-300°C. Initially, the temperature range was adjusted so that the microprocessor would turn the circuit on to rapidly ramp up to the maximum temperature. The microprocessor clock controlled the total duration at the preset temperature and started the cool-down process at the programmed time.

HPLC System

The complex process of changing from an organic mobile phase to an aqueous phase and finally evaporating the solvents prior to thermal desorption of the solutes requires sophisticated LC and GC valves.

A DuPont Pump Model 870 was used for the analytical mobile phase and samples were injected onto the column with the modified Micromeritics 725 Autosampler. The original Micromeritics valve supplied with the unit had several undesirable characteristics. Loops were difficult to change, the valve was prone to clogging which resulted in crushed vials, and reproducibility was not as good as would be expected from a loop sampling device. A Rheodyne Model 7000 valve (Figure 12) was substituted for the Micrometrics valve to provide better accuracy and precision. A variable wavelength UV detector was connected to the output of the LC column to monitor species which have UV chromophores. When a species of interest elutes from the column, the flow is switched to a Vortex Dynamic Mixer (Figure 16). When the organic content of the mobile phase is lowered, a hydrophobic solute will be retained longer on the concentrator column instead of being eluted almost instaneously. The same principle can also be applied to normal-phase separations. The polar modifier in the normal-phase would be diluted by mixing the analytical column mobile phase with a pure alkane such as n-hexane. The visible flowrate of the diluting pump allows a reduction of 75% in the modifier using the present system.

Figure 16

Vortex Dynamic Mixer

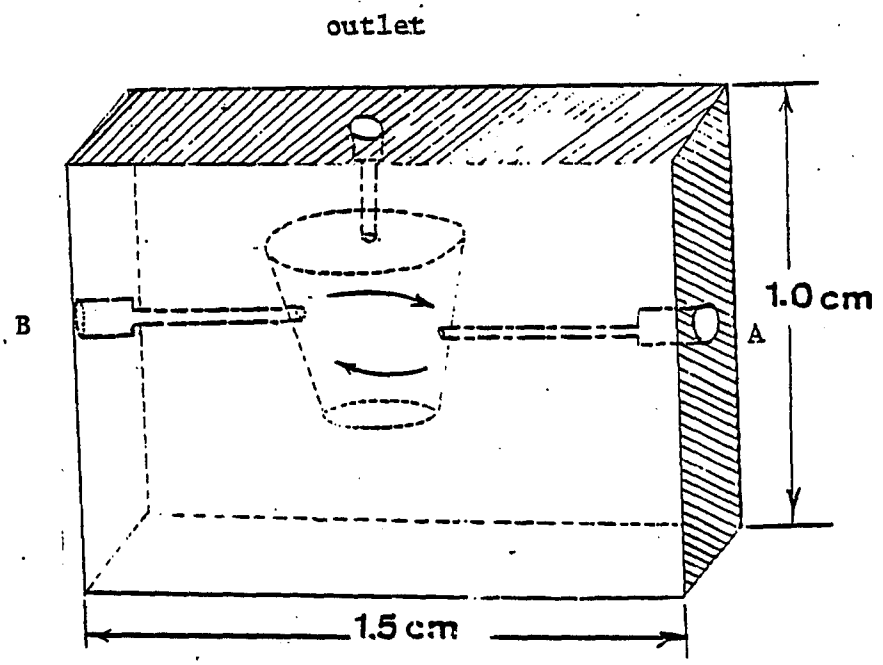

VORTEX DYNAMIC MIXER

The mixer is designed for low dead volume and to provide efficient mixing of the two liquid streams which meet at that point. Tubing from the HPLC column is connected to port "A", while the diluting solvent pump (Beckman Model 110A, Beckman Instruments, Palo Alto, CA) is connected to port "B". The streams are blended in such a way as to cause a vortexing action within the conical section of the mixer. The output of the mixer contains a mobile phase which is lower in organic content. The final composition can be controlled by the analog output of the SLIC-1400 which regulates the flowrate of pump B.

The concentrator column is connected as detailed in Figure 17. A Rheodyne Model 5704 (Rheodyne, Cotati, CA) is controlled by a tandem actuator operated by the same air supply used for the other valves. The sequence starts in position number one and the mixed mobile phase from the dynamic mixer is pumped through the concentrator column. The packing material can be varied as discussed in Chapter 6. The microprocessor advances the valve controlling the pneumatic air supply to the tandem system (Figure 18). A stream of nitrogen flows through the concentrator column in the backflush mode in position 2 and continues to flow for a timed interval which has been established to achieve a certain dryness of the packing material. In position 3, water or any other solvent is pumped through the concentrator column in the backflush mode to elute the trapped solutes from the concentrator column to a Tenax-GC column figure 19.

Figure 17

Concentrator Column Valves

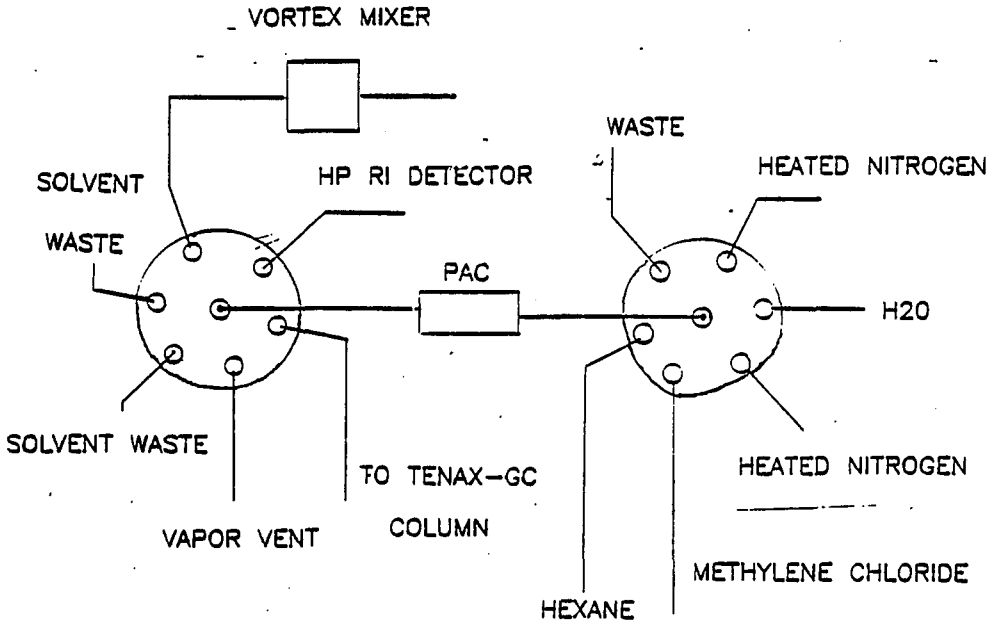

FLUID CONTROLS LC-GC/PID INTERFACE

Figure 18

Tandem Air Supply System

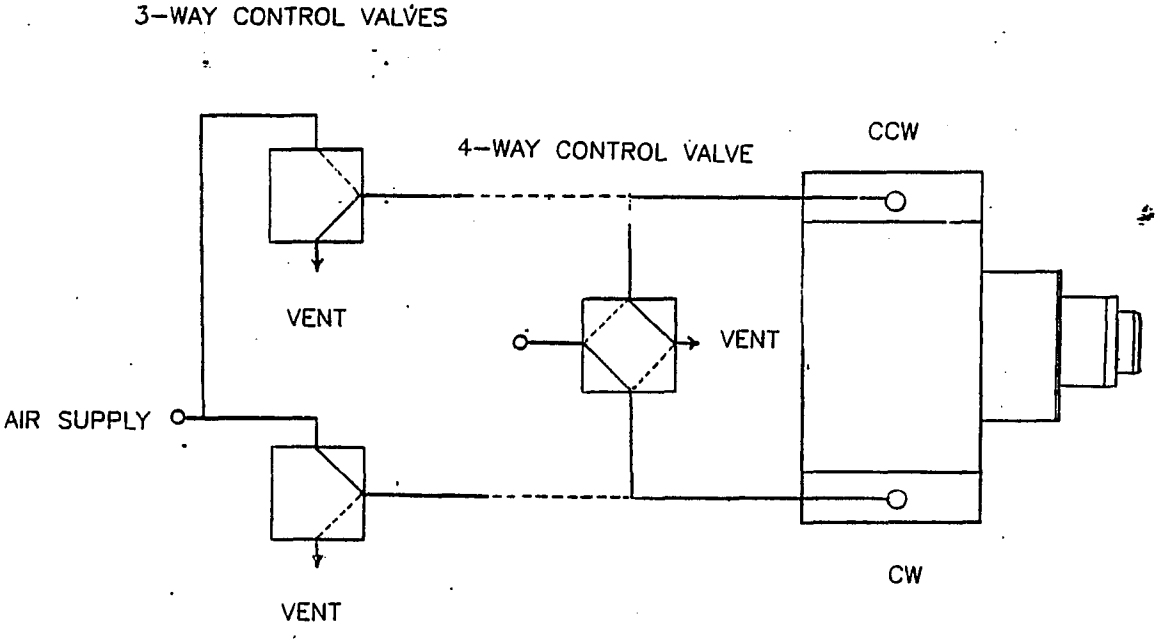

TANDEM AIR SUPPLY SYSTEM

Heated nitrogen again purges most of the water from the column once the solutes are focused on the Tenax-GC column. The valve is advanced to position 5 at a time when only residual water remains and methylene chloride displaces the remainder of the reverse-phase solvent from the concentrator column. The concentrator column is then reintroduced into the normal-phase line for conditioning with 6 or 7 void volumes of mobile phase solvent as preparation for the next fraction switched from the analytical column.

The trapped material was thermally desorbed from the Tenax-GC column shown in Figure 19, and the vapors swept into the PID detector. This packing material, Tenax-GC, a porous polymer based on 2, 6 diphenyl-p-phenylene oxide is often used for trapping organics from water samples. Tenax-GC is also suitable as a GC stationary phase for the separation of high boiling polar compounds such as alcohols, polyethylene glycol compounds, diols, phenols, mono-and diamines, ethanolamines, amides, aldehydes and ketones[37-60]. The Tenax-GC used for the LC-GC interface was 80/100 mesh (Altech Associates, Deerfield, ILL) and was conditioned in a vacuum oven at 250°C for 24 hours prior to use to remove all of the volatiles which may be initially present in the material.

Figure 19

Tenax - GC Trapping Column

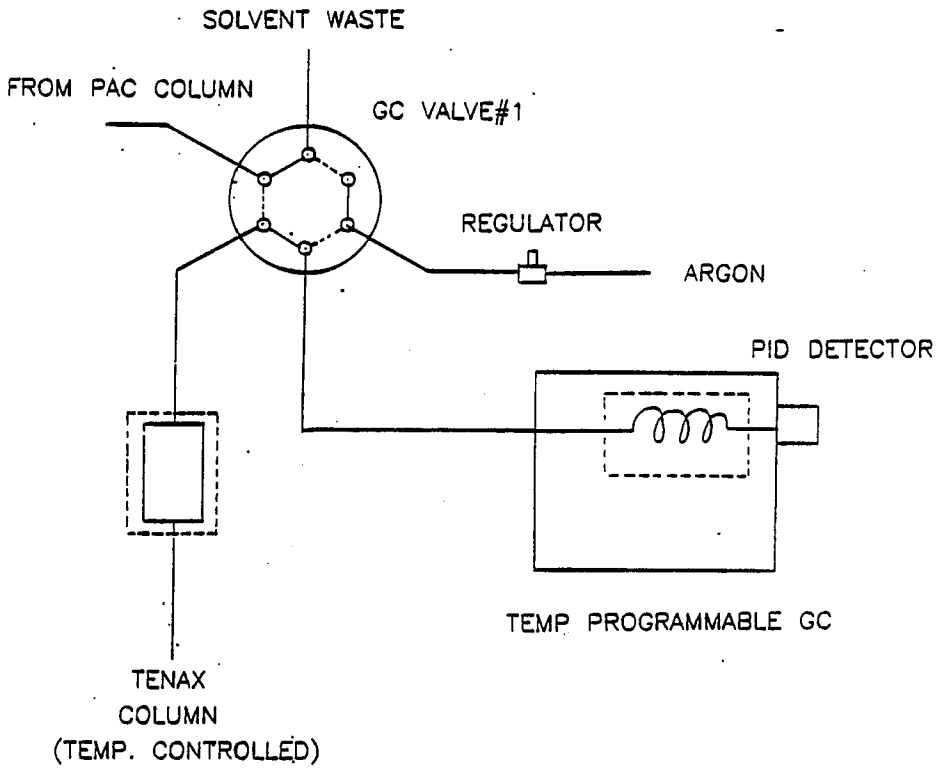

GC VALVES AND PID DETECTOR

Some of the outstanding features of Tenax are the high operating temperatures possible, stable baselines after short conditioning times, short retention times and relatively low temperatures required for effective separations. Thermogravimetric analysis shows no weight loss up to 400°C while at 450°C a loss of 3.3% results[67].

The thermal desorption section of the interface contains two GC valves (Carl, Instruments, Anaheim, CA). These valves are housed in a Carle Model 4300 Valve oven which can be set at any predetermined temperature. For accurate GC analysis, switching valves and transfer lines should be maintained at a temperature equal to or greater than the column temperature to prevent sample condensation in the valve, or sample adsorption on the wall of the transfer tubes.

The oven was mounted on the front of a Perkin-Elmer Model 3290 GC (Perkin-Elmer Corporation, Norwalk, CT). In Figure 12, GC valves #1 & #2 are Model 5621 Carle Mini Valves. GC valve number 2 is a Model 5634 Carle Mini Sampling Valve. Both of these valves were contained within the valve oven. In Figure 20, the solutes were loaded onto the Tenax-GC Trap from the concentrator column or directly from the analytical column depending on the particular analytical procedure. Figure 21, shows the valve in the backflush position. The valve remained in the orientation shown in "A" until most of the moisture was flushed from the valve using a stream of N_2 or Ar. It was then rotated to position "B".

Figure 20

GC Valves in Loading Position - "A"

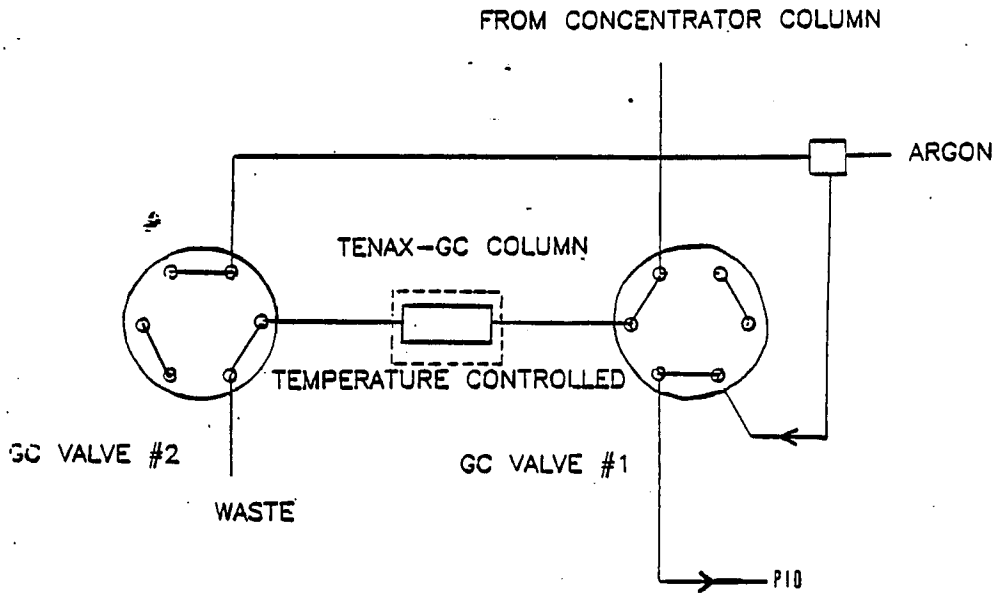

GC VALVES IN POSITION "A"
LOADING

Figure 21

GC Valves in Backflush Elution Position - "B"

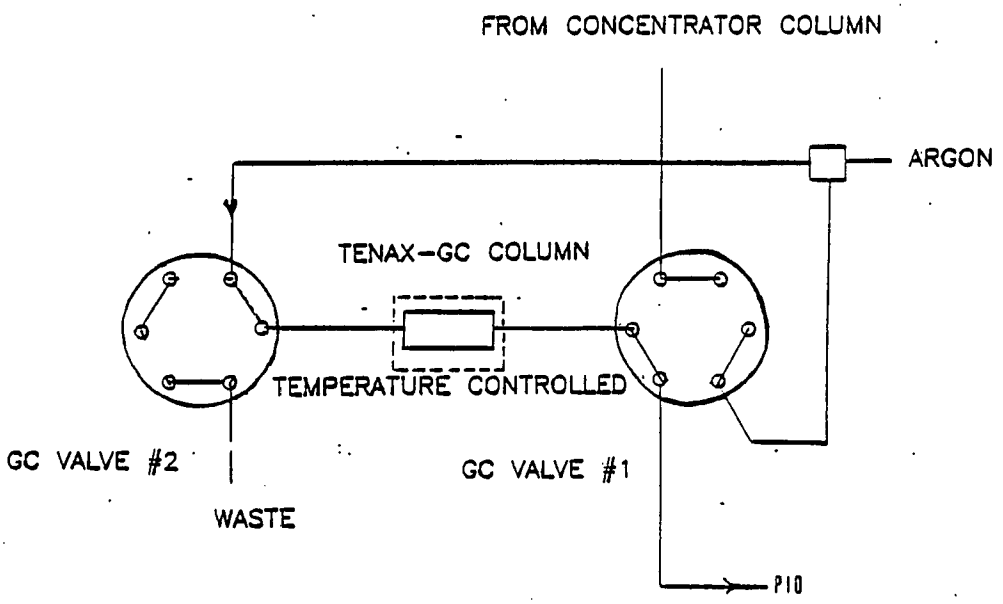

GC VALVES IN POSITION "B"
BACKFLUSH

The PID detector used for the automated system was manufactured by HNU Systems (Newton, MA) and was operated with a VUV lamp with an output at 10.2 eV which was the wavelength which we explored with the detector described in Chapter 3. The specifications of the HNU detector (Table VIII) are very similar to the values which we determined. This commerical unit was used because of the range of available lamps and their higher maximum operating temperatures.

Table VIII

HNU PID Specifications

Linear dynamic range	$>10^7$
Noise Level	$1.5X\ 10^{-14}$ amps
Background current	$1.5\ X\ 10^{-11}$ amps
Minimum detectable level	2 pg (benzene)
Maximum linear level	~30 ug (benzene)
Sensitivity	0.3 Coulombs/gram (benzene)

References Chapter 5

(1) Driscoll, J.N.; Ford, J.; Jaramillo, L.F.; Gruber, E.T.; J. Chromatogr., 158, 171 (1978).

(2) Horvath, C.; "Practice of Gas Chromatography" Ettre, L., ed.; Interscience Publishers: New York, NY 1967.

(3) Ducass, A.; Gonnard, M.F.; Arpino, P; Guiochon, G.; J. Chromatogr., 148, 321 (1978).

(4) Bertsch, W.; Anderson, E.; Holzer, G.; Chromatographia, 10, 449 (1977).

(5) Huber, J.F.K.; Vander Linden, R.; Ecker, E.; Oreans, M.; J. Chromatogr. Sci., 8, 692 (1970).

(7) Scott, D.; Chilcote, D.D.; Lee, N.E.; Anal. Chem., 45, 85 (1972).

(8) Harvey, M.C.; Stearns, S.D.; Am. Lab, 13, 151 (1981).

(9) Berry, V.V.; J. Chromatogr., 199, 219 (1980).

(10) Burns, D.A.; Pharm. Tech, 53, 420 (1981).

(11) Gfeller, J.C.; Stockmeyer, M.; J. Chromatogr., 198, 164 (1980).

(12) DeJung, G.J.; J. Chromatogr., 183, 203 (1980).

(13) Koch, D.D.; Kissinger, P.T.; Anal. Chem., 52, 27 (1980).

(14) Hulpke, H.; Wertmann, U.; Chromatographia,, 13, 39 (1980).

(15) Davis, G.C.; Kissinger, P.T.; Anal. Chem., 51, 1960 (1979).

(16) Wahlund, K.G.; Lund, U.; J. Chromatogr., 122, 267 (1976).

(17) Erni, F.; Keller, H.P.; Morin, C.; Schmitt, M.; J. Chromatogr., 204, 65 (1981).

(18) Majors, R.E.; J. Chromatogr. Sci., 18, 571 (1980).

(19) Apfell, J.A.; Alfredson, T.V.; Majors, R.E.; J. Chromatogr., 206, 43 (1981).

(20) Erni, F.; Frei, R.W.; J. Chromatogr., 149, 561 (1978).

(21) Martin, M.; Verrillon, F.; Eon, C.; Guicochon, G.; J. Chromatogr., 125, 17 (1976).

(22) Miller, R.L.; Ogan, K.; Poile, A.F.; Am. Lab., 13, 52 (1981).

(23) Minavik, M.; Pope, M; Mostecky, J.; J. Chrom. Sci., 19, 250 (1981).

(24) Snyder, L.R.; Dolan, J.W.; Van Der Wal, S.J.; J. Chromatogr., 203, 3 (1981).

(25) Willmott, F.W.; Mackenzie, I.; Dolphin, R.J.; J. Chromatogr., 167, 31 (1978).

(26) Little, C.J.; Thompkins, D.J.; Stahel, O.; Frei, R.W.; Werkhoven-Goewie, C.E.; J. Chromatogr., 264, 183 (1983).

(27) Ramsteiner, K.A.; Bohm, K.H.; J. Chromatogr., 260, 33 (1983).

(28) Karger, B.L.; Giese, R.W.; Snyder, L.R. TRAC, 2, 156, (1983) Wiley: New York, NY,.

(29) Sonnefeld, W.J.; Zoller, W.H.; May, W.E.; Wise, S.A.; Anal. Chem., 54, 723 (1982).

(30) Majors, R.E.; J. Chrom. Sci., 18, 571 (1980).

(31) DeJong, M.L.; "Programming and Interfacing the 6502", Howard W.; Sams: Indianapolis, IN, 1979.

(32) Peatman, J.; "Microcomputer-Based Design", McGraw-Hill, New York, NY, 1977.

(33) Titus, J.A.; Titus, C.A.; Rony, P.R.; Larsen, D.G.; "Microcomputer-Analog Converter Software and Hardware Interfacing", Howard W. Sams: Indianapolis, IN, 1978.

(34) Johnson, C.; "RCA Solid-State Power Circuits Designers Handbook", RCA: Sommerville, NJ, 1980.

(35) Van Wijk, R.; J. Chrom. Sci., 8, 418 (1970).

(36) Tanaka, T.; J. Chromatogr., 153, 7 (1978).

(37) Daemen, J.M.H.; Dankelman, W.; Hendricks, M.E.; J. Chrom. Sci., 13, 79 (1975).

(38) Bertsch, W.; Anderson, E.; J. Chromatogr., 112, 701 (1975).

(39) Bertsch, W.; Chang, R.C.; Zlatkis, A.; J. Chrom. Sci., 12, 175 (1974).

(40) Black, M.S.; Rehg, W.R.; Sievers, R.E.; Brooks, J.J.; J. Chromatogr., 142, 809 (1977).

(41) Bruner, G.; Bertoni, G.; Severini, C.; Anal. Chem., 50, 53 (1978).

(42) Dowty, B.; Laseter, J.L.; Anal. Lett., 8, 25 (1975).

(43) Dowty, B.J.; Green, L.E.; Laseter, J.L.; Anal. Chem., 48, 946 (1976).

(44) Dowty, B.; Green, L.E.; Laseter, J.L.; J. Chrom. Sci., 14, 187 (1976).

(45) Holzer, G.; Shanfield, H.; Zlatkis, A.; Bertsch, W.; Juarez, P.; Mayfield, H.; Liebich, H.M.; J. Chromatogr. , 142, 755 (1977).

(46) Janak, J.; Ruzickova, J.; Novak, J.; J. Chromatogr., 99, 689. (1974)

(47) Kuo, P.P.K.; Chian, E.S.K.; DeWalle, F.B.; Kim, J.H.; Anal. Chem., 49, 1023 (1977).

(48) Leoni, V.; Puccetti, G.; Grella, A.; J. Chromarogr., 106, 119 (1975).

(49) May, W.E.; Chesler, S.N.; Cram.; S.P.; Gump, B.H.; Hertz, H.S.; Enagonio, D.P.; Dyszel, S.M.; J. Chrom. Sci., 13, 535 (1975).

(50) Mieure, J.P.; Pietrich, M.W.; J. Chrom. Sci., 11, 5 (1973).

(51) Parson, J.S.; Mitzner, S.; Env. Sci. and Tech., 9, 105 (1975).

(52) Pellizzari, E.D.; Bunch, J.E.; Berkley, R.E.; McRae, J.; Anal. Lett., 9, 45 (1976).

(53) Pellizzari, E.D.; Carpenter, B.H.; Bunch, J.E.; Env. Sci. and Tech., 9, 556 (1975).

(54) Russel, J.W.; Env. Sci. and Tech., 9, 1175 (1975).

(55) Vanhaelen, M.; Vanhaelen-Fastre' R.; Geeraerts, J. Chromatogr., 144, 108 (1977).

(56) Versino, B.; Knoppel, H.; DeGroot, M.; Peil, A.; Poelman, J.; Schauenburg, H.; Vissers, H.; Greiss, F.; J. Chromatogr., 122, 373 (1976).

(57) Zlatkis, A.; U.S.# Patent 4,003,257, 1977.

(58) Zlatkis, A.; Bertsch, W.; Lichtenstein, A.; Shunbo, F.; Liebich, H.M.; Coscia, A.M.; Fleischer, N.; Anal. Chem., 45, 763 (1973).

(59) Zlatkis, A.; Lichtenstein, H.A.; Tishbee, A.; Chromatographia., 6, 67 (1973).

(60) Zlatkis, A.; Liebich, H.M.; Clin. Chem., 17, 592 (1971).

(61) Zlatkis, A.; Bertsch, W.; Bafus, D.A.; Liebich, H.M.; J. Chromatogr., 91, 379 (1974).

(62) Zlatkis, A.; Lichtenstein, H.A.; Tishbee, A.;Bertsch, W.; Shunbo, F.; Liebich, H.M.; J. Chrom. Sci., 11, 299 (1973).

(63) Brown, P.; Purnell, C.J.; J. Chromatogr., 178, 79 (1979).

(64) Van Wijk, R.; J. Chrom. Sci., 8, 418, (1970)

Chapter 6

Applications of the LC-GC-PID Interface in Pharmaceutical Assays

Part I - Phenobarbital

New methods of detection and quantitation are always of interest to the pharmaceutical industry, where the development of more active drugs in turn requires more sophisticated analytical procedures. The photoionization detector (PID), by its very nature, is suitable for selective and sensitive determinations in very complex pharmaceutical and biological matrices.

In this chapter, the applications of the LC-GC PID interface will be explored for both a normal and reverse-phase HPLC system. The normal phase system was investigated in more detail since it involves a greater challenge to optimize conditions and establish a reproducible assay. In each case, conditions are described for the concentration, elution and adsorption prior to thermal desorption into the PID.

Drug administration to laboratory animals is usually accomplished, in long-term toxicological studies, by incorporating the drug into the animals' feed, dosing and studying the increased animal mortality. Analytical methodology is required to ensure that the proper doses are administered, and that the drug is uniformly distributed and stable in the feed mix under the storage conditions used.

Laboratory animal feeds are complex mixtures which present a formidable separation problem due to the broad spectrum of interfering substances they contain. Most established HPLC methods for the determination of drug substances in animal feeds[1-6] have employed extensive manual sample cleanup methods. These methods were found to be unacceptable in terms of accuracy and efficiency especially at the lower end of the 0.1 - 50 ppm concentration range used in most initial dosing studies. Alternative methods of sample preparation were developed to extract more easily drugs from a feed matrix and to remove many of the interfering substances while maintaining maximum sensitivity.

Phenobarbital [5-ethyl-5-phenyl-2,4,6- (1H,3H,5H) - pyrimidinetrione],

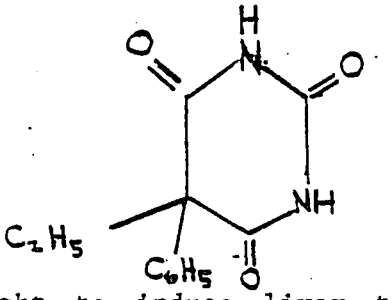

(I)

a compound thought to induce liver tumors in mice, was selected as a model compound since a sensitive procedure is required to detect low levels in animal feed spiked with this material. Analytical methodologies are, therefore, required to verify that accurate dosages are administered and that the chemical is stable and uniformly distributed in the spiked diet. A published procedure is currently used to determine residues of phenobarbital in animal chow at levels as low as 0.14 ppm[2], but it requires an initial methanol extraction followed by a 2-step liquid-liquid cleanup at pH's 13 and 1.

The automated LC-GC PID was evaluated using mixtures of phenobarbital in animal feed. The development of the assay proceeded in the following order:

1) Optimization of the chromatography
2) Study of extraction solvents and recovery of drugs
3) Specificity studies of drug separations
4) Validation of the assay procedure

After review of published assays for phenobarbital, both a reverse-phase and normal-phase system were investigated to optimize the chromatography required specifically for this difficult separation. In both cases, the LC was used as an automated sample cleanup method to provide a "heart-cut" suitable for GC PID detection[12-29]

Experimental

The LC instrumentation consisted of two Altex Model 112A pumps, an Altex Model 421 controller, a Waters Associates WISP Autosampler, a DuPont column oven, a Model 773 Kratos variable wavelength UV detector and an HP 3390 integrator (Figure 22). When the initial conditions were established, the LC instrumentation in Chapter 5 was used to collect the data.

Procedures

A stock solution of phenobarbital (I) in 50/50 acetonitrile/water was prepared from USP reference material at a concentration of 0.15 mg/ml. Solutions were prepared every 12 hours because phenobarbital degrades in solution. All other reagents were Burdick and Jackson (Muskegon, MI) HPLC grade solvents. Two mobile phases were prepared so gradient elution techniques could be used to optimize the reverse-phase chromatography. Mobile Phase A contained 1% acetic acid, 10% acetonitrile and 89% distilled water. Mobile Phase B contained 1% acetic acid, 90% acetonitrile and 9% water. The two limits were established to prevent precipitation of the phenobarbital on the column during the gradient runs.

Figure 22

Gradient Elution HPLC System

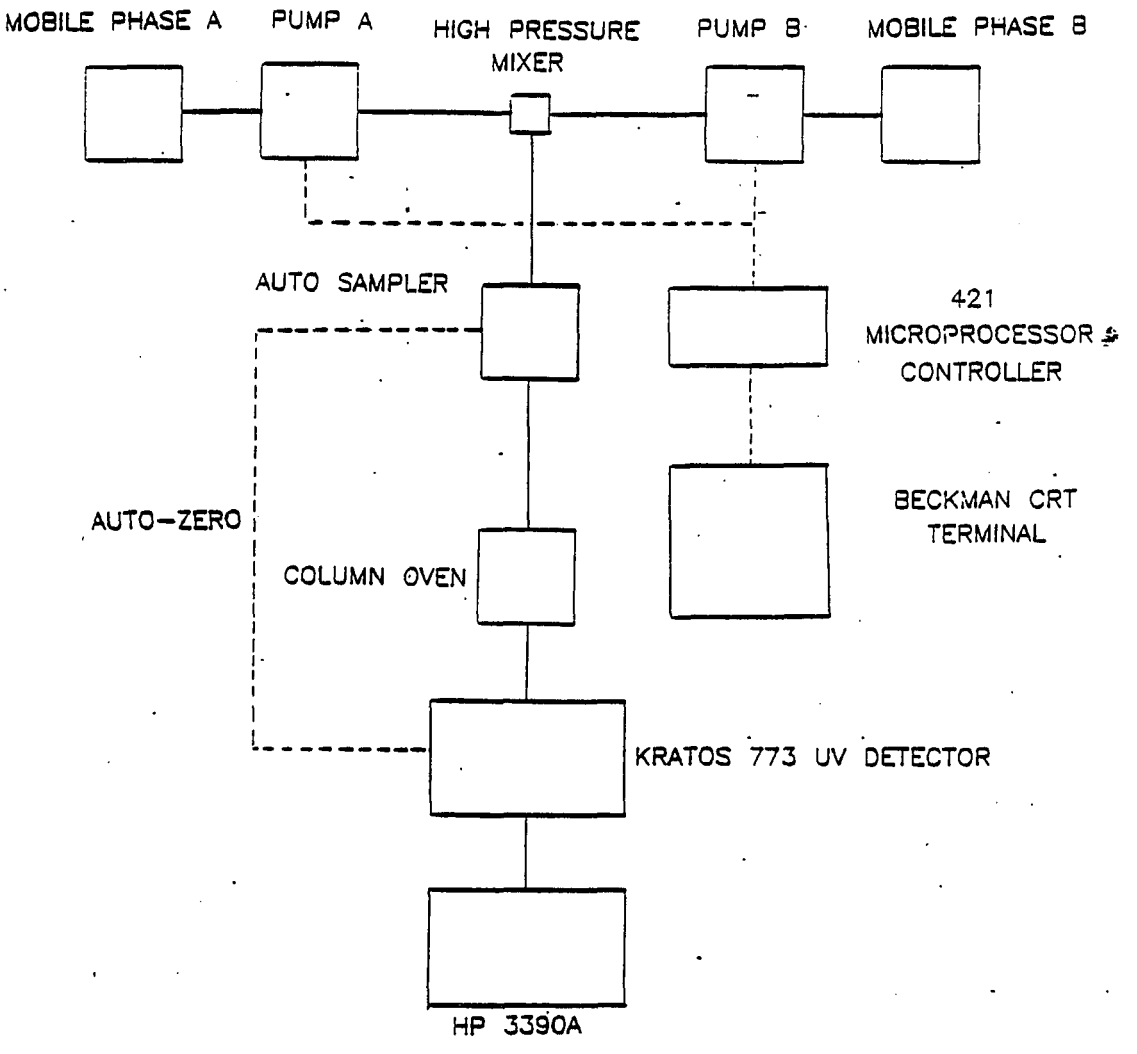

GRADIENT ELUTION HPLC SYSTEM

A stepwise gradient was formed in each LC run so that the composition of the mobile phase was changed by 5% acetonitrile. The retention characteristics were determined as well as peak symmetry for quantification. The chromatogram in Figure 23 shows the optimum conditions: 1% acetic acid, 30% acetonitrile and 69% water.

Extraction of Phenobarbital from Feed Matrix

The HPLC conditions described above were used in the recovery study with actual feed samples. The animal feed samples (Purina Laboratory Chow, Ralston Purina Co., St. Louis, MO) were spiked with known amount of phenobarbital and then extracted using a series of solvents. A solvent should be selected which will provide a high drug recovery while minimizing the extraction of components from the feed matrix itself.

Figure 23

Separation of Phenobarbital and Heptyl Paraben (Internal Standard)

Column:	Zorbax C_8, 4.6 mm x 25 cm
Mobile Phase:	30% acetonitrile, 69% water, 1% glacial acetic acid
Temperature:	35°C
Flowrate:	2.0 ml/min.
Sample:	1. 0.15 mg/ml Phenobarbital 2. 0.10 mg/ml Heptyl Paraben (4-Hydroxybenzoic Acid Heptyl ester)

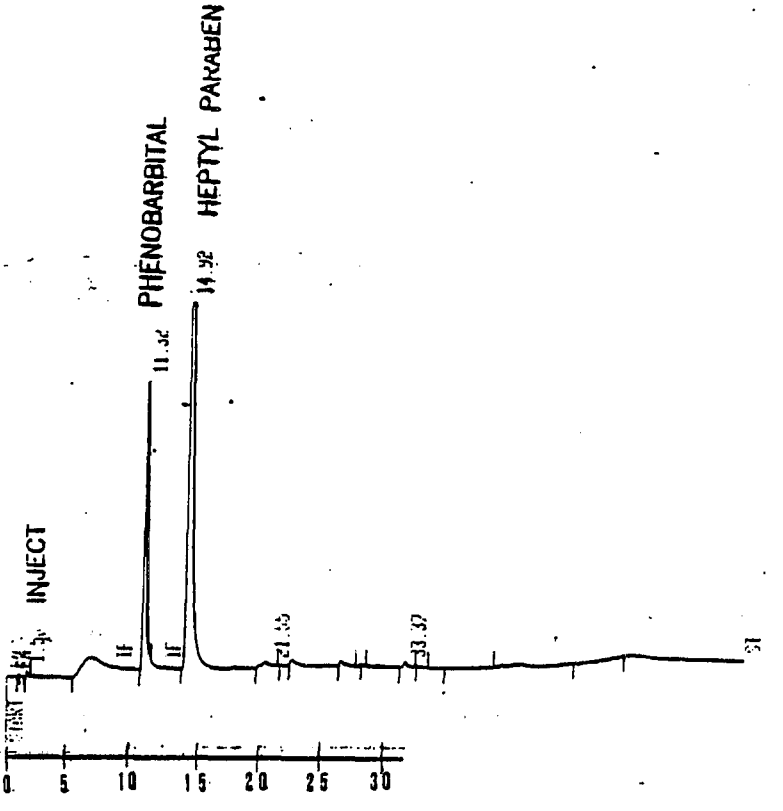

SEPARATION OF PHENOBARBITAL

AND HEPTYL PARABEN

The extraction study was performed by pipetting 5.00 ml of a stock standard solution of phenobarbital (1 mg/ml) into nine 250 ml RB flasks. The animal chow (10.0 grams) was added to 8 flasks; while the remaining round bottom flask was used for the external standard. One hundred ml of each were added to individual flasks, which were then shaken on a Model 8-500 mechanical shaker (Kraft Instruments Co., Mineola, NY) for 30 minutes. The solvents were decanted through a silanized glass wool plug into another series of 8 RB flasks. This procedure was repeated 3 times to provide an exhaustive extraction of the phenobarbital. All of the solutions, including the 5.00 ml of external standard, were evaporated to dryness at 35°C under reduced pressure using a Buchi Rotovap (Brinkman Instruments, Westbury, NY). A Heptyl paraben internal standard was prepared by dissolving 0.10 mg/ml of the material in 50/50 acetonitrile/water. Each flask received 5.00 ml of the internal standard solution and the residual within the flask was dissolved by mechanically shaking the flask for 10 minutes.

Figure 24

Plot of Concentration of the High, Middle and Low Phenobarbital Standards Versus Area Ratio

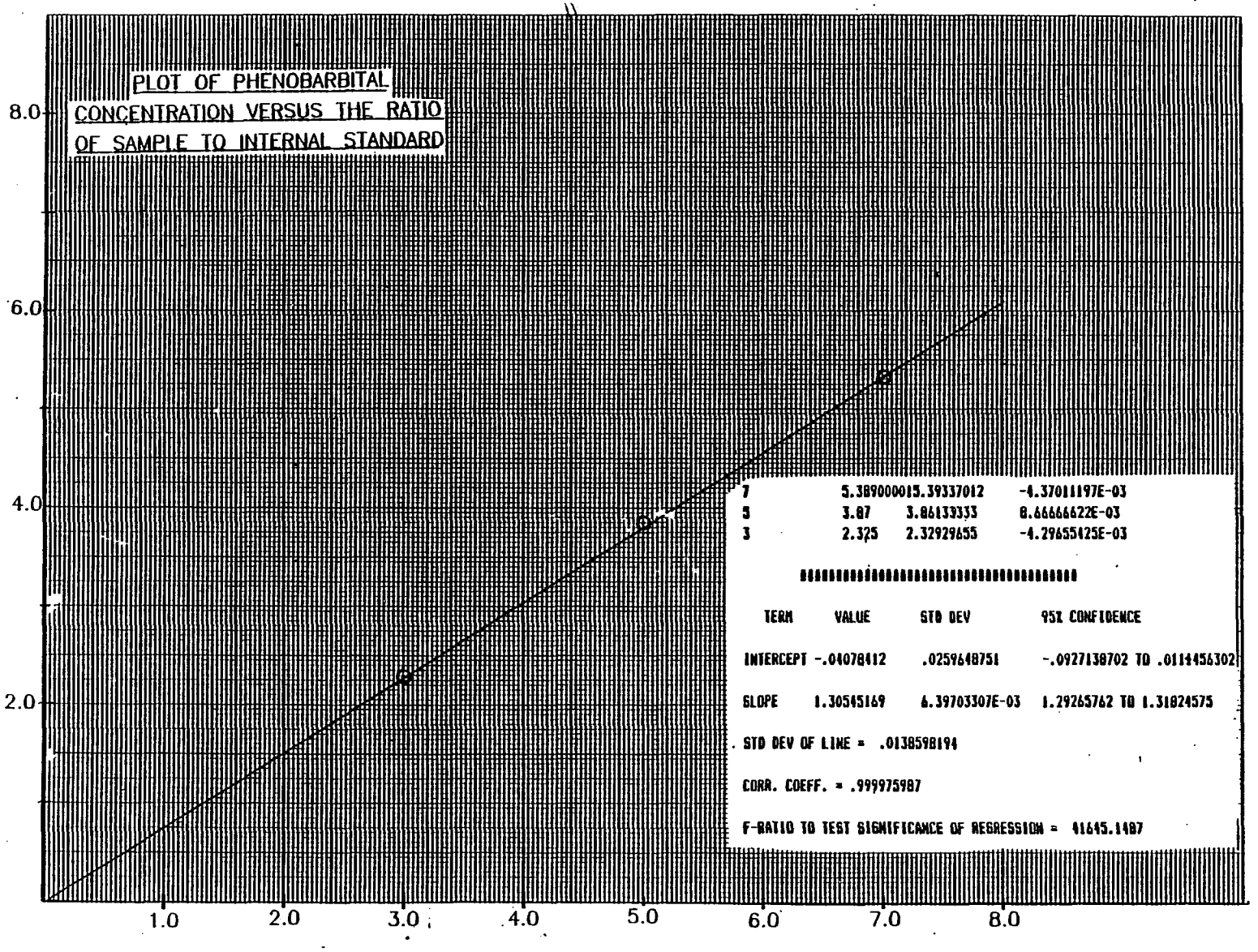
PLOT OF PHENOBARBITAL
CONCENTRATION VERSUS THE RATIO
OF SAMPLE TO INTERNAL STANDARD
8.0
6.0
4.0
2.0
1.0
2.0
3.0
4.0
5.0
6.0
7.0
8.0
7 5.389000015.39337012 -4.37011197E-03
5 3.87 3.86133333 8.66666622E-03
3 2.325 2.32929655 -4.29655425E-03
TERM VALUE STD DEV 95% CONFIDENCE
INTERCEPT -.04078412 .0259648751 -.0927138702 TO .0111456302
SLOPE 1.30545169 6.39703307E-03 1.29265762 TO 1.31824575
STD DEV OF LINE = .0138598194
CORR. COEFF. = .999975987
F-RATIO TO TEST SIGNIFICANCE OF REGRESSION = 41645.1487

The resulting solutions were placed in LC vials and automatically injected into the HPLC system described in Figure 22. The peak areas obtained were compared with a standard curve which bracketed the valves by using high, middle and low standards. Recovery data is presented in Figure 25. The data were obtained using a least squares program (Appendix I) to calculate the percent recoveries listed in Table IX. The standard curve was also linear, showing an excellent fit of the data points (Figure 26). The adjusted recovery data were obtained by subtracting the recovery for the external standard from the values calculated for each extraction solvent. Chromatograms are included in Appendix I showing the phenobarbital in each solvent extract. By comparing the extraction efficiencies in Table IX with the chromatograms in Appendix I, methanol is seen to have high phenobarbital extraction efficiency, but also extracts a large number of peaks from the feed matrix. Therefore, acetonitrile with the next highest recovery but fewer feed peaks, is the solvent of choice.

Figure 25

Recovery of 5 mg of Spiked

Phenobarbital from Animal Feed

RECOVERY OF 5mg PHENOBARBITAL FROM ANIMAL FEED

SOLVENT	mg RECOVERED	% REC.	ADJ % REC.
HEXANE	0.25	5.0	29.4
METHYLENE CHLORIDE	1.32	26.5	50.9
CHLOROFORM	1.54	30.8	55.2
ETHYL ACETATE	1.61	32.2	56.6
M-t-Bu ETHER	1.11	22.3	46.7
ACETONE	2.44	48.8	73.2
ACETONITRILE	2.38	47.5	71.9
METHANOL	3.58	71.5	95.9
EX. STD.	3.78	75.6	---

Table IX

Solvents Used to Extract Phenobarbital
from Animal Feed

SOLVENT PROPERTIES

Solvent	Boiling Point	Viscosity	Dielectric Constant
(A) Hexane	69	0.30	1.88
(B) methyl-t-Butyl ether	142	0.64	2.8
(C) methylene chloride	40	0.41	8.9
(D) ethyl acetate	77	0.43	6.0
(E) chloroform	61	0.53	4.8
(F) acetone	56	0.30	12.4
(G) acetonitrile	82	0.34	37.5
(H) methanol	65	0.54	32.7

Normal-Phase Separation

The reverse-phase separations discussed above indicate a substantial amount of extractable material in the animal feed mixtures even with a acetonitrile solvent. Therefore, a normal-phase system was investigated to determine if lipids, fat soluble vitamins and other large lypophilic molecules which were coextracted along with phenobarbital could be separated more effectively using a nonpolar mobile phase. After an initial series of optimization experiments, a mobile phase consisting of 79% n-hexane, 18% methyl-t-butyl ether and 3% methanol provided an excellent separation of phenobarbital on a Whatman 4.6 mm x 25 cm Partisil 5 propyl-amino-cyano (PAC) column. Figure 26 shows the separation of hexobarbital and phenobarbital.

An injection of the acetonitrile extract was made on the normal-phase system by evaporating off the acetontrile using a Buchi Rotovap (Brinkman Instruments, Westbury, NY) and reconstituting the residue in methanol, which did not cause solvent incompatability problems.

Figure 26

Separation of Hexobarbital and Phenobarbital

Column:	PAC 5 μm 4.6 mm x 25 cm Whatman
Eluent:	79% Hexane, 18% methyl-t-Butyl-ether, and 3% methanol
Flowrate:	2.0 ml/minute
Temperature:	25°C
Detector:	Kratos Model 773, 0.05 AUFS @ 235 nM
Sample:	10 μl injected of 1.0 mg/ml soluion of hexobarbital and phenobarbital

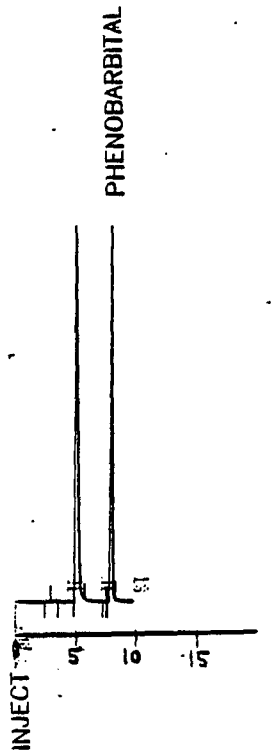

SEPARATION OF HEXOBARBITAL AND PHENOBARBITAL

Figure 27

Data Showing Phenobarbital Recovery

Using a Least Squares Program

Sample #	Ratio	Factor	Assay (mg)	Relative % Recovery	Adjusted % Recovery
1) A	2.376	1	3.061	$\frac{2.376}{5.0} \times 100\% = 47.5\%$	71.9%
2) B	3.575	1	3.061	$\frac{3.575}{5.0} \times 100\% = 71.5\%$	95.9%
3) C	1.611	1	2.062	$\frac{1.611}{5.0} \times 100\% = 32.2\%$	56.6%
4) D	1.541	1	1.971	$\frac{1.541}{5.0} \times 100\% = 30.8\%$	55.2%
5) E	1.114	1	1.413	$\frac{1.114}{5.0} \times 100\% = 22.3\%$	46.7%
6) F	.248	1	.283	$\frac{0.248}{5.0} \times 100\% = 5.0\%$	29.4%
7) G	1.324	1	1.688	$\frac{1.324}{5.0} \times 100\% = 26.5\%$	50.9%
8) H	2.439	1	3.143	$\frac{2.439}{5.0} \times 100\% = 48.8\%$	73.2%
9) Ex.Std	3.781	1	4.895	$\frac{3.781}{5.0} \times 100\% = 75.6\%$	100%

The chromatogram in Figure 28 shows that most of the background material is eluted earlier in this normal-phase system as opposed to the previous separations using reverse-phase. Therefore, the final assay procedure was developed to utilize the better resolution of the feed matrix components using a normal-phase LC system.

Assay Specificity

It is important to ascertain whether the peaks represent pure components or more than one compound. The Food and Drug Administration requires that evidence be presented to show that a peak being detected is a single species. Several approaches to this problem can be taken.

Figure 28

Separation of Acetonitrile Feed Extract
Using a Normal Phase System

Column:	4.6 x 25 cm Whatman PAC 5 µm
Eluent:	79% Hexane, 18% methyl-t-Butyl-ether, and 3% methanol
Flowrate:	2.0 ml/minute
Temperature:	25°C
Detector:	Kratos Model 773, 0.05 AUFS @ 235 nM
Sample:	10 µl of methanol reconstituted acetonitrile extract of 10.0 gms of animal feed (Ralston Purina Lab Chow, St. Louis, MO).

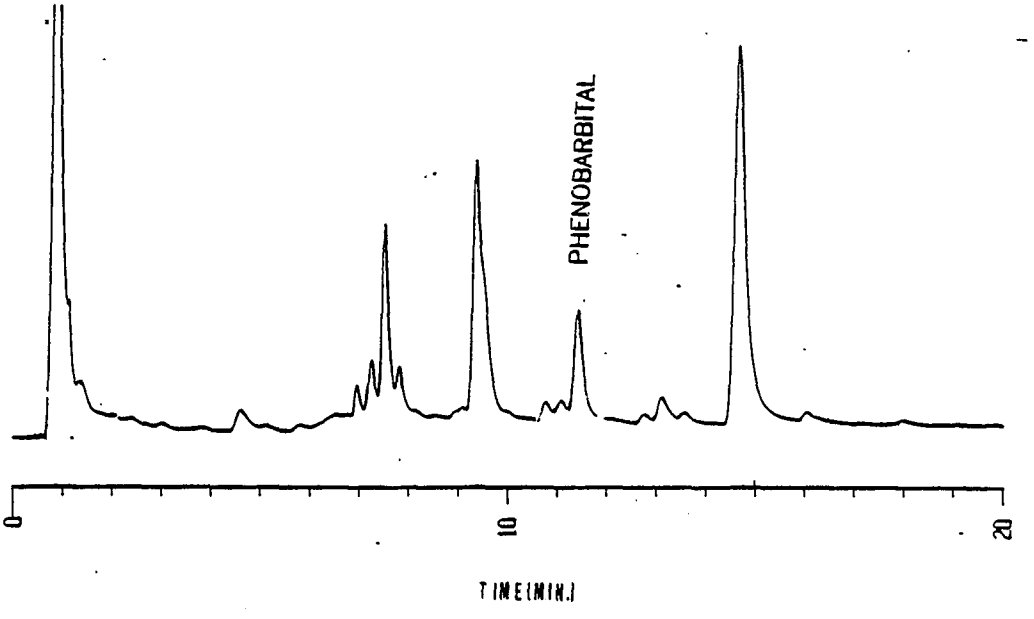

SEPARATION OF ACETONITRILE FEED EXTRACT
USING A NORMAL PHASE SYSTEM

The first is to collect fractions, evaporate the mobile phase and perform direct probe mass spectrometry on the residue. This technique requires a tedious collection of effluent until several micrograms are accumulated. The data presented in Figures 29 & 30 shows that a good correlation was achieved with the reference mass spectra for phenobarbital. On this basis, it is apparent that only phenobarbital was present under the peak in the chromatogram in Figure 28.

A second approach is the use of a photodiode array spectrophotometer. A HP1040A spectrophotometer with flow through cells, supported with an HP 82901M Flexible Disc Drive, HP 85 Terminal and HP7470A Plotter (Hewlett Packard, Avondale, PA)., was used.

Figure 29

Mass Spectra Obtained from the Collection of Mobile Phase Corresponding to the Retention Time of Phenobarbital in Figure 28

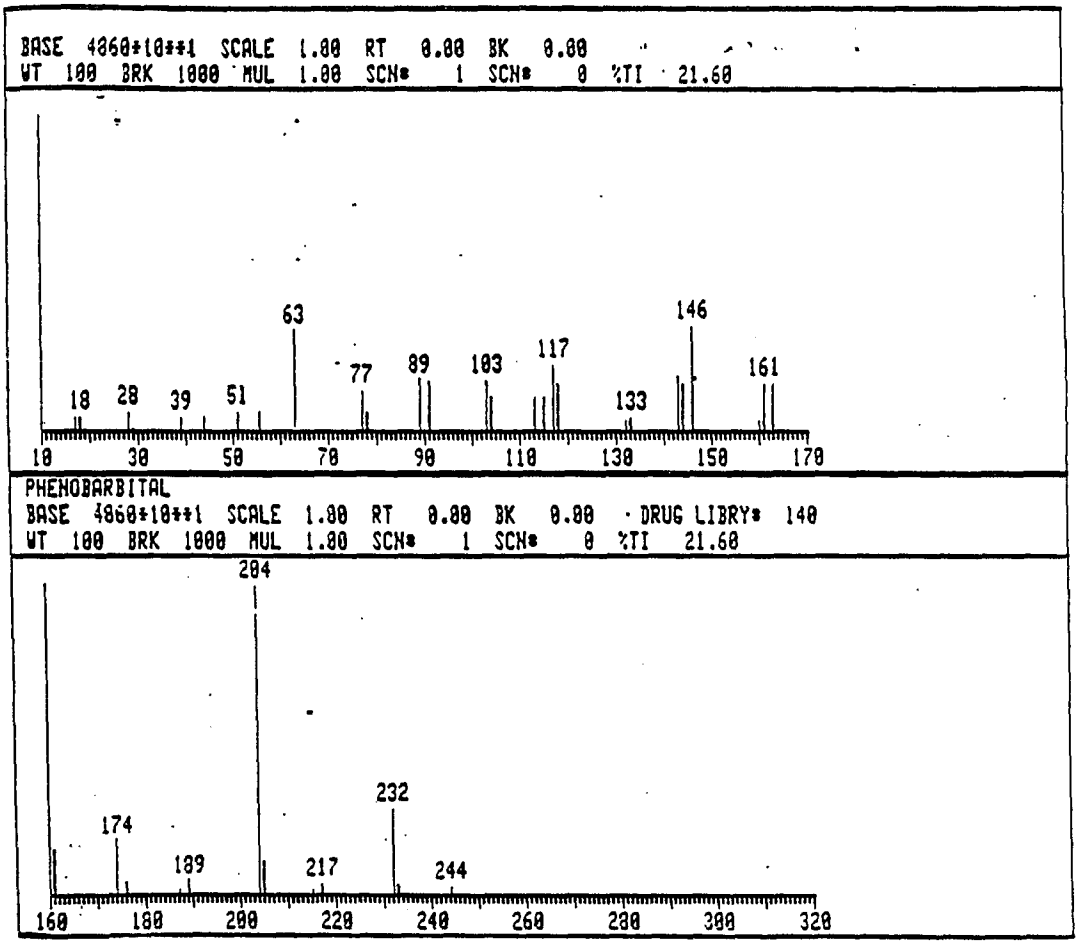
BASE 4860+10++1 SCALE 1.00 RT 0.00 BK 0.00
WT 100 BRK 1000 MUL 1.00 SCN# 1 SCN# 0 %TI 21.60
18
28
39
51
63
77
89
103
117
133
146
161
10
30
50
70
90
110
130
150
170
PHENOBARBITAL
BASE 4860+10++1 SCALE 1.00 RT 0.00 BK 0.00 DRUG LIBRY# 140
WT 100 BRK 1000 MUL 1.00 SCN# 1 SCN# 0 %TI 21.60
284
232
174
189
217
244
160
180
200
220
240
260
280
300
320

Figure 30

Reference Mass Spectra of Phenobarbital

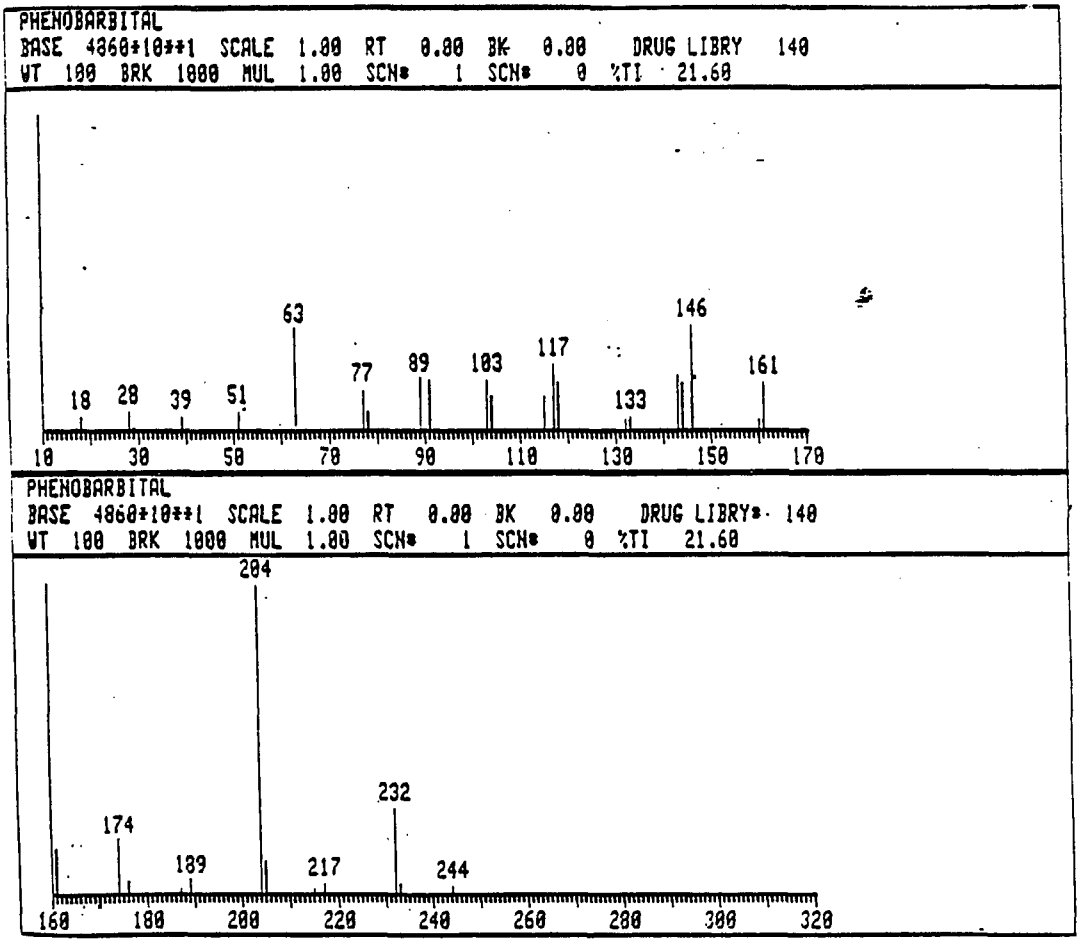

RERERENCE MASS SPECTRA OF PHENOBARBITAL

Figure 31

Separation of Phenobarbital Degradation Products

Column:	4.6 x 25 cm Whatman PAC 5 µm
Eluent:	79% Hexane, 18% methyl-t-Butyl-ether, and 3% methanol
Flowrate:	2.0 ml/minute
Temperature:	25°C
Sample:	10 µl of stock solution of Phenobarbital in 1 mg/ml after degradation in sunlight for 1 week.

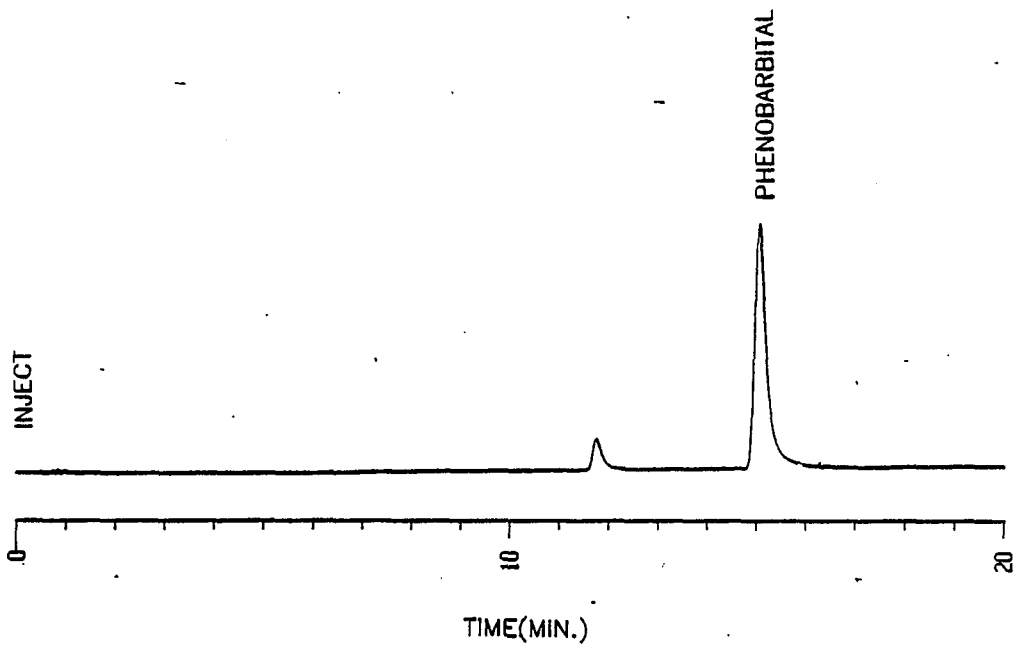

SEPARATION OF PHENOBARBITAL

DEGRADATION PRODUCTS

Separation of phenobarbital degradation products, as shown by the chromatogram which the HP 1040A stored, is shown in Figure 31. The phenobarbital standard (1mg/ml) was allowed to stand for 1 week under the same conditions listed in Figure 28. The two peaks which have eluted corresponding to retention time of 11.4 and 14.7 minutes were stored on the HP disc storage system. A software program normalizes the data and plots it as a function of wavelength versus absorbance in mAV units. Corresponding spectra are shown in Figure 32. It should be noted that the spectra are all very similar, which indicates that most of the phenobarbital moiety remains intact with only minor changes in the structure.

Figure 32

HP 1040A Spectra of Phenobarbital Degradation Products

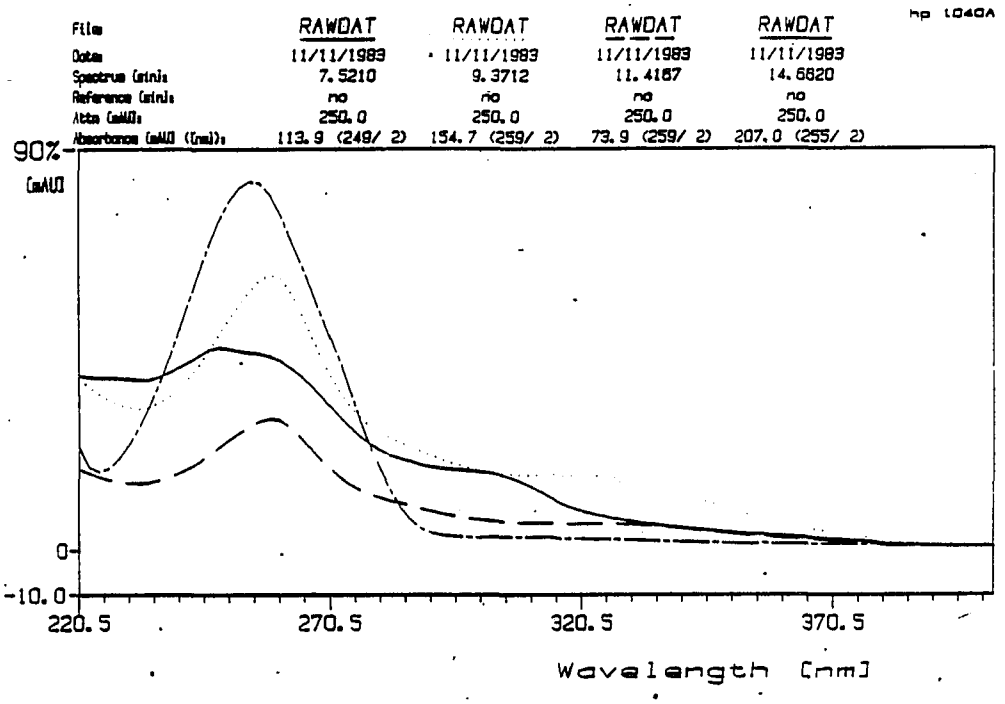

HP 1040A SPECTRA OF PHENOBARBITAL

DEGRADATION PRODUCTS

Optimization of the Automated System

At this point, the separation of the phenobarbital from the animal feed background had been acheived. The LC-GC PID interface now has to be optimized to trap the solute on the concentrator column (Figure 17) reproducibly. The experimental setup utilized two DuPont Model 870 HPLC pumps, a vortex mixer (Figure 33) and a Model 165 variable wavelength UV detector (Beckman Instruments, Palo Alto, CA). The experimental system is shown in Figure 33. The two parameters which were investigated were the type of packing material for the concentrator column and the requirements of solvent mixing to trap all of the phenobarbital on the concentrator column.

Experimental

Stainless steel tubing (4.6 mm x 3 cm) was used for each of the packing materials listed in Table X. The material was packed into the short column using the modified tap-fill method.

Figure 33

Optimization of Trapping Conditions on

a 3 cm Concentrator Column

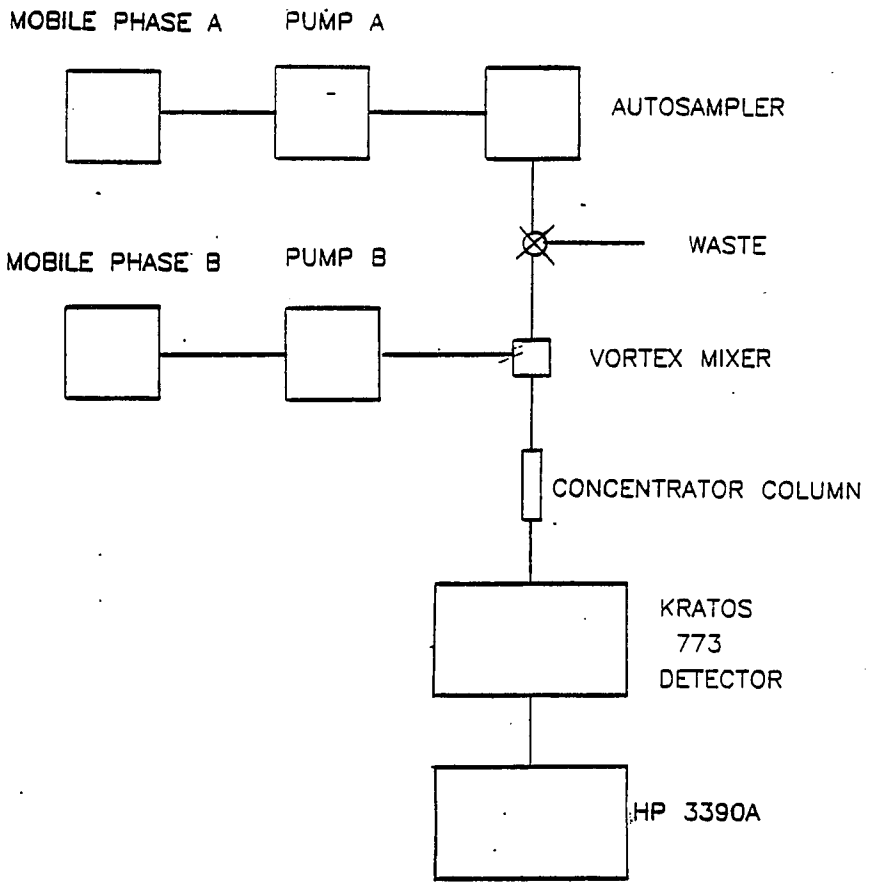

OPTIMIZATION OF TRAPPING CONDITIONS
ON A 3cm COLUMN

Table X

Packing Material Used in the Concentrator Column and the Retention Time of Phenobarbital Using a 50/50 Mixture of Mobile Phase A and B

Packing Material	Retention Characteristics Phenobarbital (minutes)
1) Zorbax BP-CN	6.2
2) Permaphase ETH	3.5
3) Co:Pell PAC [cyano-amino groups on 30-38 µm porous layer beads]	not eluted at 30 minutes
4) Baker Cyano [Irregular shaped 40 µm]	5.3
5) Baker Diol [Irregular shaped 40 µm]	2.3
6) HC Pellosil [high capacity Silica gel bonded to 30-38 µm glass beads]	7.0
7) Whatman Pre-column Gel [37-53 microns]	5.7

Mobile phase A consisted of 79% n-hexane, 18% methyl-t-butyl ether and 3% methanol which is the same as the solvent system used for the analytical HPLC system. Mobile phase B was 100% n-hexane and activated the concentrator column prior to the injection of the phenobarbital standard into the vortex mixer.

Data was collected by pumping mobile phase A and B at flowrates of 2.0 ml/minute. A 10 µl sample of a Phenobarbital Standard (1mg/ml) was injected while mobile phase A was flowing to waste and mobile phase B conditioned the concentrator column. Valve 1 was rotated to allow the mixing of the two mobile phases. A slight variation in the baseline was noticed which was due to refractive index effects of solvent mixing and the increase in flowrate. The retention time of the Phenobarbital was recorded and compared with other packing materials.

As noted in Table X, the Whatman PAC retains the phenobarbital without showing that is breaking through and eluting from the packing material. This selectivity was observed and is the major reason for selecting the Whatman 4.6 mm x 25 cm 5 µm PAC column for the analytical separation.

The second part of the experiment included the variation of flowrate on pump B to determine if an optimum solvent blend could be achieved. Complete trapping was noted even at flowrates of 1.0 ml/minute of the pure n-hexane mobile phase. Therefore, the 1.0 ml/minute flowrate for the diluting solvent was selected with the Co:Pell·PAC trapping material.

Elution of Phenobarbital from the Concentrator Column

Once the phenobarbital is concentrated, the next problem is its elution from the concentrator column and trapping onto Tenax-GC prior to thermal adsorption. A packing material which retains the solute too strongly will require excessive time to elute. The HPLC system in Figure 34 was used to evaluate this section of the automated interface. Tenax GC was selected as described in Chapter 5 since it allows the thermal desorption of polar solutes and can be cycled many times without degradation.

Figure 34

Optimization of Elution from the Concentrator Column and Trapping on Tenax-GC

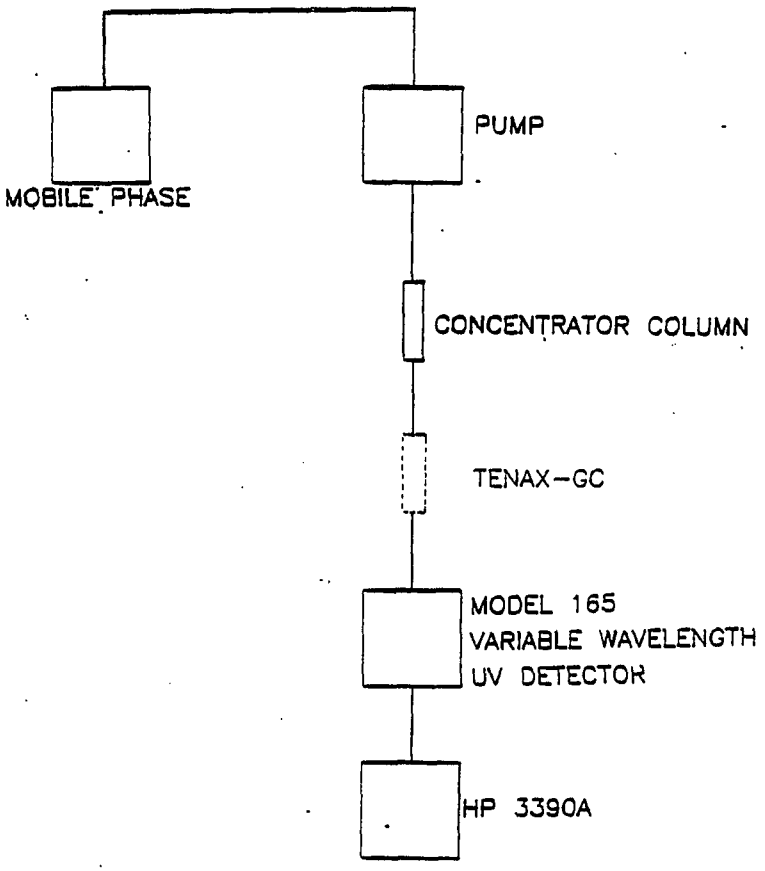

OPTIMIZATION OF ELUTION
FROM A TENAX-GC COLUMN

Experimental

The concentrator column was loaded with the phenobarbital as described in the previous section using the vortex mixer and the two mobile phases. Verification of the retention of phenobarbital on the concentrator column was obtained, because no detectable peak was observed after 10 minutes of pumping the 1:1 mixture of mobile phase A and B. The column was dried using nitrogen for 10 minutes.

A mobile phase of 100% water was selected since it was predicted that the high polarity would readily elute the phenobarbital from the Co:Pell PAC, but also would permit the adsorption onto Tenax-GC

Initially, the concentrator column was connected directly to the Model 165 variable wavelength UV detector. The wavelength, as in previous experiments, was set at 235 nM for maximum sensitivity for the barbiturate. A peak was detected after 10 minutes as shown in Figure 35. When the Tenax-GC Column (4.6 mm x 3 cm) was included in series, the peak did not appear at that retention time and after monitoring the system for 20 minutes, no peak was detected. Therefore, again the phenobarbital was trapped, but this time on the Tenax-GC column.

Thermal Desorption of Phenobarbital from Tenax-GC

Samples of 10 µl of Phenobarbital standard (50 µg/ml) were introduced onto a 4.6 mm x 3 cm stainless steel Tenax-GC column using the experimental arrangement in Figure 36. The Tenax column was heated in the P-E 3290 column oven for 10 minutes prior to connection to the PID. The system was allowed to stabilize and the temperature was programmed to desorb thermally the phenobarbital and carry the vapor into the PID.

Figure 35

Elution of Phenobarbital from

a Co:Pell PAC 4.6 mm x 3 cm Concentrator Column

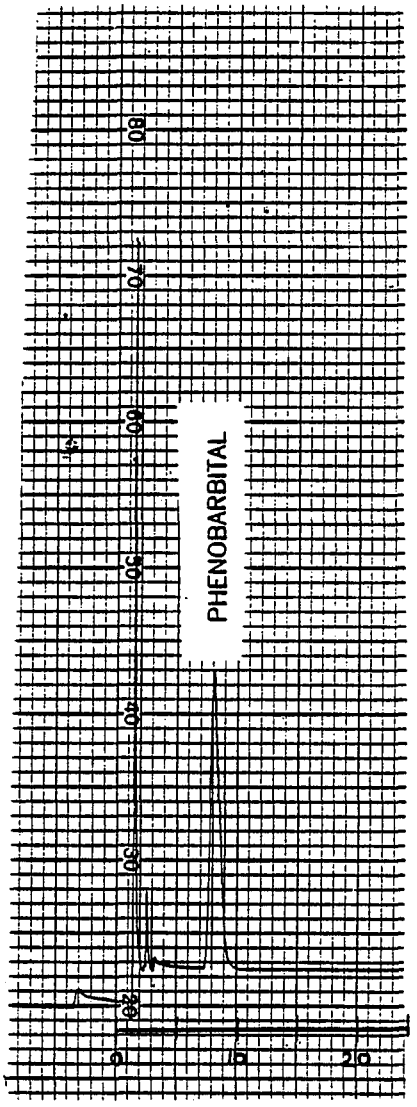

ELUTION OF PHENOBARBITAL FROM

A CO:PELL PAC COLUMN

Figure 36

Experimental System to Evaluate the Thermal Desorption of Phenobarbital from Tenax-GC

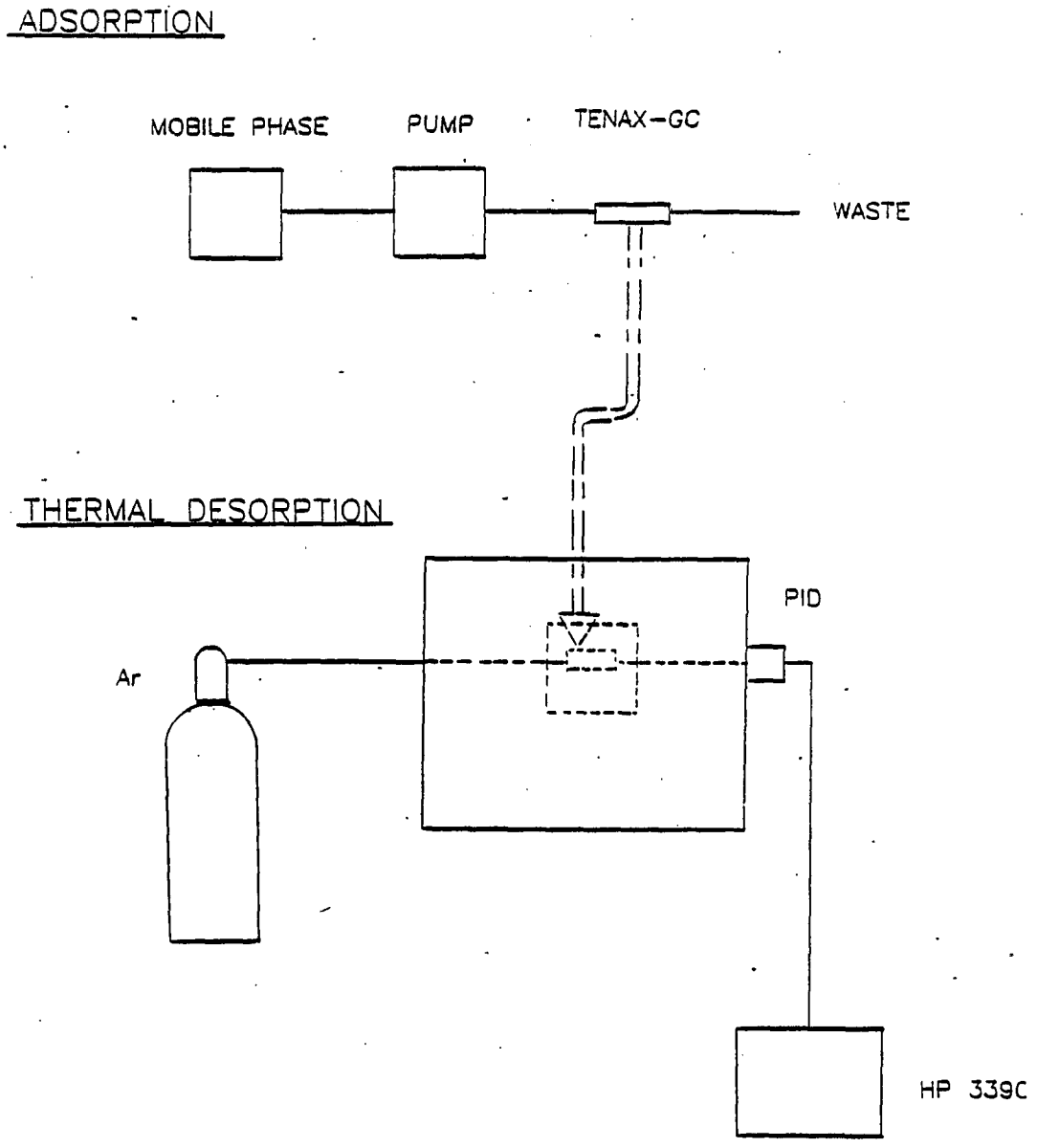

EXPERIMENTAL SYSTEM TO EVALUATE THE THERMAL DESORPTION OF PHENOBARBITAL FROM TENAX-GC

It was noted that more than one peak would appear after several initial experiments. At first, it was thought that impurities were present in the Tenax-GC that were being desorbed simultaneously. Figure 37 shows 5 peaks which resulted when a temperature of 200°C was used over 3 minutes. The possibility of pyrolysis was also considered and after reviewing several articles by Nelson et al[40], it was concluded that the phenobarbital was degrading on the surface of the Tenax-GC at these elevated temperatures. The temperature was reduced to a maximum of 150°C and the chromatogram in Figure 38 shows the resulting separation. The unstable baseline is caused by the temperature programming, but it does not influence the quantitation.

Figure 37

Thermal Desorption of Phenobarbital from Tenax-GC and the Thermal Degradation Products Formed

GC:	P-E Model 3290 Temperature Programmable
Column:	Glass lined stainless steel tubing, 4.6 mm x 3 cm - all connections were made with glass lined 0.30 x 1/16 inch SS tubing
Temperature Program:	50°C - 200°C, 3 minutes
Carrier Gas:	Argon @ 40 ml/minute
PID Detector:	HNU Model PI-52-02
Input Attenuation:	10
Coarse Detector Offset:	10
Fine Detector Offset:	8.0
Polarity	Positive
Recorder Attenuation:	1

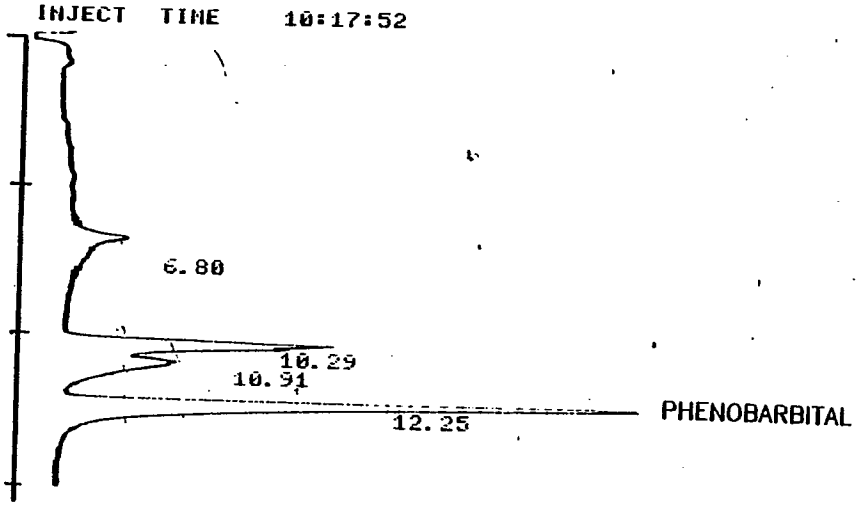
INJECT TIME 10:17:52
6.80
10.29
10.91
12.25
PHENOBARBITAL

Figure 38

Optimized Desorption of Phenobarbital from Tenax-GC

GC:	P-E Model 3290 Temperature Programmable
Column:	Glass lined stainless steel tubing, 4.6 mm x 3 cm - all connections were made with glass lined 0.30 x 1/16 inch SS tubing
Temperature Program:	50°C - 150°C, 3 minutes
Carrier Gas:	Argon @ 55 ml/minute
PID Detector:	HNU Model PI-52-02
Input Attenuation:	100
Coarse Detector Offset:	10
Fine Detector Offset:	8.0
Polarity	Positive
Recorder Attenuation:	1

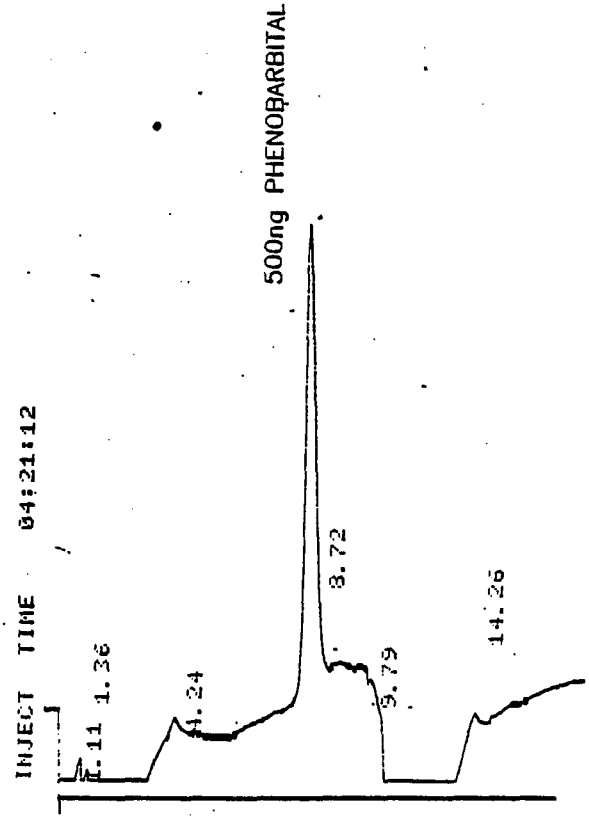

OPTIMIZED DESORPTION OF PHENOBARBITAL FROM TENAX-GC

Figure 39

Comparison of Methods

COMPARISON OF METHODS

Standard HPLC Method

Sample Pretreatment:	MeOH Extraction followed by a liquid-to-liquid clean-up at pH 13 and 1. a silica column removes remaining interference.
HPLC Column:	uBondpak C18, 4 mm x 30 cm
Detector:	UV @ 210 nm, 0.04 AUFS
Mobile Phase:	40% MeOH/60% H_2O
LDL:	0.14 ppm (700 ng)
Time:	15 minutes per sample

HPLC-GC-PID

Sample Pretreatment:	MeCN Extraction after acidification with HCl. millipore samples and inject onto HPLC
HPLC Column:	5 µ Whatman Pac, 4.6 x 24 cm
Mobile Phase:	75% Hexane, 3% MeOH, 22% m-t-Bu Ether
Detector:	Model PI-52, Input Attn. 8, 200 C, 3% SP-2250 Chrom. AW
LDL:	0.006 ppm (30 ng)
Time:	5 minutes per sample

Results and Discussion

A comparison of the standard HPLC method and the HPLC-GC/PID procedure is given in Figure 39. It should be noted that instead of an extensive sample pretreatment, a simple acidification and extraction into acetonitrile is only required. Therefore, the new assay procedure is more practical for large numbers of samples used in most toxicology studies. The time required for sample preparation used in the automated procedure is 5 minutes per sample compared with a per sample time of 15 minutes by the Bowman method[42]. In addition, the assay sensitivity has been increased by a factor of more than twenty which is important in trace analysis. The precision for the assay with n=3 was 2.4% relative standard deviation at the 500 mg level of Phenobarbital. This deviation was greater than the 1.4% reported by Bowman[42], but within acceptable experimental error. With further optimization of experimental conditions, the detection limit for phenobarbital can be reduced to approximately 80 pg based on data published by HNU Systems.

Part II - Amantadine

Amantadine is an orally active antiviral agent which is used to reduce signs of infection among individuals who have been exposed to type A and C influenza viruses.[44-47] It is 90% effective also in preventing influenza[48]. The chemical name is tricyclo [3.3.1.1] decan-1-amine and is represented by the structure (II)

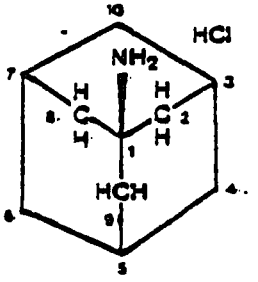

(II)

Amantadine is found in the heart, kidney, liver and lungs after oral administration. After an oral dose of 2.5 mg/kg, maximum concentration of 0.3 μg/ml is reached in 1-4 hours[49] with a plasma half-life of 9-15 hours[50].

Assays to determine purity are usually performed by GC since Amantadine is thermally stable. The structure has been characterized as being extremely stable, as predicted from the equatorial position of the amino group and the facile rearrangement of the ten carbon hydrocarbons to amantadine (III).

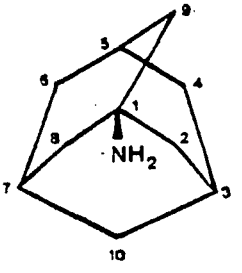

(III)

Figure 40

Separation of Amantadine Spiked into Animal Feed Using Capillary GC

Column: J & W Scientific, SE-30 Capillary Column

GC: H-P 5880A with capillary column inlet and a Flame Ionization Detector

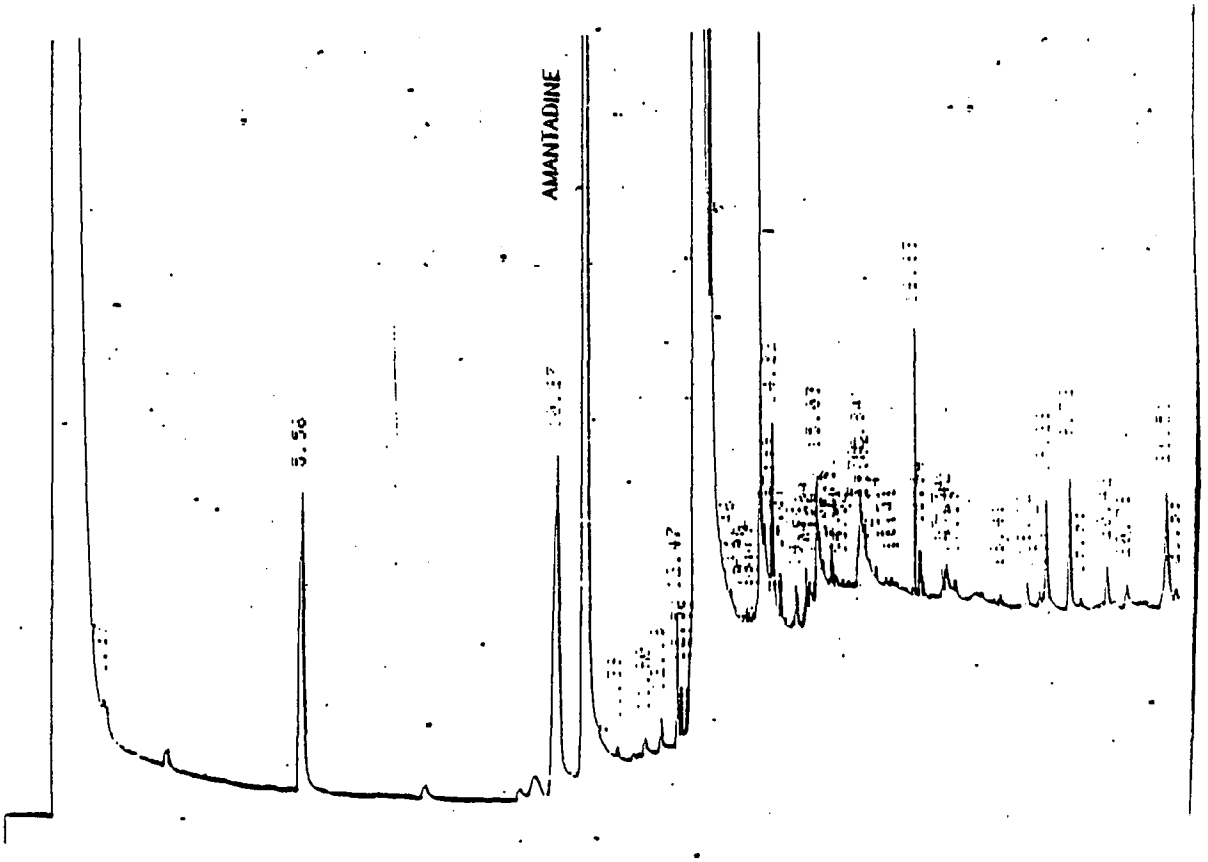

SEPARATION OF AMANTADINE SPIKED IN ANIMAL FEED
FEED USING A CAPILLARY GC COLUMN

A separation of amantadine in a feed extract shows that even using a capillary GC column with a FID detector, interfering components are still present and the resolution is not as good as an HPLC system. Figure 40 shows a typical separation of Amantadine using a capillary column.

At least some of the peaks appear to be caused by the thermal breakdown of components in the feed matrix since the number of peaks increase with increasing injector temperature.

The higher dosage levels of Amantadine obviates the trace level demands on the toxicological assay, but since interference results from feed components, an HPLC automated cleanup is preferred. Therefore, an LC method was first developed to achieve a separation from the feed background, and then the automated system to trap the samples was optimized.

Experimental

The LC instrumentation consisted of a DuPont Model 870 pump, a Waters Associates WISP Autosampler, DuPont column oven, Model 773 Kratos Variable wavelength UV detector and a HP 3390 integrator. The experimental system is illustrated in Figure 41.

Figure 41

HPLC System to Separate Amantadine

from an Animal Feed Matrix

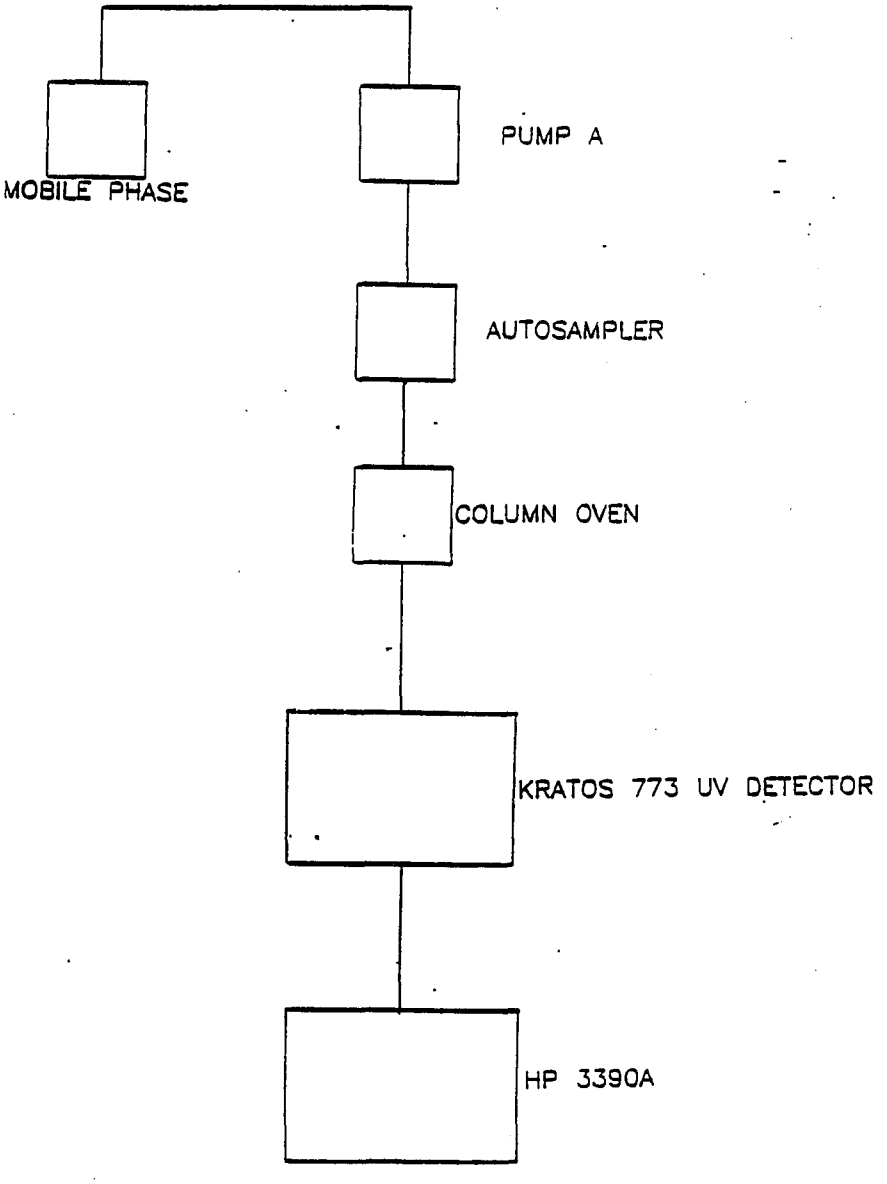

HPLC SYSTEM TO SEPARATE

AMANTADINE FROM ANIMAL FEED

The mobile phase used for the separation was similar to that described by Kirschbaum[51] and consisted of a mobile phase of methanol-water-85% phosphoric acid (60:40:0.1) with 1% of triethylamine to act as a competing base and improve the symmetry of some of the peaks. Since Amantadine has negligible absorbance in the UV region, a refractive index detector (Hewlett-Packard, Avondale, PA) was used as a detector. A typical separation is shown in Figure 42. The resolution on this chromatographic system allows the peak to be selectively trapped and then thermally desorbed into the GC/PID detector.

Optimization of the Automated System

Again, once the Amantadine is separated from the animal feed background, the LC-GC PID interface has to be optimized to trap the solute prior to thermal desorption.

Figure 42

Separation of Amantadine from an Animal Feed Matrix
Using Reverse-Phase Liquid Chromatography

Column:	DuPont Zorbax® C_8, 4.6 mm x 25 cm
Eluant:	Methanol-Water-85% Phosphoric Acid (60:40:0.1) with 1.0% triethylamine added per liter
Flowrate:	2.0 ml/minute
Temperature:	35°C
Detector:	H-P Refractive Index Detector @ 0.01 RI Units
Sample:	50 µl each of a 2 mg/ml solution of Amantadine in a animal feed spiked solution

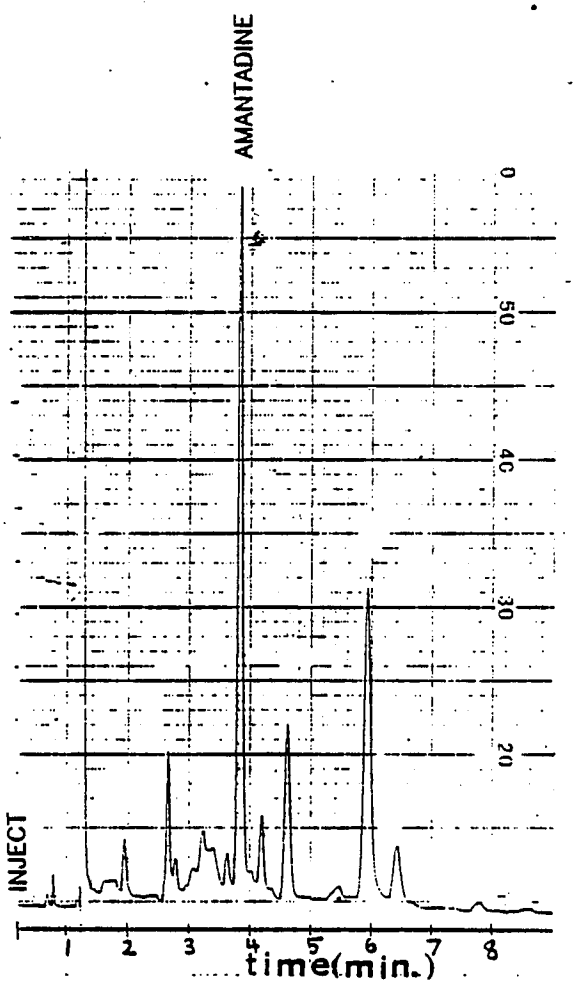

SEPARATION OF AMANTADINE FROM AN ANIMAL FEED MATRIX

The mobile phase can be diluted with water and the solute trapped directly on the Tenax-GC in a reverse-phase system. This eliminates the need for the concentrator column and thus the most complex section of the LC-GC/PID interface is obviated.

Experimental

Glass lined stainless steel tubing (4.6 mm x 3 cm) was used for the Tenax-GC packing. Again, the material was packed into these short columns using the modified tap-fill method. Figure 43 shows the experimental system used to evaluate if the Amantadine was quantitatively trapped. The instrumentation was the same used to optimize the phenobarbital separation (Figure 25) except for the use of a RI detector.

Figure 43

Optimization of Trapping Conditions

for Amantadine on a 4.6 mm x 3 cm Tenax-GC Column

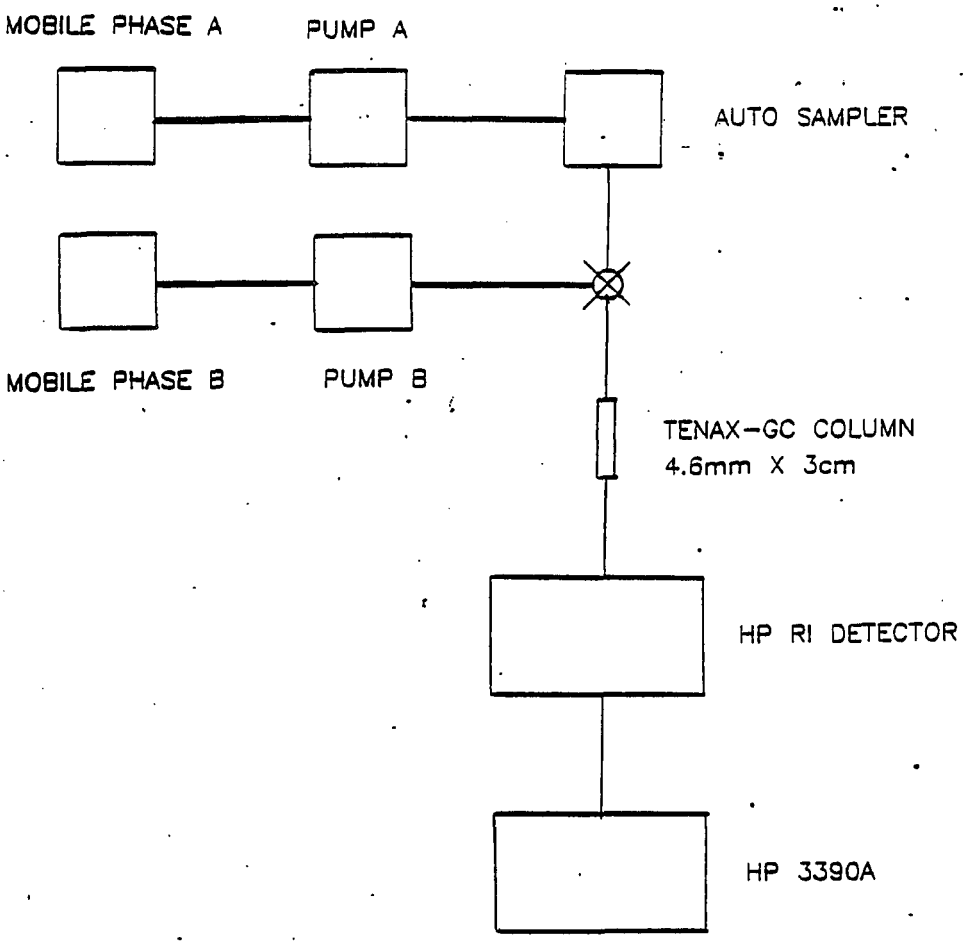

OPTIMIZATION OF AMANTADINE TRAPPING CONDITIONS

Mobile phase A was the same as the mobile phase used for the analytical separation of Amantadine from the animal feed mixture. Mobile phase B was 100% water and activated the Tenax-GC prior to the injection of the Amantadine standard into the vortex mixer.

Data was collected by pumping mobile phase A and B at flowrates of 2.0 ml/minute. A 50 µl sample of Amantadine standard (2mg/ml) was injected while mobile phase A was flowing to waste and mobile phase B conditioned to Tenax-GC column. Valve 1 was rotated to allow the mixing of the two mobile phases. From this experiment, it was determined that a flowrate of 1.5 ml/minute of pump B would retain the Amantadine on the Tenax-GC column for longer than 15 minutes.

Thermal Desorption of Amantadine from Tenax-GC

Since the amantadine is very stable and elutes from the Tenax-GC at a temperature of 180°C, the decomposition problems that were encountered with phenobarbital did not occur in this assay. Figure 44 shows the automated thermal desorption of spiked samples of Amantadine in animal feed. The precision for the assay with n=3 was 1.5% relative standard deviation at 10 µg level of Amantadine. This deviation was better than the phenobarbital assay presumably since fewer steps were involved and therefore less chance of losing a portion of the solute.

The limit of detection for amantadine is approximately 250 ng based on a signal 2 times the background level. When a flame ionization detector (FID) was compared to the PID, a 20 fold increase in sensitivity was achieved using the automated PID interface.

Figure 44

Optimized Desorption of Amantadine from Tenax-GC

GC:	P-E Model 3290 Temperature Programmable
Column:	Glass lined stainless steel tubing, 4.6 mm x 3 cm - all connections were made with glass lined 0.30 x 1/16 inch SS tubing
Temperature Program:	50°C - 180°C, 4 minutes
Carrier Gas:	Argon @ 40 ml/minute
PID Detector:	HNU Model PI-52-02
Input Attenuation:	10
Coarse Detector Offset:	10
Fine Detector Offset:	8.0
Polarity	Positive
Recorder Attenuation:	1

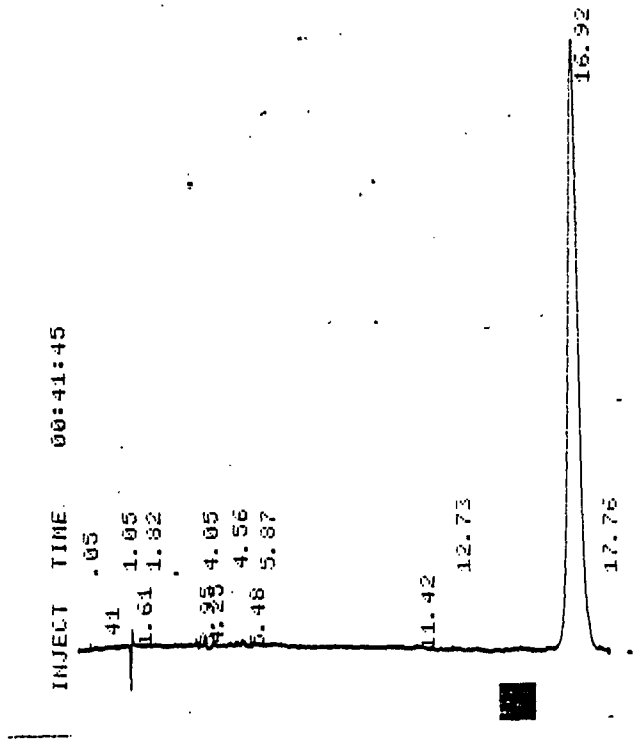

OPTIMIZED DESORPTION OF AMANTADINE

FROM TENAX–GC

Conclusions

The microprocessor-controlled system described in this thesis can detect trace levels of pharmaceuticals in very complex animal feed matrices. In general, the HPLC can rapidly separate the active components from excipients while the PID detector achieves a 40 fold increase in sensitivity compared to UV units.

Thus, combining LC with vapor phase detection shows great promise as a highly selective and sensitive technique. The LC-GC PID is another novel hyphenated technique combining ideas from two useful chromatographic systems.

References Chapter 6

(1) Bowman, M.C.; Nony, C.R.; J. Chromatogr. Sci., 15, 160 (1977).

(2) Bowman, M.C.; Rushing, L.G.; J. Chromatogr. Sci., 16, 23 (1978).

(3) Hucker, H.B.; Stauffer, S.C.; J. Chromatogr. Sci., 15, 357 (1977).

(4) Allred, M.C.; Dunmire, D.L.; J. Chromatogr. Sci., 16, 533 (1978).

(5) Quadrel, R.R.; Bogdansky, F.M.; J. Chromatogr. Sci., 18, 622 (1980).

(6) Tan, H.S.I.; Brake, N.W.; Keily, H.J.; Dalal, K.J.; Higson, H.G.; J. Pharm. Sci., 68, 1413 (1979).

(7) Van Der Hoeven, T.; Biochem. Biophys. Res. Commun., 100, 1285 (1981).

(8) Buddrus, J.; Herzog, H.; Cooper, J.W.; J. Magn. Reson., 43, 453 (1981).

(9) Toon, S.; Rowland, M.; J. Pharm. Pharmacol., 32, 8 (1980).

(10) Kraak, J.C.; Smedes, F.; Meijer, J.W.A.; Chromatographia, , 13, 673 (1980).

(11) Couri, D.; Del Villar, C.S.; Toy-Manning, Pamela; J. Anal. Toxicol., 4, 227 (1980).

(12) Sprague, K.; Poklis, A.; J. Can. Soc. Forensic Sci., 13, 31 (1980).

(13) Harbin, D.N.; Lott, P.F.; J. Chromatogr., 3, 243 (1980).

(14) Rydzewski, R.S.; Gadsden, R.H.; Phelps, C.A.; Ann. Clin. Lab. Sci., 10, 89 (1980).

(15) Miller, J.M.; Tucker, E.; Am. Lab., 11, 17 (1979).

(16) Hodnett, C.N.; Eberhardt, R.D.; J. Anal. Toxicol., 3, 187 (1979).

(17) Baker, J.K.; Raules, D.O.; Borne, R.F.; J. Med. Chem., 22, 1301 (1979).

(18) Baker, J.K.; Anal. Chem., 51, 1693 (1979).

(19) Draper, P.; Shapcott, D.; Lemieux, B.; Clin. Biochem. (Ottawa), 12, 52 (1979).

(20) Baker, J.K.; Skelton, R.E.; Ma, Ch-Y; J. Chromatogr., 168, 417 (1979).

(21) Johansson, I.; Wahlund, D.G.; Acta. Pharm. Sci., 14, 459 (1977).

(22) Kabra, P.M.; Stafford, B.E.; Marton, L.; Clin. Chem. (Winston-Salem, NC.), 23, 1284 (1977).

(23) Kabra, P.M.; Gatelli, G.; Stanfill, R.; Marton, L.J.; Clin. Chem. (Winston-Salem, NC), 24, 1020 (1978).

(24) Twitchett, P.J.; Gorvin, A.E.P.; Moffat, A.C.; J. Chromatogr., 120, 359 (1976).

(25) Henry, D.; Block, J.N.; Anderson, J.L.; Carlson, G.R.; J. Med. Chem., 19, 619 (1976).

(26) Twitchett, P.J.; Moffat, A.C.; Moffat, A.C.; J. Chromatogr., 111, 149 (1975).

(27) Atwell, S.H.; Green, V.A.; Haney, W.G.; J. Pharm. Sci., 64, 806 (1975).

(28) Chan, M.L.; Whetsell, C.; McChesney, J.D.; J. Chromatogr. Sci., 12, 512 (1974).

(29) Szaba, G.K.; Browne, T.R.; Clin. Chem. (Winston-Salem, NC), 28, 100 (1982).

(30) Snyder, L.; Kirkland, J.; "Introduction to Modern Liquid Chromatography", 2nd ed.; J.; Wiley & Sons: New York, NY, 1979; Chapter 4.

(31) Nelson, D.F.; Kirk, P.L.; Anal. Chem., 34, 899 (1962).

(32) Nelson, D.F.; Kirk, P.L.; J. Chromatogr., 12, 167 (1963).

(33) Bowman, M.C.; Rushing, L.G.; J. Chromatogr. Sci., 16, 23 (1978).

(34) Jaramillo, L.F.; Driscoll, J.N.; J. Chromatogr., 186, 637 (1979).

(35) Warnck, J.E.; Maleque, M.A.; Bakry, N.; Eldefrawi, A.T.; Albuquerque, E.; Mol. Pharm., 22, 82 (1982).

(36) Starewicz, P.M., Sackett, A.; Kovacic, P.; J. Org. Chem., 43, 739 (1978).

(37) Sunko, D.E.; Hirsl-Starcevic, S.; Pollack, S.K.; Hehre, W.J.; J. Am. Chem. Soc., 101, 6163 (1979).

(38) Stetter, H.; Smulders, E.; Chem. Ber., 104, 917 (1971).

(39) Uchiyama, M.; Shibuya, M.; Chem. Pharm. Bull., 17, 841 (1969).

(40) Bleidner, W.E.; Harmon, J.B.; Herves, W.E.; Lynes, T.E.; Hermann, E.C.; J. Pharmacol. Exp. Theory, 150, 484 (1965).

(41) Kirschbaum, J.; "Analytical Profiles of Drug Substances", Vol. 12, Academic Press: New York, NY, 1979.

Appendix I

Chromatograms Showing the Separation of an Animal Feed Extract After Extracting with the Solvents Indicated

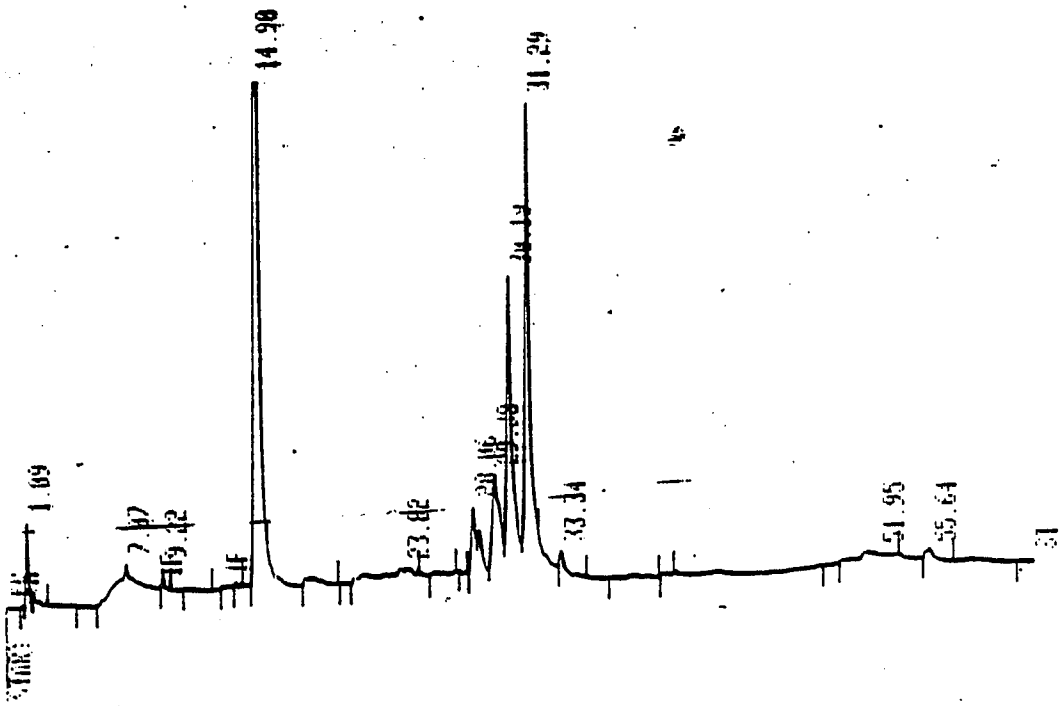

Acetonitrile

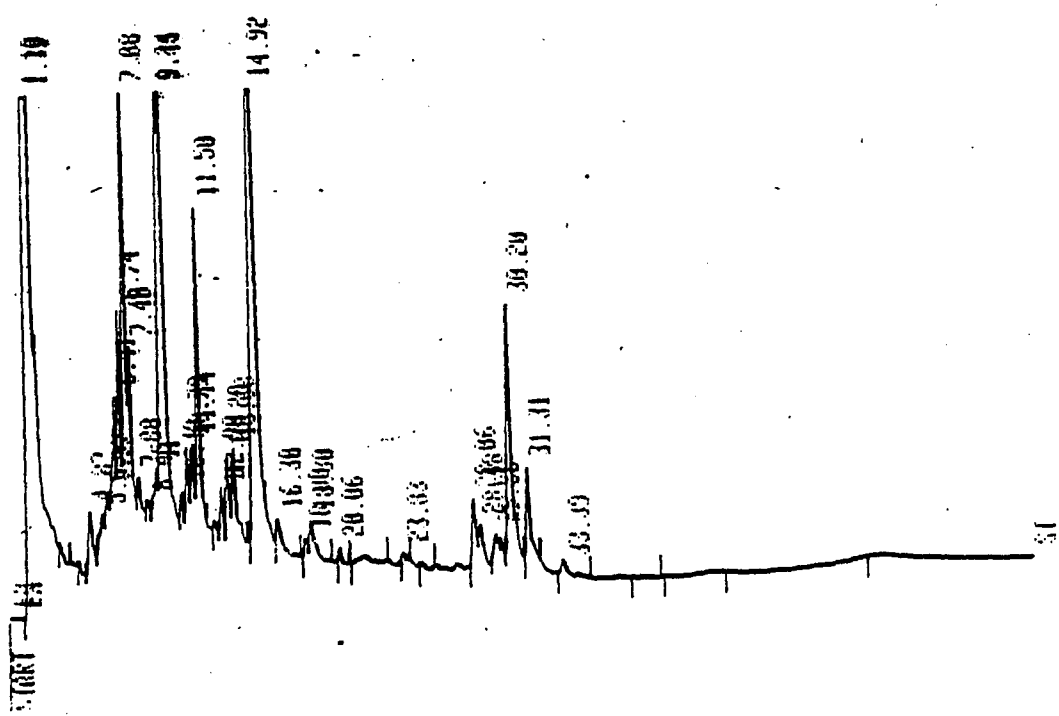

Methanol

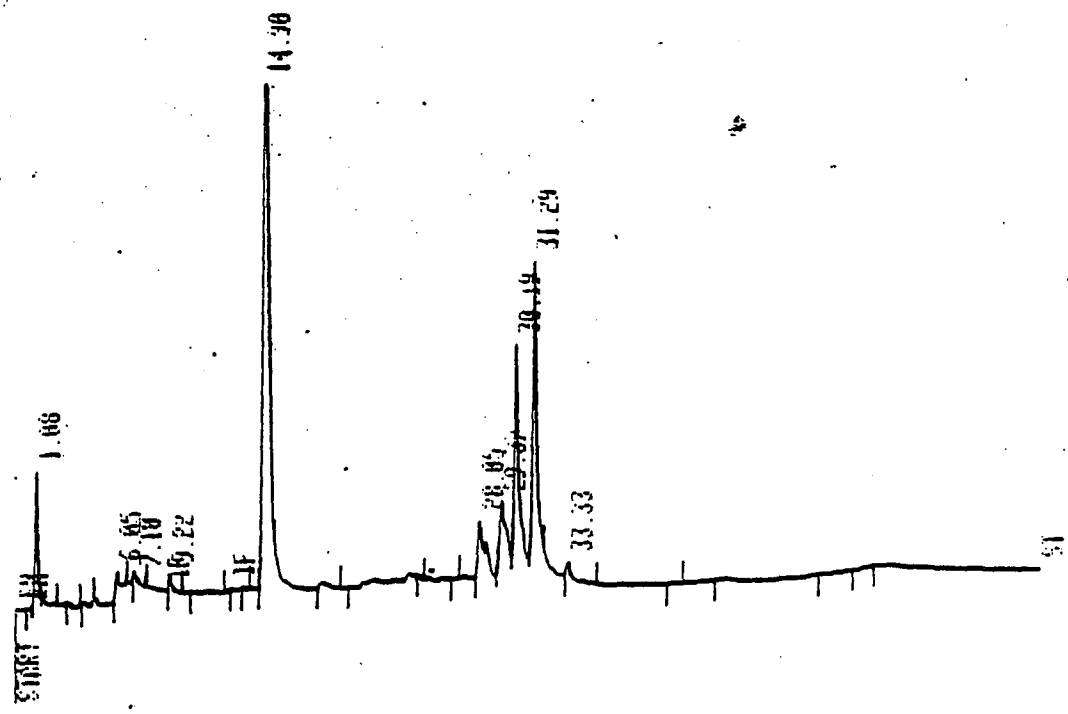

Ethyl Acetate

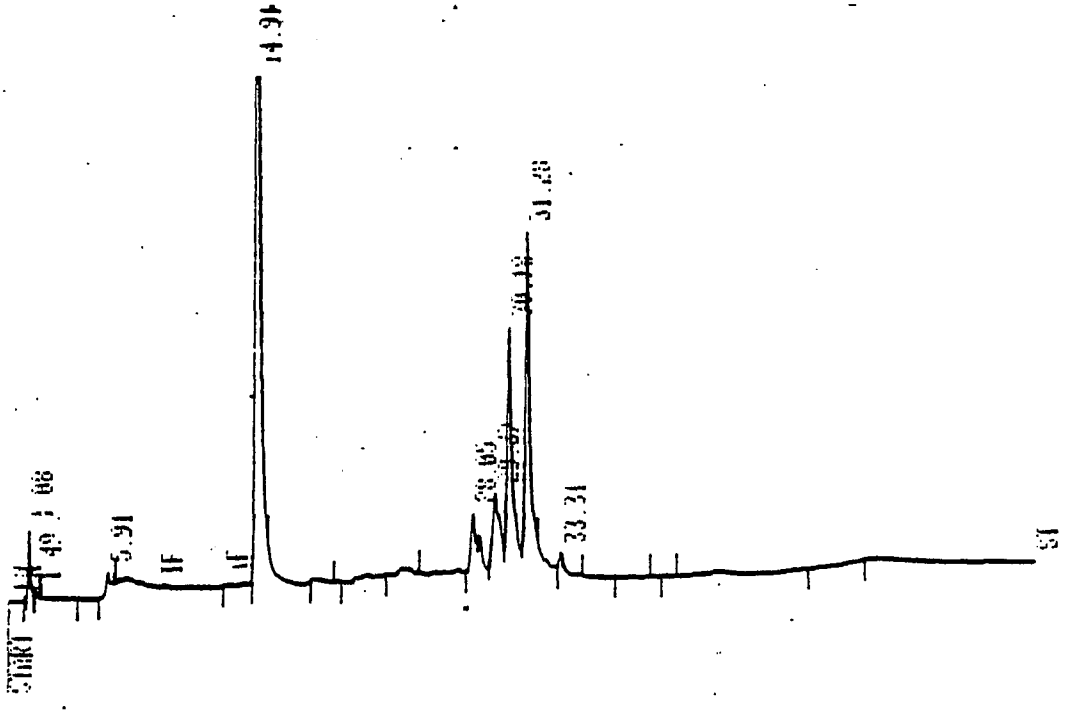

Hexane

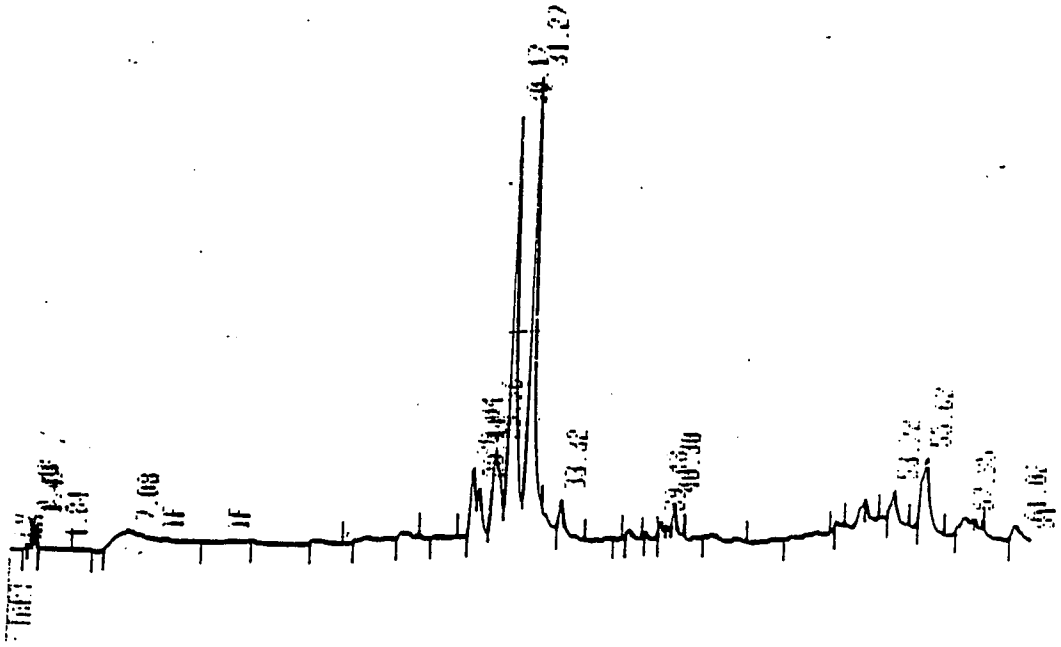

Methylene Chloride

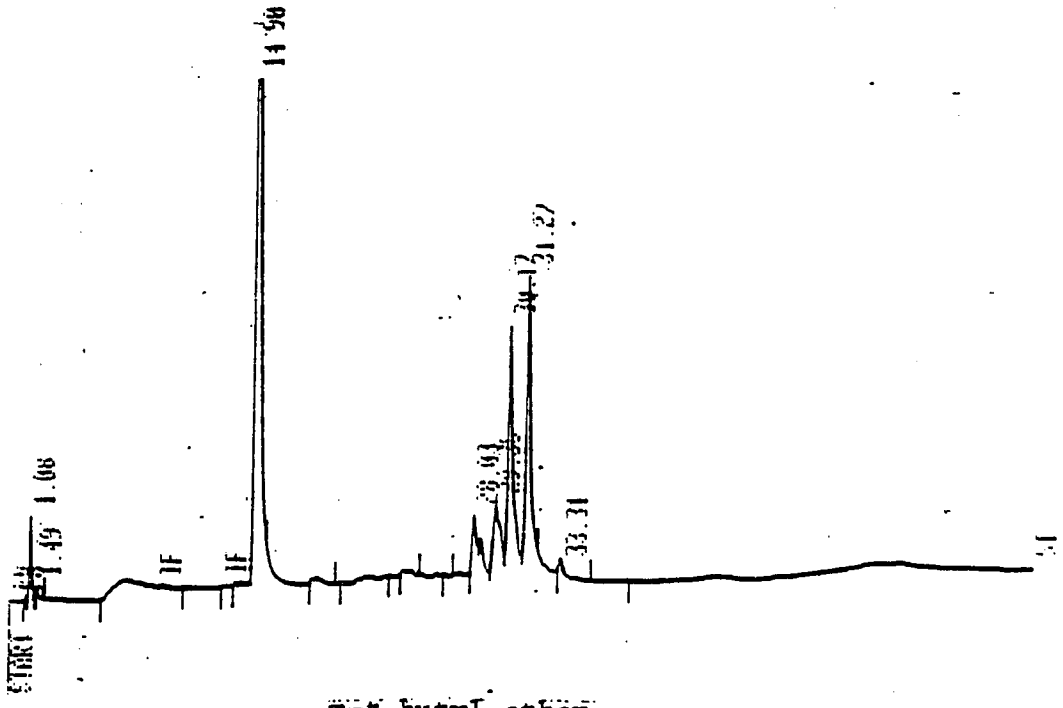

m-t-butyl ether

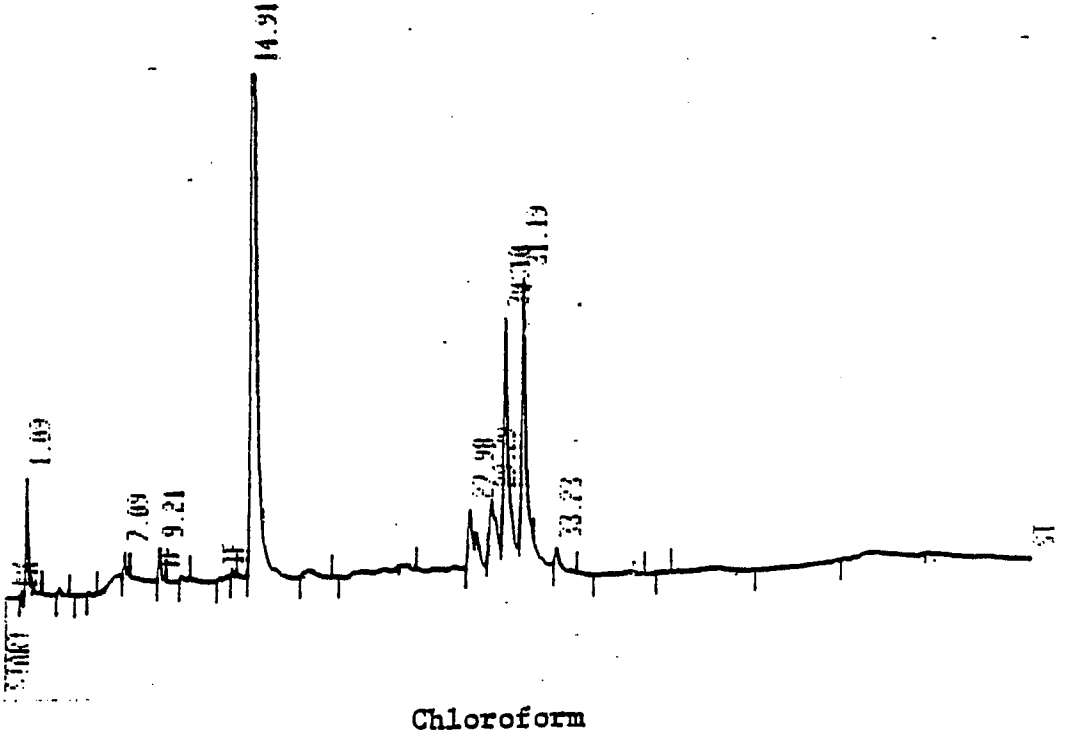

Chloroform

Appendix II

Calculation of Sample Peak Area Using a 3-Point Standard Curve and Least Squares Program

```
]LIST

10 D$ =  CHR$ (4): REM  CTRL-D
20  LEAST SQUARES PROGRAM
30  DIM C(25),R(25)
40  DIM P(100),U(100),L(100)
45 Z8 = 0
50 E1 = 1
60  IF E1 = 1 THEN 190
70 N = 0
80 C(1) = 0
90 C(2) = 0
100 C(3) = 0
110  PRINT "INJECTION (VIAL) NUMB
     ER OF SAMPLE   ";
120  INPUT V
130  IF V = 0 THEN 1990
140 R(1) = 0
150 R(2) = 0
160 R(3) = 0
170  IF N = 2 THEN 400
180  GOTO 550
190  INPUT "# OF STANDARDS :";K
200  PRINT "ENTER MG/FLASK, RATIO
      FOR EACH STANDARD:"
210  FOR I = 1 TO K
220  INPUT C(I),R(I)
230  NEXT I
240  PRINT "PT. NO.","CONC.","RAT
     IO"
250  PRINT
260  FOR J = 1 TO K
270  PRINT J,C(J),R(J)
280  NEXT J
290  PRINT
```

```
300  PRINT "DATA OKAY ";
310  GOSUB 4000
320  IF Z = 1 THEN 380
330  INPUT "CORRECT DATA PT. #";I

340  IF I > = K THEN 360
350 K = I
360  INPUT C(I),R(I)
370  GOTO 240
380  PRINT
390 N = K
400  IF N ↑ 2 THEN 550
410  IF N ↑ 1 THEN 430
420 R(2) = 0:C(2) = 0
430 B1 = (C(1) - C(2)) / (R(1) -
     R(2))
440 B0 = C(1) - B1 * R(1)
450  IF N = 1 THEN 1670
460  PRINT "          ##########
     ######################"
470  PRINT
480  PRINT
490  PRINT " TWO POINT CALIBRATIO
     N CURVE PARAMETERS:"
500  PRINT
510  PRINT "SLOPE= ";B1;" Y-INTER
     CEPT= ";B0;" MG/FLASK"
520  PRINT
530  PRINT "          ##########
     ######################"
540  GOTO 900
550 S1 = 0:S2 = 0:S3 = 0:S4 = 0:S
     5 = 0
560  FOR I = 1 TO N
570 S1 = S1 + R(I)
580 S2 = S2 + R(I) ↑ 2
590 S3 = S3 + C(I)
600 S4 = S4 + C(I) ↑ 2
610 S5 = S5 + C(I) * R(I)
620  NEXT I
630 M1 = S1 / N
640 M2 = S3 / N
650 T1 = S2 - S1 ↑ 2 / N
660 T2 = S4 - S3 ↑ 2 / N
670 T3 =  SQR (T1 / N)
680 T4 =  SQR (T2 / N)
690 T5 = S5 - S1 * S3 / N
700 T7 = T5 / (N * T3 * T4)
710 Q = T7 * T7
720 B1 = T5 / T1
730 B0 = M2 - M1 * B1
740 T8 = B1 * T5
750 T9 =  ABS (T2 - T8)
760 S =  SQR (T9 / (N - 2))
770 S6 = S /  SQR (T1)
780 Z = 1 / N + M1 ↑ 2 / T1
790 S7 = S *  SQR (Z)
800 F = T8 * (N - 2) / T9
810  PRINT "WANT TO SEE A PLOT ";

820  GOSUB 4000
825 Z8 = Z
830  IF Z = 0 THEN 880
840  GOSUB 5000
```

```
870  POKE  - 16303,0
880  IF E1 $  † 1 THEN 1150
890  PRINT
900  PRINT "DO YOU WANT TO USE FA
     CTORS ";
910 M = 1
920  GOSUB 4000
930 G = 0
940  IF Z = 0 THEN 1010
950 G = 1
960  PRINT "CONSTANT FACTORS";
970  GOSUB 4000
980  IF Z = 0 THEN 1010
990  INPUT "INPUT THE CONSTANT FA
     CTOR :";M
1000 G = 0
1010  PRINT "THE SAMPLE RATIOS ?
     (LAST ONE = 999)"
1020 J = 1
1030  PRINT "ENTER RATIO FOR SAMP
     LE  ";J;":";
  7HPT+,I
        ON I
5590R
     560 RISI 610 IQ = 3
5620  IF (IX - IQ) $ 0 THEN 5690
5630  IF (IY - IQ) $ 0 THEN 5690
5640  IF (IX + IQ) † 279 THEN 569
     0
5650  IF (IY + IQ) † 191 THEN 569
     0
5660  HPLOT (IX - IQ),(IY - IQ) TO
     (IX - IQ),(IY + IQ)
5670  HPLOT  TO (IX + IQ),(IY + I
     Q) TO (IX + IQ),(IY - IQ)
5680  HPLOT  TO (LX - IQ),(IY - I
     Q)
5690  RETURN
5700  END
```